Journal of Marine Technology and Environment

Vol. II, year 2013

ISSN 1844-6116

YEAR VI, 2/2013
ISSN 1844 – 6116
JOURNAL OF MARINE TECHNOLOGY AND ENVIRONMENT

This Journal has been founded in 2008 as a biannual publication of
Constanta Maritime University/ROMANIA

TOPICS

- Marine Science and Engineering
- Marine Environmental Issues
- Marine Renewable Energy and Sustainability
- Maritime Safety
- Marine Chemistry
- Marine Corrosion and Material Science
- Ship Design, Building Technologies
- Ocean Engineering
- Advanced Technologies for MET
- Advances in numerical methods for marine engineering
- Algorithms for multidisciplinary problems in marine engineering
- Other related topics

JOURNAL ADDRESS
Journal of Marine Technology and Environment
Constanta Maritime University, 104, Mircea cel Batran Street, 900663, Constanta, Romania
Tel: +40 241 664 740/ 107
Fax: +40 241 617 260
E-mail: jmte@imc.ro
http://cmu-edu.eu/jmte/

EDITURA NAUTICA
Constanta Maritime University
Constanta Maritime University, 104, Mircea Cel Batran Street, 900663, Constanta, Romania

CONTENTS

STUDY OF CORROSION RESISTANCE OF CONTACT RIVETS OF ELECTRICAL APPARATUS WITH NANOSTRUCTURED COATINGS OF THE TI/TIN TYPE

[1]APRAHAMIAN BOHOS, [2]GAYDARDZHIEV ALEXANDER, [3]STREBLAU MAIK

[1,2,3]*Technical University of Varna, Bulgaria*

The article presents the results of studies of corrosion resistance, in particular the resistance of contact rivets of electrical apparatus with nanostructured multilayer coatings of the Ti/TiN type – the so-called superlattices, to salt sea mist. The possibility of using these contact bodies at sea has been experimentally proven.

Keywords: corrosion, salt mist, contact rivets of electrical apparatus, multilayer coatings

1. INTRODUCTION

Corrosion is a process of spontaneous deterioration of metals as a result of their chemical or electrochemical interaction with the environment. Such deterioration advances under the influence of the oxygen in the air, moisture, sulfur oxides, nitrogen, and the action of other chemically active substances.

The processes in the atmosphere or in a gaseous medium at ambient temperature, and sometimes at elevated temperature when the formation of even the thinnest layers of electrolyte (greater than 10 μm) onto the surface of metal is possible, refer to the electrochemical corrosion. Electrochemical corrosion is the most common form of corrosion of ships at sea.

Corrosion damage may be complete or local, uniform or non-uniform. The rate of corrosion in the equipment is measured in grams of damaged metal for 1 h on 1 m^2 metal surface. If its value does not exceed 0,1 g/m^2, the metal is considered to be corrosion-resistant; if the value reaches and exceeds 3 g/m^2 – the metal is somewhat resistant. Metals that lose more than 10 g/h on an area of 1 m^2 are considered not resistant to corrosion [1].

Tests should be conducted according to standard IEC 60068-2-11 [2] and its national equivalents. The standard is used to test the relative resistance to corrosion of protective coatings, when exposed to a salt mist (spray) climate at an elevated temperature. Test specimens are placed in an enclosed chamber and exposed to a continuous indirect spray of neutral (pH 6.5 to 7.2) salt water solution, which falls-out on to the specimens at a rate of 1.0 to 2.0 ml/80 cm^2/hour, in a chamber temperature of +35℃. This climate is maintained under constant steady state conditions. The test duration is variable.

Contact rivets of electrical apparatus of various types of nanostructured multilayer coatings of the Ti/TiN type have been tested [3]. The aim is to demonstrate the applicability of the obtained specimens in ship conditions.

2. METHODS AND APPARATUS FOR CONDUCTING THE TESTS

The tests were conducted in the Laboratory for material analysis and testing and calibration of measuring facilities (LMTC) of the “Acad. A. Balevski” Institute of Metal Science of the Bulgarian Academy of Sciences.

Testing of test pieces was made in an aerosol chamber Aerozol-Korrosionsprufkammera Type 1000 – Switzerland (Figure 1), in accordance with standards BS EN ISO 7384:1996 and BS EN ISO 9227:2007, in a medium of neutral salt mist - 5% NaCl, temperature T = 35.0℃, pH of the collected solution in the ran ge from 6,5 to 7,2 at 25℃ for the duration of 100 hours.

Test specimens are placed at an angle of 15° to 30° to the vertical and they not shield one another from environmental influences in this arrangement.

The difference with the standard test is that a constant elevated temperature of T = 35.0℃ must be maintained in the chamber.

Fig. 1. General view of aerosol chamber Aerozol-Korrosionsprufkammera Type 1000

3. DESCRIPTION OF THE TESTED SAMPLES

Samples of contact bodies of contactor K6E with material of the base according to Table 1 were tested. General view of the tested samples is shown in Figure 2.

Table 1: Main characteristics of the base material of the tested contact bodies. % IACS – electrical conductivity according to the International Association of Classification Societies

№	Composite material	Chemical composition %	Density q/cm3	Hardness Hb	Electrical conductivity m/ohm.mm %IACS
1	**Silver cadmium oxide**	Ag-CdO 10 / 15 / 20	10.0 / 9.9 / 9.8	80 / 85 / 90	49 / 45 / 41 82 / 75 / 68

The coatings have been applied through electric arc application in a vacuum chamber and exhibit the characteristics shown in Table 2.

Table 2: Main characteristics of the material of the coating of tested contact rivets

Number of mode	Structure of superlattices	Gas medium and pressure in the working chamber	Total thickness of coating, nm
11	Ti/TiN/Ti/TiN	Ti-100% Ar(p=0.2 Pa) TiN-100% N_2(p=0.2 Pa)	88
12	Ti/TiN/Ti/TiN	Ti-100% Ar(p=0.2 Pa) TiN-100% N_2(p=0.7 Pa)	94
13	Ti/TiN/Ti/TiN/Ti/TiN	Ti-100% Ar(p=0.2 Pa) TiN-100% N_2(p=0.2 Pa)	128
14	Ti/TiN/Ti/TiN/Ti/TiN	Ti-100% Ar(p=0.2 Pa) TiN-100% N_2(p=0.7 Pa)	173
15	Ti/TiN/Ti/TiN/Ti/TiN/Ti/TiN	Ti-100% Ar(p=0.2 Pa) TiN-100% N_2(p=0.2 Pa)	170
16	Ti/TiN/Ti/TiN/Ti/TiN/Ti/TiN	Ti-100% Ar(p=0.2 Pa) TiN-100% N_2(p=0.7 Pa)	180
17	Ti/TiN/ Ti/TiN/Ti/TiN/Ti/TiN/Ti/TiN	Ti-100% Ar(p=0.2 Pa) TiN-100% N_2(p=0.2 Pa)	234

The coatings have been formed by alternating the specified layers in the relevant medium, and the corresponding thickness has been obtained for each mode.

Fig. 2. General view of a set of contacts for contactor K6E before testing for corrosion resistance

4. RESULTS OF THE TESTS

Upon the expiration of test time, the samples have the appearance shown in Figure 3. The number of contact plates corresponds to the number of the mode in Table 2. "0" is an uncoated plate.

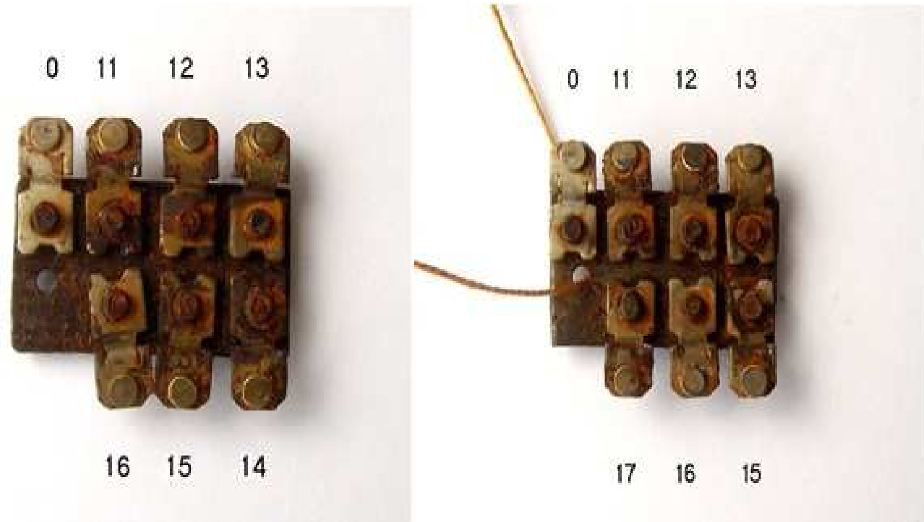

Fig. 3. Samples (groups 1 and 2) of contact plates after their testing for a duration of 100 hours in a neutral salt mist medium

Assessment of the coating has been made in accordance with BS EN ISO 10289:2006.

Test results are shown in Table 3. The following information has been presented in the table: Rp is a numerical rating which characterizes the ability of the coating to protect the base metal from corrosion; appearance rating – Ra, which includes a numerical rating and symbols intended to describe the general appearance of the sample, including all defects caused by exposure; and suitability rating - Rp/Ra, which is a combination of the numerical rating of protection (Rp), slash, followed by a numerical rating of appearance (Ra).

Table 3: Results obtained from testing the corrosion resistance of the samples

Corrosion resistance test results			
Mode	**Rating of protection** R_P	**Rating of appearance** R_A	**Rating of suitability** R_P / R_A
0	10	ND	10/ ND
11	10	ND	10/ ND
12	10	ND	10/ ND
13	10	0MA	10/0MA
14	10	0VsA	10/0VsA
15	10	0VsA	10/0VsA
16	10	0VsA	10/0VsA
0	10	ND	10/ ND
11	10	0SA	10/0SA
12	10	0MB	10/0MB
13	10	0VsA	10/0VsA
14	10	ND	10/ ND
15	10	0SA	10/0SA
17	10	ND	10/ ND

The designations used in Table 3 are as follows:

Numerical rating of protection R_P depending on the corrosion of base metal and of appearance R_A depending on the deterioration of the quality of the coating	
10	No defect
9	Affected surface between 0% and 0,1%
8	Affected surface between 0,1% and 0,25%
7	Affected surface between 0,25% and 0,5%
6	Affected surface between 0,5% and 1,0%
5	Affected surface between 1,0% and 2,5%
4	Affected surface between 2,5% and 5,0%
3	Affected surface between 5,0% and 10%
2	Affected surface between 10% and 25%
1	Affected surface between 25% and 50%
0	Affected surface above 50%
Degree of damage	
Vs	Very small
S	Small
M	Moderate
X	Significant
Types of damage of the coating established as a result of exposure	
A	Darkening and/or discoloration due to damage of the coating
B	Darkening with small or no visible corrosion of the coating

There is accumulation of corrosion products of iron with a characteristic color (hematite and magnetite). They are located on the bearing plate and along the adjustable screws, which are not subject to assessment.

In general, the coatings of group samples № 1 and 2 are unaltered (no defect); they only have different degrees of darkening with no apparent corrosion of the coating. As far as the behavior of the coatings according to the numbering of modes is concerned, no significant differences are noted. Differences in the degree of darkening do not give sufficient information which mode of application, and its corresponding thickness, is most appropriate.

5. CONCLUSIONS

It can be summarized that all tested samples were resistant to salt mist for the duration of 100 hours and fulfill the requirements of Standard EN ISO 10289:2006 - Methods for corrosion testing of metallic and other inorganic coatings on metallic substrates - Rating of test specimens and manufactured articles subjected to corrosion tests (ISO 10289:1999). This conclusion is consistent with the high corrosion resistance of coatings of the Ti/TiN type, known in the reference literature.

The area to be analyzed is too small for us to be able to determine which of the modes of the coating application demonstrated the best behavior in salt mist conditions. In order for a complete study to be made and for the best mode to be determined, the exact exploitation conditions must be known and, depending on that, the samples shall be subjected to the respective model resistance tests.

Such tests are, however, expensive and are only justified in the event of introducing new products into mass production.

However, the study demonstrated that the developed contact rivets of electrical apparatus with nanostructured coatings of the Ti/TiN type are fully applicable to ships at sea.

REFERENCES

[1]. Raychev R., - ***Corrosion and material protection***, Novi Znania Publishing House, Sofia, 2006.

[2]. Standard IEC 60068-2-11, - ***Environmental testing, Part 2 Tests – Test Ka: salt mist,*** Third Edition, 1999

[3]. Aprahamian B., A.Gaydardzhiev, - ***Improvement the durability of contact rivets of ship electrical apparatus by use of multilayer titanium nitride coatings,*** Journal of Marine Technology and Environment, Constanta Maritime University, Romania, vol. 2, 2011, p. 17 – 24, 2011

VIRTUAL DIALOGUES WITH RUDOLF DIESEL: A SAMPLE OF TEACHING/LEARNING MATERIALS FOR BEGINNERS IN MARINE ENGINEERING

[1]DEMYDENKO NADIYA, [2]SERHIY SKIDANCHUK, [3]SERHIY OCHKOVSKIY, [4]VIACHESLAV VIGOVSKIY

[1,2,3,4]*Kyiv State Maritme Academy, Ukraine*

This paper presents the materials of experimental class-room activity which is a part of the project approved by the Ministry of Education and Science of Ukraine. The project aims to create a Study Pack of Maritime English Introductory Course. One of the objectives is to find out methodological principles based on the interdisciplinary co-operation with specialists who are teaching major subjects. The great part of work has been done by senior students. The authors are thankful to the Department of Marine Engineering for the reasonable approach to the initiative, participation and assistance in preparatory work.

Keywords: interdisciplinary co-operation, experimental class-room activity, early specialisation

1. AIMS AND OBJECTIVES OF THE EXPERIMENT

The experimental class-room activity suggests the free discussion on one of the professional topics studied by the first-year students trained in Marine Engineering. The concept of "early specialisation" presumes the introduction of materials taught by the specialist teachers to the 1st year Maritime English syllabus. In terms of "twinning" (two teachers side-by-side), the particular requirements for the teachers emerge:

a) maximum attention to coordination in contents: the selection of topics depends on the scope of information in lectures and practical classes on professional subjects;
b) maximum attention to the English language proficiency: the 1st year students should be trained for level B 1 according to the European framework of foreign languages proficiency;
c) the scenario and the class-room activity plan are worked out by the two parties – the language teacher and the subject instructor; they conduct the class-room activity together;
d) participation of senior students has been planned according to the project's objectives; it aims to increase their motivation through the development of teaching/learning materials for Marine Engineering students;
e) individual work and additional assignments for students are foreseen; the students are advised to work on the Internet searching for materials on the subject;

f) the experimental activity is conducted as a final language class-room before the examination on the subject “The English language”;
g) two departments – Department of English for Specific Purposes and Department of Power Plants and Auxiliary Machinery- analyse the outcomes of the experiment for further improvements in methodology and contents;
h) the materials of the experimental class-room activity are the supplementary part of “Guidelines on teaching English to Maritime students (first year of studies)”.

2. MATERIALS OF THE CLASS-ROOM ACTIVITY “VIRTUAL DIALOGUES WITH RUDOLF DIESEL”

1. Introductory mini-lecture illustrated by the scheme.

Scenario: Mini-lecture is delivered in English by a specialist instructor; the aim of a language teacher is to check the students’ competencies in listening, taking notes (writing), answering questions, and speaking on the subject.

Motors and heat engines

A motor is a machine or an engine that produces motion. Motor is a device that converts any form of energy into mechanical energy, especially an internal-combustion engine. An engine is a motor that converts thermal energy to mechanical work. A machine - any mechanical or electrical device that transmits or modifies energy to perform or assist in the performance of human tasks.

A motor converts one form of energy into useful work without the intentional production of heat, such as an electric motor.

A device which burns fuel creating heat to perform work is a heat engine.

Heat engines can be classified as external combustion, such as steam boiler, or internal combustion (IC). They can further be divided into the spark ignited (SI) engine or the compression ignited engine (CI). The Compression Ignited heat engine is the Diesel engine, named after its inventor, Rudolph Diesel.

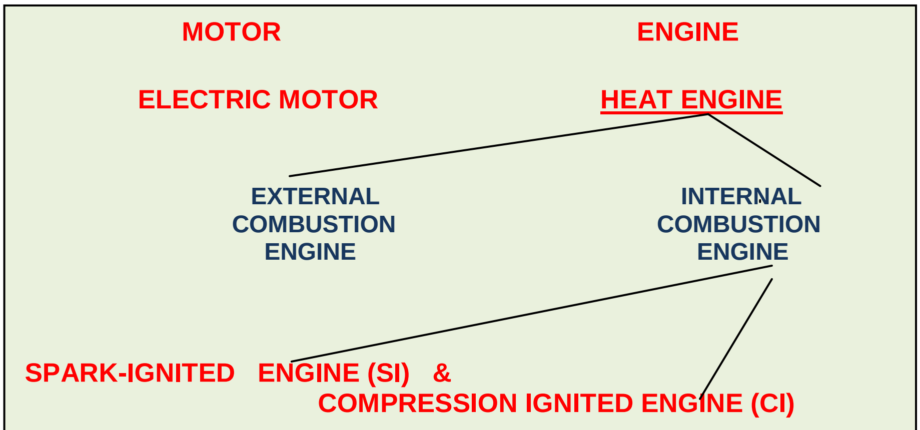

Vocabulary box:
-to produce, to convert, to perform /work/, to burn /fuel/, to divide into, to classify,

Checking comprehension and speaking:
What is a motor?
What is an engine?

What’s a heat engine?
What are the types of engines?
What’s ICE?
What’s a SI engine? What’s CI engine?

2. Introducing the inventor. Rudolf Diesel’s Biography

Scenario: role-play - a senior student is a virtual R. Diesel. He is present in the class-room and is ready to take part in the discussion. Two texts are suggested. The students prepare their questions for him.

Rudolf Diesel was born in Paris in 1858. His parents were Bavarian immigrants. Rudolf Diesel was educated at Munich Polytechnic. After graduation he was employed as a refrigerator engineer. His true love lay in engine design. Rudolf Diesel designed many heat engines. In 1893, he published a paper describing an engine with combustion within a cylinder, the internal combustion engine. In 1894, he filed for a patent for his new invention, called the diesel engine. Rudolf Diesel was almost killed by his engine when it exploded. However, his engine was the first that proved that fuel could be ignited without a spark. He operated his first successful engine in 1897. In 1898, Rudolf Diesel was granted patent #608,845 for an "internal combustion engine", the Diesel engine.

Efficiency: Diesel was aware of the inefficiencies inherent in the powertrains of the day. Steam engines were only 6% thermodynamically efficient and the gasoline engine, while better, could still manage only 12%. In 1896 he demonstrated another model with the theoretical efficiency of 75 percent (thermal efficiency figures of approaching 40%), in contrast to the ten percent efficiency of the steam engine. Application: Diesel engines were used to power pipelines, electric and water plants, automobiles and trucks, and marine craft, and soon after were used in mines, oil fields, factories, and transoceanic shipping.

Vocabulary box:
To invent – an inventor – an invention
To study – to research – to investigate
A model – a design – a patent
To apply - an application
Efficient – inefficient – efficiency

3. Dialogues with R. Diesel

Scenario: Listening and speaking skills are developed through professional conversations. The specialist instructor checks the knowledge of the basics of thermodynamics. The language teacher is checking correct usage of terms.

Question One: How did you make the heat engine so efficient?

R. Diesel’s answer: “My invention has a reference to improvements in internal combustion engines. The process consists in first compressing air or a mixture of air and a neutral gas or vapour to a degree producing a temperature above the igniting point of the fuel to be consumed, then gradually introducing the fuel for combustion in the compressed air while expanding against resistance.”

Qustion Two: How is it possible to increase the motive power?

R.Diesel’s answer:

Motive power.

I was confident that there was a better way to use the energy from the fuel that the most efficient steam plant used. At the time, 90% of the fuel was wasted. Then I read a book. A book by Sadi Carnot, a gifted engineer with a specialization of thermodynamics. His book

”Reflexion sur la puissance motrisse de feu” was published in 1824 and cut right to the heart of the heat engine, and gave us the “First Law of Thermodynamics”; which is “heat and mechanical energy are convertible to each other, but are never created or destroyed, only changed in form”.

4. Mini-lecture “Carnot cycle”

Scenario: the information is delivered in English by the subject instructor. The discussion is at the chalkboard with the formula on it. The knowledge on physics is assessed by the subject instructor; the skills of speaking on the professional topic are assessed by the language teacher.

All standard heat engines (steam, gasoline, and diesel) work by supplying heat to a gas, the gas then expands in a cylinder and pushes a piston to do its work. The catch is that the heat and/or the gas must somehow then be dumped out of the cylinder to get ready for the next cycle. How efficient such a heat engine can be: what’s the most work we can possibly get for a given amount of fuel? The simplest cyclical model: an ideal gas enclosed in a cylinder, with external connections supplies and takes away heat, and a frictionless piston for the gas performs (and absorbs) mechanical work.

The efficiency question was first posed—and solved—by Sadi Carnot in 1820.

The efficiency of an ideal engine operating between two temperatures will be equal to the fraction of the temperature drop towards absolute zero that the heat undergoes. This turns out to be exactly correct, even though the reasoning is based on a false model.)

Efficiency of the Carnot Engine. The efficiency of the engine, defined as the fraction of the ingoing heat energy that is converted to available work, is $\boxed{\text{efficiency} = \frac{W}{Q_H} = 1 - \frac{T_C}{T_H}.}$

5. The differences between Otto cycle and Diesel cycle

Scenario: the text is to be read and analysed to compare the Otto cycle and the Diesel cycle. The comprehension question is: *What’s the difference between the two cycles?*

Nikolaus Otto was born in Germany on 10th June 1832. In 1876 he developed the first 4-stroke cycle internal combustion engine. His engineering work led to the first practical use of the 4-stroke cycle. Nikolaus Otto died on 26th January 1891.

The gasoline engine inherently has problems with efficiency and/or fuel. In order to improve the efficiency one must increase the compression ratio of an internal-combustion engine. The diesel engine can use much higher compression levels than the gasoline engine reaching higher efficiency. In addition, the diesel engine can use fuel that is not nearly as refined as the high-octane gasoline fuel (thus cheaper).To make this possible, Rudolph changed the Otto cycle and created the Diesel cycle. The difference is that during compression phase, no fuel is present in the cylinder and thus no self-ignition can happen. The fuel is only injected at the moment the ignition is wanted – when injected into the hot pressurized air the diesel fuel self-ignites immediately (the diesel-air mixture, as we said already, is happy to ignite even at relatively low temperatures).

The Diesel cycle is a compression ignition (rather than spark ignition) engine. This cycle can operate with a higher compression ratio than the Otto cycle because only air is compressed and there is no risk of auto-ignition of the fuel. Although for a given compression ratio the Otto cycle has higher efficiency, because the Diesel engine can be operated to higher compression ratio, the engine can actually have higher efficiency than an Otto cycle when both are operated at compression ratios that might be achieved in practice.

6. Classification of marine diesel engines

Scenario: Developing skills in reading and writing. The schemes of two stroke and four stoke diesel engine are displayed in front of the students. The short characteristics of two diesel types is produced by the students individually. They may exchange questions on the specific features of diesel engines design. The information about four stroke diesel engine is filled in on the cards distributed to the students.

The compression ignited internal combustion engine has two main designs: the four stroke cycle, and the two stroke cycle engine. They burn a wide variety of hydrocarbon fuel, which is still common. Heavy fuel oil, intermediate fuel oil and marine diesel oil are the most common hydrocarbon fuel. The two stroke and four stroke titles refers to the mechanical action of the machinery, in particular the piston within the cylinder, to achieve the theoretical Carnot heat cycle, as define by the laws of thermodynamics.

Two-stroke cycle: the piston makes two strokes for every explosion.

It takes two strokes to complete a power cycle: one stroke down, one stroke up – one turn of the crankshaft. The power stroke occurs at every down stroke.

Four-stroke cycle: the piston makes four strokes for every explosion. Describe / write down the definition of a four-stroke cycle.

7. Marine diesel engines manufacturers

Scenario: the pictures of different models are produced on displays. The students prepare information about marine diesels they know.

Two-stroke marine diesel engines. In the world of ships, these engines are large and tall to increase the efficiency of the power stroke. The large physical size of these power plants tends to slow them down (around 100 rpm). The builders of large, slow speed, two stroke engine are Sulzer of Switzerland, producer of the first big two stroke design, and Burmeister & Wain (B&W) of Denmark, the pioneers of the engine's application to ship design.

Four-stroke marine diesel engines. Many companies build four stroke Diesel engines. Caterpillar, Cummins, Detroit Diesel engines are the most popular engine manufacturer for highway trucks and smaller applications. MAN (the company that first developed Rudolph Diesel's engine), MAK, MTU, Wartsila, Deutz - offer a wide range of power plants. The four stroke is seen in application demanding a compact power plant with smaller physical size, especially the engine's height. This height becomes a problem on many coastal ships, such as ferries.

8. Classification: slow, medium and high speed diesel engines

Scenario: the text is discussed as the example of marine diesels' classification and applications of different designs. Attention is paid to pronunciation of numbers in speech.

-SLOW-SPEED ENGINES 100-300 RPM (revolutions per minute)
-MEDIUM-SPEED ENGINES 300-900 RPM
-HIGH-SPEED ENGINES Over 900 RPM

Diesel engines are sub-divided into three categories: slow, medium and high speed. Slow speed are considered to be up to 300 rpm such as most big two stroke engines commonly found on ships. Medium speed engines dwell in the 300 - 900 rpm range. They are most common on smaller ships and power plants driving electrical generators and / or the propeller. High speed engines are the most common. Their high revolutions are ideal for driving vehicles such as a bus and a yacht. All Diesel trucks and vehicles on our roads use this class of Diesels, having an rpm over 900.

9. Engine design: Parts of a marine diesel engine

Scenario: developing students' communicative skills and suggests assessment in professional knowledge. Visual aids have been made by senior students.

Parts of a two-stroke engine. The heart of the two stroke engine consists of a cylinder liner with inlet ports about 2/3 of the distance from the top of the liner. The cylinder head, also known as cylinder cover, contains the exhaust valve. The piston within the cylinder is connected to the crankshaft by the connecting rod. On the larger engines, the power is transmitted to a cross head assembly first. The cross head slide up and down with the piston and transmit power from it to the connecting rod and crankshaft.

Parts of a four-stroke engine. The four stroke is similar to the two stroke. But its inner working is quite different. One primary difference is the cylinder liner does not have the inlet ports. Another is the combustion air is drawn into the cylinder by the piston. This action is controlled by an inlet valve in the cylinder head. With no need for a blower, this becomes the most radical difference between the four and two strokes engines and as such, the four strokes are called naturally aspirated engines.

10. Rudolf Diesels questions

Scenario: the students answer the questions of virtual R. Diesel. Free discussion is organised involving students and teachers.

1. What types of engines are used now?
2. What are the manufacturers?
3. What's the engines' efficiency?

3. CONCLUSIONS

In MET the domination of skills development over knowledge delivery is being obvious. This is the sphere of practical methodology which usually has certain achievements in non-English speaking countries. Coordination between subject and language teachers lies in an area where both knowledge and skills may be improved. This is the core idea of any corporative research activities.

The interdisciplinary cooperation purposes to develop new teaching/learning materials to improve students' language and professional skills and abilities. The fact is that marine engineers experience the lack of training in professional English. However, "training in handling various types of electrical equipment and cargo computers is vital, including the all important engines and machinery in the engine room. Here a problem has been highlighted in that operational and maintenance manuals may be in the languages of the original manufacturers i.e. German, Japanese, Norwegian etc. This situation is gradually being addressed yet, even if manuals are provided in English, (the presumed 'common' language on board), if the crew are multi-nationals, translation may be necessary by an English speaker who might not be an electrical engineer or computer expert." [Short, 2006].

In our project, the priorities are given to general English competencies which include abundant communicative work on the level of a sentence/phrase and a text/description, narration, etc. The linguistically centered model [Demydenko, 2012] presumes the implementation of units on professional topics aiming the assessment of ME abilities as the outcome through skills development. The 1st-year students trained in Marine engineering attain better results when taught professional materials in English. The teaching/learning materials should be supplemented by additional tasks for the web search. The work in the Internet increases the students' motivation for their further professional training.

REFERENCES

[1]. Demydenko Nadiya - ***Teaching Maritime English: A Linguistic Approach,*** Journal of Shipping and Ocean Engineering 2, pp. 249-254, 2012

[2]. Short Valerie - ***Maritime English: Valuing a common language,*** Nautical Briefing, 'Seaways' in The Journal of The Nautical Institute October, pp.1-12, 2006

[3]. Source of materials: www.dieselduck.net

SUSTAINABLE PORT DEVELOPMENT IN CONNECTION WITH ENVIRONMENTAL REGULATIONS

[1]GRANCHAROVA VALENTINA, [2]GRANCHAROV IVAYLO

[1,2]Naval Academy “Nikola Y Vaptsarov”, Bulgaria

Modern ports as a part of logistics chain and the transport networks are under sustainable development and process optimization. Port expansion should always be considered in the context of environmental legislation and its implementation in different national laws. The paper discusses the introducing of major environmental requirements for port development activities.

Keywords: port development, environmental management, port activities

1. PORT DEVELOPMENT ACTIVITIES AND THEIR IMPACT TO THE ENVIRONMENT

Port sustainable development have the potential to impact on environmental and human resources. There are no established uniform criteria for assessment the adverse effects of port development because they vary by countries and depend on local or regional characteristics. Generally environmental effects in relation to port development can be categorized into following groups: water quality; coastal hydrology; contamination of bottom sediments; marine and coastal ecology; air quality; noise and vibration; waste management; and socio-cultural impacts. Water quality includes five components: general features such as temperature, salinity, pH, colour, transparency, oil and grease, and organic material concentration, measured by total organic carbon (TOG), chemical oxygen demand (GOD) or biochemical oxygen demand (BOD); turbidity measured by suspended solids (SS); eutrophication-related factors, measured by dissolved oxygen (DO), nitrogen (N) and phosphorus (P); harmful or toxic substances, including heavy metals such as mercury, cadmium, lead, and pesticides; and sanitation-related factors determined by measuring the amount of coliform bacteria. Coastal hydrology embrace factors and physical phenomena in the shore zone(such as currents, tidal flow, littoral drifts, erosion of beach, water drainage, sediment deposition, groundwater flow). Marine and coastal ecology encompasses aquatic fauna and flora. Air quality depends on dust, originate from dry bulk cargo handling and storage, construction work on land, and road traffic and concentration of harmful substances such as sulfur dioxide (SO_2), nitrogen dioxide (NO_2), carbon monoxide (CO), and hydrocarbons (HC), emitted from ships, vehicles and various equipment used for port activities. Noise and vibration generated by construction equipment, truck traffic, work vessels and other similar sources could be considerably reduced by adoption of low noise equipment or installation of sound insulation fences. Waste management relates to liquid and solid wastes, disposed of in the port area. These wastes include dredged materials, garbage and oily mixtures discharged from ships, wastes from cargo operations, and all types of discharges from municipal and waterfront industry activities.

The port activities can be divided mainly to following groups: activities for development and operational activities. Building renovation, quay enlargement, dredging of navigational channels are some of the development activities common to all ports. Activities, concerning maintenance of vehicle and equipment, storage and handling of cargo are typical operational activities in ports (see Fig.1). Dredging for channel deepening can cause major changes to the intertidal and sublittoral areas and consequently in the type of aquatic habitats. The change of littoral drift may lead also to erosion or accretion in shore zones. Altered currents or reflected waves may endanger small ships maneuvering near structures. The reduction in sediment load being transported upstream and shoreline configuration by erosion or accretion or shoaling may alter flow velocities and directions. Therefore capital dredging operations should be designed as a part of sustainable dredging and sediment management schemes. Damage prevention or avoidance measures should always be preferred to compensation measures and to include a predefined and validated scheme to monitor the potential impacts and a framework to adapt the mitigation and compensation measures to the actual impacts.

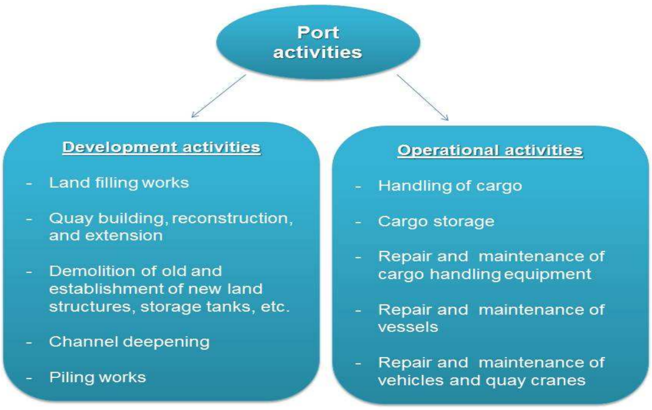

Fig. 1. Type of port activities

The physical removal of bed sediment can also remove important habitats of aquatic organisms. Resuspension of sediments in water leads to an increase in the level of suspended solids (SS) and in the concentration of organic matter, possibly to toxic or harmful levels. It also reduces sunlight penetration. The presence of new waterside structures, including breakwaters, pontoons and harbour arms, can impact on the water quality by encouraging accumulation of debris and oil or by stagnating the water. Structures can also lead to changes in maintenance dredging practices and navigation. The establishment of new structures in inland waterways will physically remove waterside habitats and may interfere with the movements of certain sorts. Landfills are often used to increase the available areas for port operations. Breakwaters and landfills may change current patterns and cause stagnation of water behind the structures. During filling for land reclamation purposes, fine sediment from the filling material can escape into water with implications similar to dredging. The demolition of old storage tanks and pipelines and the associated breaking of equipment can introduce contaminants into surface water via runoff and eventually into groundwater supplies.

The performing of cargo handling operations can result in the introduction of contaminants into the ambient air, surface water, ground water supplie, and soil and harbour sediment. Other sources of pollution in ports include accidental spills of fuel oil or bulk or liquid cargo, as well as the introduction of non-native marine species via the release of ballast water. Runoff from raw material storage, spills from bulk cargo handling, and wind-blown dust are possible sources of contamination of port water. Frequent spillage of organic cargo can spend dissolved oxygen. As a consequence the nutrient level in water will increase, which brings effect to aquatic life. Certain ores such as iron ore can result water discoloration and changes in the acidity or the salinity of the water. The presence of fertilisers in water lead to eutrophication of algal blooms and the released toxins may endanger some animals. Environmental consequences generated by activities of industrial ports can be easily prevented by increase of awareness on types of pollutants produced by factories and industrial ports. The monitoring of potential environmental threats can help by setting up of work procedures and emergency plans, which have to be followed strictly. The monitoring of marine water quality around the port can also serve the presence of polycyclic aromatic hydrocarbons, which are generated from petrochemical industries and oil refineries (ESPO, 2012).

2. ENVIRONMENTAL LEGISLATION

The Ports themselves have become highly complex centers where, alongside traditional loading and offloading operations, new installations carry out goods processing and industrial transformation as well as cargo storage operations. In order to respond to the rapid growth in international trade, some ports are periodically required to expand their infrastructure. This gives them a new important role in the production and consumer chain and creates new needs to minimize environmental risks in their installations and processes. The accomplishment of port development projects has to be in fully conformity of environmental legislation in port sector, including the EU nature directives and standards.

The last issue of ESPO Green Guide 2012 has following tasks: 1/ defines a common vision of the port sector on environmental sustainability; 2/promotes the efforts of European port authorities in the field of environmental management; 3/ demonstrates evidence of the progress achieved by the sector over time; 4/ provides guidance to ports in establishing and developing further their environmental management programmes; 5/ highlights the main environmental challenges that ports face and demonstrates response options; 6/ develops a common approach towards responsible action, while respecting the diversity of ports, their competences and their abilities.

An Environmental Management System (EMS) is an instrument that can help ports meet the goal of providing a healthy environment. The most commonly used framework for performing of EMS is the International Standard EN ISO 14001, which specifies requirements for an environmental management system to enable an organisation to formulate a policy and objectives taking into account legislative requirements and information about significant environmental impacts. Innovation of one environmental management system requires organisations to identify and evaluate the environmental impacts associated with their activities, products or services. The Standard ISO 14001 defines an environmental impact as “any change to the environment, whether adverse or beneficial, wholly or partially resulting from an organisation’s activities, products or services”.

Environmental problems need to be addressed during the port design, construction and operational phase. Integrated spatial planning offers opportunities for anticipating difficulties and adverse environmental impacts and avoiding potential conflicts and delays in port project development. Integrated coastal zone management (ICZM) paves the way for ports for such strategic planning. The Water framework directive (WFD) of EU establishes an integrated framework for the sustainable management of surface waters and groundwater with the aim of reaching good ecological status in all waters by 2015 (European

Commission, 2011). For heavily modified water bodies, e.g. for navigation purposes or for the construction of port basins, the objective is to reach good ecological potential.

3. ENVIRONMENTAL FRIENDLY DEVELOPMENT

From a port authority environmental management perspective, three levels of potential intervention can be identified; the level of own port authority operations, that of the operations within the port area, the level of the transport and the level of logistics chain. The degree of influence a port authority can have towards taking actions to improve the environmental performance varies between the levels identified above and depends on the different objectives and functions, institutional framework and overall competence of the port authority. Port authorities should formulate and periodically update their vision or business plan for the development of the port. In this vision information regarding the trends for sustainability and the environment on a port area level should be provided. By collecting, combining and aggregating (individual) data, a specific environmental policy can be developed and performed at the port area scale. Global data can also can give assistance to detection of potential port development restrictions and can help on the prioritising and setting of environmental actions. In most cases port authorities have an exclusive or shared operational and financial responsibility for the management of port infrastructure (e.g. docks, quays). This infrastructure management accomplishment, and especially competences for environment-related infrastructure such as infrastructure connected to shore side electricity, bunkering systems, smart grids, waste water treatment etc., could also be a useful instrument for port authorities in order to realise environmental ambitions.

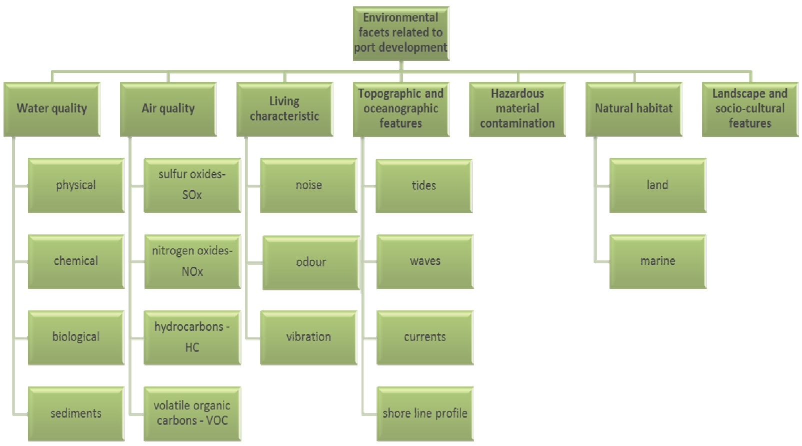

Fig. 2. Classification of environmental facets related to port development

The ports' development always is connected with exploitation of resources, direction of investments, orientation of technology and institutional change. The design and expansion of one terminals starts usually with determination of cargo flow and calculating the service time, the number and productivity of cranes per berths and also the used cargo handling equipment. After that the attention should be directed to protecting of environment from pollutions. The monitoring of environment is a sensory component of environmental management and is an appropriate performance indicator. For prediction the environmental impact can be used model, which simulate dispersion of the pollutant (water quality model) or define the pollution distribution in the atmosphere (temperature models). The proposed from authors classification from a view point of environmental components (presented in

Figure 2) can be very useful by creating of checklist for environmental impacts of port development. In Table 1 are described the major sources influencing on the environment state, their typical effects, and the respective measures, which have to be taken for preserving the environment in the vicinity of port area.

Table 1 Major sources influencing on the environment state

	Environmental effects	Measures against adverse effects
Impacts of port location	stagnation of water behind the water structures	careful site selection and port design
	alteration of wave refraction, diffraction and reflection	model experiment or computer simulation for developing of appropriate design
Impacts of construction	increasing of suspended solids, reducing of sunlight penetration and turbid water	appropriate selection of equipment in pile driving and dredging, proper use of silt curtains, careful planning od setting ponds and overflow weirs for landfills, suitable transport of construction materials and proper disposal of dredged materials
	leakage of harmful substances into ground water caused by disposal of dredged material on land	carefully planning the steepness of the dredging slope and the deviation from the shore line
	dust from construction activities	use of appropriate methods for controlling dust emissions (water scattering in the construction site) and proper transportation of materials.
Impacts of ships traffic and discharges	any kind of clandestine dumping or accidental spills from ships	providing of relevant methods for detecting of dumping and spills into water, ensuring of warming systems for accidental pollution necessary reception facilities acc. to MARPOL annexes and related IMO Conventions.
	airborne pollutants generated by ships while both maneuvering and berthing	proper detection of emissions from ships and observing of requirements of Annex VI of MARPOL
Impacts of cargo operation and waterfront industry	spills from bulk cargo handling	use of cover conveyor or pneumatic unloader for minimizing influence of wind and rain
	effluent from waterfront industries	regularly monitoring of water quality and separation of water front industry from the harbours
	dust from bulk cargo handling	monitoring of air quality to ensure acceptable level of emissions in accordance with environmental management plan
	gases released from cargo handling equipment	
	releasing of VOC during load/discharge of liquid cargoes or cleaning of storage tanks or equipment	

Environmental actions in sea ports are to be selected for each port individually and applied gradually (Kruse C. J., 2005). The presence of a port in coastal area leads to a concentration of land transport with trucks and trains and increasing of emissions of CO_2. Congestion at ports leads to increased energy consumption, operational pollution and loss of time and comfort. To reduce the congestions at port and and population exposure to health hazardous air pollutants the modal shift for transport of goods to and from the port from road to rail needs to be promoted. In order to avoid the conflicts, concerning land use and deterioration of cultural heritage and natural habitats, the ports' physical expansion must be done after reaching of efficient use of existing port areas. Therefore many of large harbours operate mainly with containerized cargoes and implement automated systems for performing of cargo handling operations.

A challenge for the future is to find solutions that may accommodate increased activity in the land/sea transfer and at the same time minimizing the environmental and societal impacts.

4. CONCLUSIONS

Surrounding communities are increasingly interested in the impacts of port expansion, such as wetland or habitat loss, handling of sediment from dredging operations, congestion, safety, and other impacts of port growth.

An environmental management system is a problem identification and problem-solving tool that provides ports with a method to systematically manage their environmental activities, products and services and helps to achieve their environmental obligations and performance goals. Dealing responsibly with waste, and monitoring energy and water usage will make environmentally friendly outlook of ports and save investitures' money. To improve awareness of environmental impacts expansion projects should pre-assess the effects of the development and consult the competent nature conservation authorities on whether their plan or project is likely to have significant negative effects. The main aim of Environmental Code of Practice (ESPO Green Guide 2012) is to trigger port authorities commit to sustainable development and the continuous improvement of their environmental performance. Environmental policy at ports should be directed to observing and reducing impacts to the sea (from ship, land, dredging) and air pollution (dust, noise) to the minimal level, performing of environmental impact analysis in port development, prevention risk of major accidents such as vessel's collision and grounding using of Vessel Traffic System (VTS), manage waste and discharge operations (recovery, collection, recycling, supervised disposal areas).

Careful site selection and port design could minimize changes in current patterns and other coastal hydrology. Appropriate regulations on ship discharges and provision of reception facilities are indispensable for proper control of emissions and effluent from ships. Detection of spills is also important for regulating ship discharges. Since accidental spills are unavoidable, recovery vessels, oil fences, and treatment chemicals should be prepared with a view to minimizing dispersal. Proper contingency plans and a prompt reporting system are keys to prevention of oil dispersal. Periodical clean-up of floating wastes is also necessary for preservation of port water quality. Ships are a possible source of airborne emissions such as gasses, smoke, soot andfumes. NO_2 and SO_2 are typical pollutants generated by ships while both manoeuvering and berthing and may affect air pollution in the hinterland. Proper detection of emissions from ships are effective means to reduce discharges of pollutants. Prohibition of the use of heavy diesel oil as fuel could be a possible means to reduce pollutants. Accidental spills of toxic,harmful materials, oils or oily compounds, and other raw materials are also possible sources of contamination of water.

The environmental friendly outlook of port can be achieved through optimisation of port/terminal location and distribution, innovations that increase throughput while reducing intermediate storage, innovative solutions that reduce port/terminal land use, advanced planning of land infrastructure, simulations of effects on ecosystems.

REFERENCES

[1]. ESPO – ***Green guide: Towards excellence in port environmental management and sustainability***, Brussels, Belgium, 2012

[2]. European Commission – ***Integrating biodiversity and nature protection into port development,*** Brussels, Belgium, 2011

[3]. Kruse C. J. – ***Environmental management at ports – a new initiative***, 14th Biennial Coastal Zone Conference, New Orleans, USA., 2005

ENERGY EFFICIENCY IMPROVEMENT OF SHIP MOTOR DRIVEN SYSTEMS. HIGH EFFICIENT MOTORS AND DRIVES

KATELIEVA ELENA

Naval Academy " Nikola Y. Vaptsarov "- Varna, Bulgaria

The purpose of this paper is to show potential measures and practices for energy savings and to give recommendations for energy efficiency improvement of ship motor driven systems. For overall energy efficiency improvement of the ship is essential for companies to implement specific energy policy and to develop an energy management plan. As the motor driven systems are the largest energy consumer on ship optimisation of the performance of these systems will provide greatest energy savings. For achieving efficiency optimization it is necessary to determine baseline data of the system, identify and implement the most appropriate measures and practices.

Keywords energy efficiency, motor driven systems, improvement

1. INTRODUCTION

Achieving energy efficiency and environmental protection are among the main goals of scientists all over the world. These issues are particularly relevant today due to global economic growth and increased energy consumption in recent decades. Maritime transport is efficient mode of transport. The increasing shiping servises requires development of various energy-saving technologies and implementation of measures to support the maritime industry in achieving fuel efficiency and reduction of greenhouse gas emissions.

The motor driven systems are the major electricity consumer in ships and optimization of their operation will lead to greatest savings. Improved efficiency of motor driven system could be achieved by applying an integrated approach - optimizing the different components as part of the overall system. Optimization of energy efficiency of the complete system requires accurate sizing of motors, pipes, end-use equipment (pumps,fans,compressors); use of high-quality electric power; high-efficiency motors,pumps,fans; variable speed drives; optimized maintenance and operation. For this purpose it is necessary to gather baseline data of the system. The next step is to identify proper measures and best practices for optimization and make the necessary calculations to determine the energy consumption with different optimization approaches. The final stage of this process includes assessment and conclusions for the improvement.

2. ENERGY EFFICIENCY OF SHIP MOTOR DRIVEN SYSTEMS

The vessel is full of a variety of mechanisms and devices that consume energy from the ship power plant. Performance of power generation system depends on ship speed, navigational area, weather conditions and ship operation. To optimize the energy efficiency of the system it is necessary to analyze load of all electrical consumers for each mode of operation. The system load information can be obtained from the load profiles through an energy audit or by theoretical research of the different ship modes: running mode; mooring with or without load operations; maneuver and emergency operation.

The ship electricity consumers form a three main groups:

- *Continuously operating* - includes all electrical loads operating continuously in the various modes.
- *Periodically operating* - includes consumers that run regularly in the various modes, and consumers operating in the expected maximum load.
- *Occasionally operating* - includes consumers that run occasionally and their power is not taken into account when calculating the system load.

The consumers can be classified for their intended purpose in the following groups: motor driven systems, radio navigation devices, lighting, electrothermal equipment and control devices. This systems include: mechanisms servicing the main engine, auxiliary engines and boiler installation; deck machinery; fans; refrigeration and air conditioning; galley consumers; workshops; lighting; auxiliary systems; radio navigational equipment.

The biggest load of ship power plant is obtained by running mode, maneuverable mode and mooring with load operations. Continuously operating consumers and those working periodically in the expected maximum load have the most significant impact on the load of the ship's power plant. They include the mechanisms servicing the main engine, refrigeration and air conditioning equipment, deck machinery, fans, which are part of ship motor driven systems.

The motor driven systems are the major electricity consumer on the ship, they includes continuously operating mechanisms with high power and have the most significant influence on the system load. The main motor driven systems are: steering; anchoring and mooring; lifting; life boat winch; motor driven systems of pumps, fans, compressors; electric tow winches; antiheeling systems. The steering electric drive systems provide control and safe navigation of the ship, they are among the most important consumers of electricity. These systems operate continuously or periodically in the different modes. The deck machinery, refrigeration and air conditioning are also consumers with high power, although operating periodically, they affect the power system loading too. The motor driven systems of pumps, fans and compressors are the most numerous and increasing their efficiency will provide the greatest energy savings.

Implementation of energy management is very important for achieving the energy efficiency improvement. Each company should develop management strategy and formulate goals and measures for energy efficiency improvement. International Maritime Organization (IMO) developed a Ship Energy Efficiency Management Plan (SEEMP). The SEEMP seeks to improve a ship’s energy efficiency through four steps: planning, implementation, monitoring, and self-evaluation and improvement. These components could be applied in improvement of the efficiency of ship motor-driven systems:

- **Planning**

During the planning process, the company must determine the baseline data of the system and review current practices and energy usage. To plan and carry out energy audits of the system. For effective management it is important to identify suitable optimization measures and determine main goals. It is necessary to develop implementation plan and choose monitoring method. The company should make the necessary calculations to compare different measures and demonstrate potential cost savings.

- **Implementation**

On this stage upon completion of the planning the operator should make implementation of the most appropriate measures and practices. It is important record-keeping for each measure.

- **Monitoring**

This stage includes continuous and consistent data collection. The company should verify the savings with measurements, assess implementation and effectiveness of measures, and system's operation. There are different software tools that can be used to estimate savings and compare actual with calculated savings.

- **Self-evaluation and improvement**

This is the final stage in the energy efficiency management cycle when each measure can be assessed and the results apply into the next improvement cycle.

Energy efficiency of the system relates the amount of energy used to useful work or number of units manufactured [1]:

$$E_{system} = \frac{system\ output}{total\ \ power\ input} = \frac{units\ \ produced}{\left[power\ required\ / \left(E_{components} \times F_{system\ effect\ \ factor} \right) \right]} \tag{1}$$

, where $E_{components}$ is component's efficiency in the system;
$F_{system\ effect\ factor}$ is a multiplier that reflects the sum of friction and other losses of the distribution system.

To achieve the overall optimization of the energy efficiency of the drive system is necessary to increase the efficiency of each component of the system: motor, gears, end-use equipment and control mechanisms and devices.

The total system efficiency can be represented as the product of the efficiencies of each component in the motor-driven system:

$$E_{system} = E_{motor} \times E_{gear} \times E_{drive} \times E_{end-use\ equipment} \tag{2}$$

The main areas for optimization of the motor driven systems are as follows:

Electric power quality

- Maintain voltage levels - with a maximum deviation of 5% from the nameplate value
- The voltage phase balance should be within 1%
- Maintain high power factor - installing capacitors
- Detection and reduction of energy transmission losses

Motor optimization

- Use of high - efficient motors
- Selection of proper motor size
- Implementation of regular diagnostics and predictive maintenance
- Implementation of an optimized operation

Optimization of transmission and control mechanisms

- Use of variable speed drives and controllers
- Use of more efficient couplings and pipes

Optimization of end-use equipment

- Use of high-efficient pumps,fans,compressors
- Implementation of diagnostics and adequate maintenance

- Implementation of an optimized operation
- Eliminate unnecessary uses

Combining the most appropriate measures according to the characteristics of the process would provide improved system efficiency and save significant amounts of energy.

3. HIGH EFFICIENT MOTORS AND DRIVES

3.1 Motor Efficiency

An essential component of the drive system is the electric motor, which is necessary to operate with high efficiency. The most common type of motors in ship drive systems are squirrel cage induction motors. When it is underloaded the power factor of the system decreases and the motor consumes more reactive power. Therefore, according to the specific conditions and requirements it is necessary to ensure the optimal design and parameters of the motor and optimal control. It is necessary to select proper motor size according to the requirements of the motor driven system and to calculate all of the operating costs.

In order to identify the most appropriate measures for efficiency optimization it is necessary to determine the parameters and to analyse motor performance. When analysing a motor's performance it is useful to collect motor data (Table 1) and to determine both the motor load and efficiency.

Table 1: Motor data collection

N^0	Motor type	Motor Tag No.	P, kW	U, V	I, A	Speed (RPM)	Power Factor	Motor efficiency	Insulation Class	Year of manufacture	Manufacturer
1											
2											

$$ML = \frac{input\ motor\ power[kW]}{rated\ motor\ power[kW]}.100,[\%] \quad (3)$$

where the input power is $P_1 = \sqrt{3}.I.U.\cos\varphi/1000,[kW]$ (4)

I - line current, [A];
U – line voltage, [V];
cosφ - power factor

and the rated power is $P_{1r} = \dfrac{P_{2r}}{\eta_r},[kW]$ (5)

P_{2r} – rated output power (nameplate), [kW]
η_r – motor efficiency at full-rated load (nameplate), [%]

- **Motor efficiency analysis**

$$\eta_m = \frac{P_{2r}.ML[\%]}{P_1},[\%] \quad (6)$$

η_m - motor efficiency, [%];
ML - motor load, [%];

P_1 – input motor power, [kW];
P_{2r} - rated output power (nameplate), [kW]

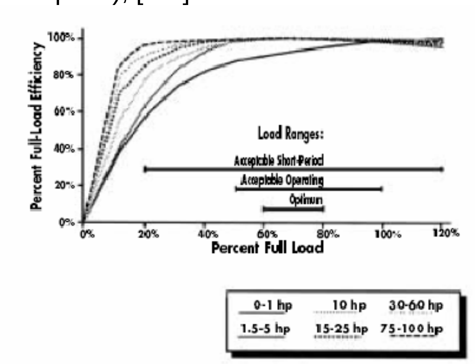

Fig. 1. Motor efficiency as function of % full load (US DOE)

There is connection between motor load and efficiency (Fig.1.). The efficiency of motors typically peaks near 75% of full load and is relatively flat down to the 50% load point [5]. According to results of motor's assessment could be recommended strategy for energy efficiency optimization.

As electricity costs typically account for approximately 95% of the lifetime motor costs [3], it is important to ensure efficient motor operation. Implementation of regular diagnostics and appropriate maintenance will provide safely and effective motor performance. The motor failure detection provide different opportunities for efficiency improvement – repair, right-sizing, replacement with standard or more efficient motor. It is necessary to assess the different options available, taking into account prices, the implementation time and future saving possibilities.

Rewinding could provide efficiency at previous levels, but sometimes results in rising losses, and reducing reliability and efficiency. It is usually best to replace fail small size (low power) and old previously rewound motors by new high-efficient. If the rewind cost exceeds 50% of a new energy-efficient motor price,it is better to buy new motor. Some operators hesitate to replace old motors because the capital cost of a new high efficient motor usually exceeds the cost of repairing the old one, that's why it is important to assess the cost of power they consume. In most cases this replacement results in significant energy and cost savings and would pay back motor's purchase price for a short period.

For replacement operators could implement permanent magnet or high-efficiency induction motors (efficiency class EFF1 or NEMA Premium® efficiency motor).

The most common permanent magnets motors are with magnets made from alloys of rare metals ($Nd_2Fe_{14}B$; Sm-Co), they have denser magnetic fields than those of conventional machines and as a result, weight and size are significantly reduced. These motors have reduced excitation losses, a higher efficiency and increased reliability. Combined with variable speed drives they are more energy efficient than conventional AC induction motors.

Improved design, materials, and manufacturing techniques enable energy-efficient motors to accomplish more work per unit of electricity consumed. There are different clasifications in the European Union and in the United States. The European Scheme to designate energy efficiency classes for low voltage AC motors established through cooperation between CEMEP(European Committee of Manufacturers of Electrical Machines and Power Electronics) and European Commission has been in operation since 1999. The motors included in this scheme are three phase AC squirrel cage induction motors in the range 1.1 to 90kW, having 2- or 4- poles, rated for 400V line, 50Hz, S_1 duty class, in standart design (Design N according to EN 600 34-12 and EN 50347) [2]:

Table 2: Efficiency of different class of motors

kW	EFF 3 2p = 2;4; η_n [%]	EFF 2 2p = 2;4; η_n [%]	**EFF 1 2p = 2 η_n [%]**	**EFF 1 2p = 4 η_n [%]**
1,1	< 76,2	≥ 76,2	**≥ 82,2**	**≥ 83,8**
1,5	< 78,5	≥ 78,5	**≥ 84,1**	**≥ 85,0**
2,2	< 81,0	≥ 81,0	**≥ 85,6**	**≥ 86,4**
3	< 82,6	≥ 82,6	**≥ 86,7**	**≥ 87,4**
4	< 84,2	≥ 84,2	**≥ 87,6**	**≥ 88,3**
5,5	< 85,7	≥ 85,7	**≥ 88,6**	**≥ 89,3**
7,5	< 87,0	≥ 87,0	**≥ 89,5**	**≥ 90,1**
11	< 88,4	≥ 88,4	**≥ 90,5**	**≥ 91,0**
15	< 89,4	≥ 89,4	**≥ 91,3**	**≥ 91,8**
18,5	< 90,0	≥ 90,0	**≥ 91,8**	**≥ 92,2**
22	< 90,5	≥ 90,5	**≥ 92,2**	**≥ 92,6**
30	< 91,4	≥ 91,4	**≥ 92,9**	**≥ 93,2**
37	< 92,0	≥ 92,0	**≥ 93,3**	**≥ 93,6**
45	< 92,5	≥ 92,5	**≥ 93,7**	**≥ 93,9**
55	< 93,0	≥ 93,0	**≥ 94,0**	**≥ 94,2**
75	< 93,6	≥ 93,6	**≥ 94,6**	**≥ 94,7**
90	< 93,9	≥ 93,9	**≥ 95,0**	**≥ 95,0**

There is software tool used for energy cost savings calculation, it is EuroDEEM database. This software provides a list of energy efficient motors and practices for optimization of whole motor system. The US Department of Energy (DOE) also publishes a free software tool - MotorMaster+, that can be used to estimate savings associated with motor replacement and repair.

Consortium for Energy Efficiency (CEE) is an award-winning consortium of efficiency program administrators from the United States and Canada, which establishes efficiency tiers at levels that exceed federal minimum requirements for appliances and equipment. Since December 19, 2010 new federal minimum requirements for 1-200 hp and 201-500 hp general purpose motors became NEMA (National Electrical Manufacturers Association) MG 1Table 12-12, equal to NEMA Premium® efficiency levels[3].

High efficient motors ensure lower operational and maintenance costs and relatively short payback periods. Rotor losses in high efficient motors are reduced by decreasing the degree of slip. This is accomplished by increasing the mass of the rotor conductors, increasing their conductivity, and increasing the total flux across the air gap between rotor and stator. [4] High efficient motors are made to higher manufacturing standards and with quality materials than the old standard motors they are meant to replace. In the most cases this replacement results in significant energy and cost savings and improved reliability.

With the following equations we could calculate potential energy and cost savings from this replacement [3]:

$$AnnualEnergySavings = P_{2r} \times ML \times T \times \left(\frac{1}{\eta_{EFF3}} - \frac{1}{\eta_{EFF1}} \right), [kWh] \quad (7)$$

where P_{2r} is rated output power (nameplate), [kW];
ML - motor load, [%];
T - annual operating time(hours), [h]
η_{EFF3}, η_{EFF1} - efficiency of standart and high efficient motor, [%];

$$AnnualCostSavings = P_{2r} \times ML \times T \times \left(\frac{1}{\eta_{EFF3}} - \frac{1}{\eta_{EFF1}} \right) \times C_E \text{, [€]} \tag{8}$$

where C_E is the electricity cost, [€/kWh]

Potential energy demand savings could be calculated with next equation[3]:

$$Energy\,Demand\,Savings = \left(\frac{P_{2r}}{\eta_{EFF3}} - \frac{P_{2r}}{\eta_{EFF1}} \right) \text{, [kW]} \tag{9}$$

3.2. Drives

The motor control is an important factor for achieving higher efficiency and reduction of power consumption of the system. The drives are devices used for operation control of the motor driven systems. There are hydraulic, mechanical and electromechancial devices (dampers, throttles and bypasses) that alter the operational speed for the applied load when the motor operates at constant speed. More efficient is VSD technology - devices that control the frequency and voltage of electric power supply of an AC induction motors. A VSD (Variable Speed Drive), also known as a ASD (Adjustable Speed Drive), VFD (Variable Frequency Drive) or Inverter offer very precise motor speed and torque control according to the process requirements. By implementing VSD a very close match between motor speed and application requirements could be achieved. In many applications variable speed control can lead to a substantial reduction in energy use.

AC drives that use Pulse Width Modulation (PWM) provide higher efficiency of the system. VSD of an AC induction motors basic design consists of four elements: Diode bridge rectifier; Intermediate DC circuit; Inverter and Control unit:

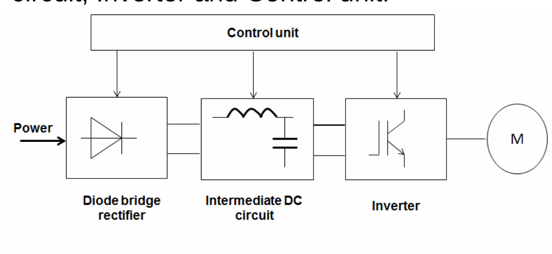

Fig. 2. Variable speed drives

The rectifier changes the incoming alternating current (AC) supply to direct current (DC). In the intermediate DC circuit, the DC voltage is filtered in a LC low-pass filter. The inverter converts the rectified and conditioned DC back into an AC supply of variable frequency and voltage. The control unit controls the whole operation of the VSD. Output frequency and voltage is controlled electronically by controlling the width of the pulses of voltage to the motor. Different types of semiconductor switches are used (MOSFET, IGBT, power bipolar transistors) to create the output, the most common being the Insulated Gate Bipolar Transistor (IGBT), which is designed to turn on and off rapidly. The IGBT combines the simple gate-drive characteristics of the MOSFETs with the high-current and low-saturation-voltage capability of bipolar transistors.

VSDs with PWM have the potential to make energy savings and increase profitability of the system.

Variable torque loads are typical of centrifugal fans and pumps and have the largest energy saving potential. This is shown by “Affinity laws” [1]:

$$Q_2/Q_1 = n_2/n_1;\ p_2/p_1 = (n_2/n_1)^2;\ P_2/P_1 = (n_2/n_1)^3 \tag{10}$$

These engineering laws show how changes of speed (n), will affect to the flow(Q), pressure(p) and power consumption(P) in the system.

For estimation of Pump system - for example using a VSD to control the flow rate from a pump rather than using simple throttle control can result in large power and cost savings.

With the following equation could be calculated potential savings for motor driven system with VSD according to the "Affinity laws"[3]:

$$Annual\,EnergyCost = \frac{P_{2r}}{\eta_{EFF1}} \times ML \times T \times n^3 \times \frac{1}{\eta_{VSD}} \times C_E \quad , [€] \tag{11}$$

where η_{VSD} is efficiency of VSD, [%];
n - % full rated speed

To assess optimization of the system associated with implementation of VSD instead of standart system with throttling valve is next equation:

$$Annual\,EnergySavings = Annual\,EnergyCost(\text{Throttling Valve})\text{-}Annual\,EnergyCost(VSD) \tag{12}$$

Potential energy demand savings for Pump system with VSD could be calculated with next equation[3]:

$$Energy\,Demand\,Savings = \frac{P_{2r}}{\eta_{EFF1}} \times ML \times \left[n_{motor}^3 - \frac{n_{drive}^3}{\eta_{VSD}} \right] \quad , [\text{kW}] \tag{13}$$

VSD technology is more efficient than any other devices used for operation control of the motor driven systems.

4. CONCLUSIONS

The standard motor driven systems could be optimized by increasing the overall efficiency - use of properly sized and energy efficient motors, inverters, more efficient couplings, pipelines and end-use equipment. Implementing energy efficiency management practices could reduce energy consumption, operational and maintenance costs. By collecting baseline data of the system, studying all possibilities for improvement and costs for implementation it is easier to choose the most appropriate energy management strategy. Lower energy consumption, fuel saving and emissions reduction would provide optimization of energy efficiency of ships and environmental protection.

REFERENCES

[1]. Canadian Industry Program for Energy Conservation(CIPEC) - ***Energy-Efficient Motor Systems AssessmentGuide***, http://oee.nrcan.gc.ca/sites/oee.nrcan.gc.ca/files/pdf/publications/industrial/2003-661 motor-system-e.pdf
[2]. CEMEP, European Commission joint research centre - ***Electric motor efficiency,Saving Europe's Energy and Environment***, http://iet.jrc.ec.europa.eu, 2003
[3]. Consortium for Energy Efficiency Inc.,- ***Motor Efficiency, Selection, and Management A Guidebook for Industrial Efficiency Programs***, http://www.motorsmatter.org, May 2011,
[4]. The Copper Development Association Inc.,- ***Introduction to Premium Efficiency Motors***, http://www.copper.org/environment/sustainable-energy/electric-motors/education/motor_text.html
[5]. US Department of Energy (US DOE).- ***Fact Sheet:Determining Motor Load and Efficiency***.Developed as part of: Motor Challenge, a program of US DOE, http://www1.eere.energy.gov/industry/bestpractices/pdfs/10097517.pdf

A THEORETICAL ANALYSIS OF A VAPOR COMPRESSION SYSTEM ON ENVIRONMENTAL AND THERMODYNAMIC BASIS

MEMET FEIZA

Constanta Maritime University, Romania

Most of ships worldwide currently use as working agent hydrofluorocarbon R134a (HFC-134a) in direct expansion refrigeration systems. International concern forces shipping sector to use refrigerants with low value of GWP (Global Warming Potential), an index comparing the climate impact of an emission of a greenhouse gas relative to that of emitting the same mass of carbon dioxide.
The widespread refrigerant on board the ships, R134a, has a 100-year GWP=1300, while its possible alternative, the hydrofluorocarbon R152a (HFC-152a) has a GWP=140. Starting from the environmental benefit shown by R152a, a thermodynamic comparison between R134a and R152a is made in this paper. Results will indicate the opportunity of the substitution.

***Keywords**:* refrigerant, environment, evaporation temperature

1. INTRODUCTION

R134a is commonly used in vapor compression systems on board the ships since has almost same thermodynamic properties as R12 (the traditional refrigerant for old ships) and a zero ODP (Ozone Depletion Potential).

But because of its high GWP (Global Warming Potential), there is a need to find its alternatives from thermodynamic and environmental points of view. This situation is reached by different stages.

Between 1830-1930, the first refrigerants in use where chosen by their availability, despite their drawbacks, like toxicity and flammability.

In the next stage, till 1990, refrigerant selection was also according safety criteria, while during the third stage (1990-2010), environmental criteria (translated by ODP) was introduced in the selection.

In present time, a refrigerant should not contribute to global warming, ozone layer depletion, should be efficient from energy point of view, non flammable, non toxic, stable, available on the market and cheap.

The environmental concern, when talking about refrigeration, is one of international level. The first symptom was the care about the ozone layer, the layer which protects the Earth from ultraviolet rays.

Ozone Depletion Potential is assessed on a scale that use CFC-11 as a benchmarck. All other components are based on the level they harm the ozone layer in relation to CFC-11.

Lately, global warming is also considered. It is expressed by the increase in global earth surface temperature, generated by the absorption of infrared emission from surface of Earth. This indicator is evaluated on a scale that uses CO_2 as the benchmarck.

World wide concern regarding the above is found in regulations. Montreal Protocol

(1987) established the requirements that initiated phase-out of chlorofluorocarbons (CFCs), in developed countries production of CFCs being phased-out since 1st of January, 1996, while production in developing countries being phased-out later (2010). Kyoto Protocol aims on phasing-out the substances contributing to global warming.

R-134a is a refrigerant belonging to this type of substances because the increased emissions of R-134a to the atmosphere are constant increasing the concentration of greenhouse gases through leaks and more over, in an indirect manner, via energetic performance of the system.

As a consequence, R-134a will be phase-out in the future, specialists being already in the search af substitutes. This paper is discussing the opportunity of replacing R-134a with R-152a. The analysis is based on the properties comparison, being useful the table bellow.

Table 1. Properties of the considered refrigerant

Refrigerant	R-134a	R-152a
Chemical name and formula	Tetrafluorethan $C_2H_2F_4$	Difluorethan $C_2H_4F_2$
Molecular weight (g/mol)	102	66
Critical temperature (^oC)	101,1	113,3
Critical pressure (MPa)	4,06	4,52
Boiling point (^oC)	–26,1	–24,0
Flammability limit (LFL)	NF	3,7
ODP	0	0
GWP (100 years)	1300	140

2. THEORETIC BASIS

The vapor compression refrigeration system uses a refrigerant in liquid state as a medium which absorbs and removes heat from a space needed to be cooled and subsequently rejects that heat elsewhere.

Such a system has four main components: a compressor, a condenser, an expansion valve and an evaporator, as seen in Figure 1.

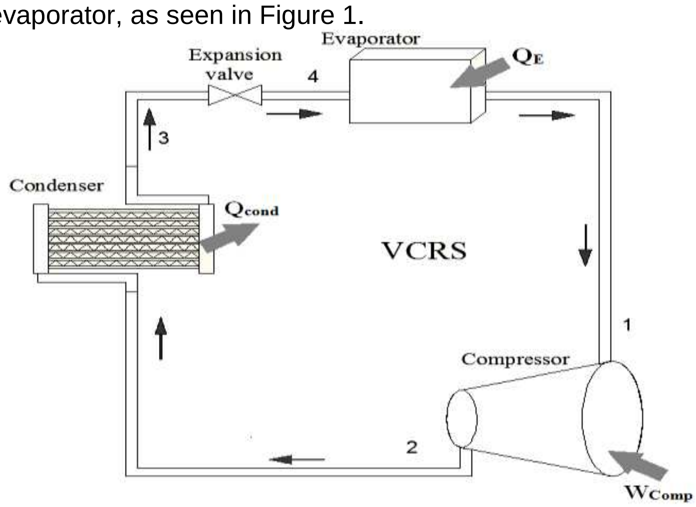

Fig. 1. Basic vapor compression system

Circulating refrigerant in saturated vapor state enters in the compressor where it is compressed to a higher pressure, getting also a higher temperature. Resulted vapors are led to the condenser where are cooled and condensed, the refrigerant releasing heat to the sea water.

The condensed liquid refrigerant (saturated liquid) is passed through the expansion valve, suffering a reduction in pressure. The pressure reduction results in the adiabatic flash evaporation of a part of the liquid refrigerant.

The auto refrigeration effect of the adiabatic flash evaporation decreases the temperature of the liquid and vapor refrigerant mixture to where it is colder than the temperature of the closed space needed to be refrigerated.

This cold mixture is then directed to the evaporator. The air from the space is cooled by the evaporation of the liquid part from the cold refrigerant mixture. The refrigerant vapor resulting from the evaporator is in saturated state again; it will be led to be compressed and the cycle repeats.

The compressor discharge temperature is calculated with:

$$T_2 = T_1 + \frac{\left(T_{2\,ISO} - T_1\right)}{\eta_{ISO}} \tag{1}$$

The volumetric efficiency of the compressor is found with the formula bellow, where C is clearance ratio:

$$\eta_{vol} = 1 + C + C\left(\frac{p_2}{p_1}\right)^{1/n} \tag{2}$$

The mass flow rate of the refrigerant is given by:

$$m_r = \frac{V_{st} N \eta_{vol}}{v_1} \tag{3}$$

where:

V_{st} – stoke volume, cm^3

N – speed, rpm.

The pressure ratio is calculated with:

$$\beta = \frac{p_{cond}}{p_{evap}} \tag{4}$$

The isentropic work input to the compressor is given by:

$$P_{CS} = m_r\left(h_2 - h_1\right) \quad \left(kJ / s\right) \tag{5}$$

where:

m_r – refrigerant mass flow rate, kg/s
h – enthalpy, kJ/kg.

The actual compressor work is found involving the isentropic efficiency (η_s):

$$P_C = P_{CS} / \eta_s \tag{6}$$

The amount of heat rejected by the condenser is given by:

$$Q_{cond} = m_r (h_3 - h_2) \quad (kJ/s) \tag{7}$$

The amount of heat absorbed in the evaporatorr is calculated as:

$$Q_{evap} = m_r (h_1 - h_4) \quad (kJ/s) \tag{8}$$

The volumetric cooling capacity is found with:

$$VCC = \frac{(h_1 - h_4)\eta_{vol}}{v_1} \quad (kJ/m^3) \tag{9}$$

Considering the first law of thermodynamics, COP (Coefficient of Performance) expresses the performance of the refrigeration cycle, and is evaluated with the ratio:

$$COP = \frac{Q_{evap}}{P_C} \tag{10}$$

3. RESULTS AND DISCUSSION

Table 2 presents the saturation pressure for R-134a and R-152a in order to have a conclusion from operating pressure point of view. Since R-152a has a saturation pressure close to the one of R134a, regarding the considered range of operating temperatures results that it can be used as a drop in substitute.

Table 2. Comparison of saturation pressures

Temperature (°C)	**–20**	**0**	**20**	**40**	**60**
Pressure (MPa) for R-134a	0,1327	0,2928	0,5717	1,0166	1,6818
Pressure (MPa) for R-152a	0,1206	0,2639	0,5129	0,9092	1,5007

Figure 2 shows the variation of refrigerant temperature at the exit of the compressor related to evaporation temperature.

Compressor's discharge temperature is a reflection of what is going on inside the compressor. Compressor discharge temperature must be monitored and kept limited, otherwise the system may start to fail worn rings, acid formation and oil breakdown; also compressor puts more work for high values of discharge temperature.

It is seen that this temperature is decreasing with the increase of evaporation temperature; also, R-152a presents lower values for the discharge temperature than R-134a.

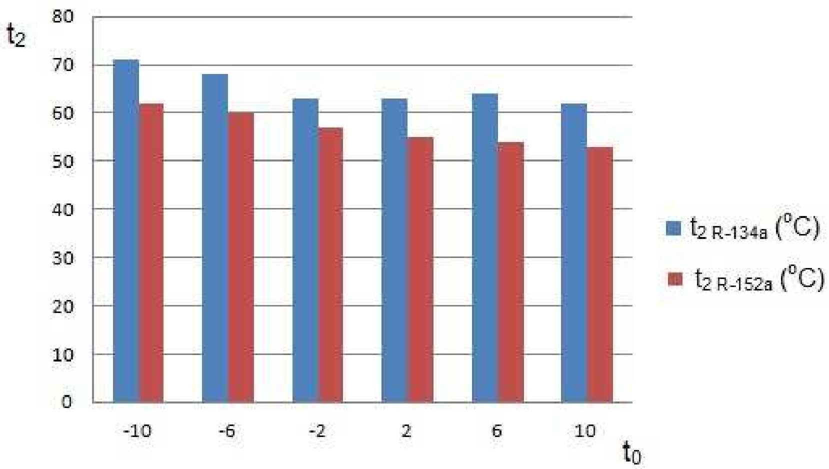

Fig. 2. Discharge temperature (t_2) versus evaporation temperature (t_0)

Figure 3 shows the variation of pressure ratio related to evaporation temperature. The higher the compressor ratio, the higher the compressor's discharge temperature will result. This situation occurs because more heat of compression will be generated when compressing the refrigerant vapor through a higher pressure range.

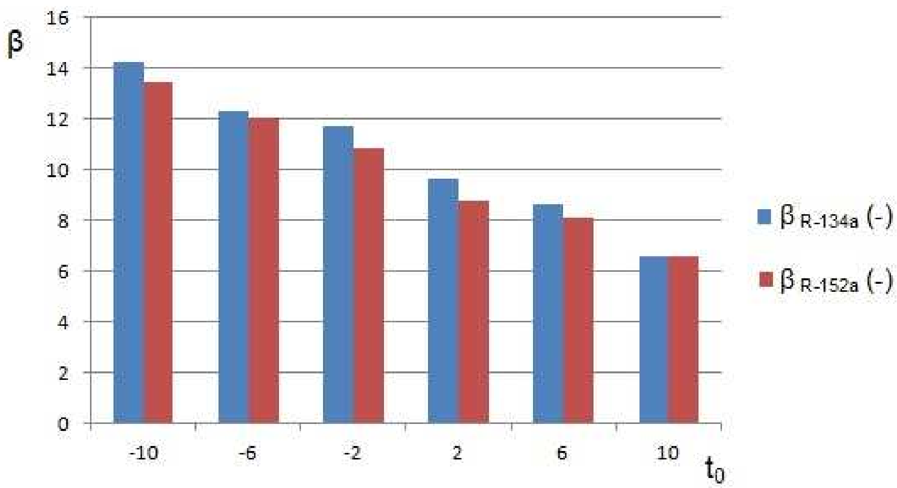

Fig. 3. Pressure ratio (β) versus evaporation temperature (t_0)

Comparison shows that pressure ratio decreases with the increase of evaporation temperature. R-152a shows slightly lower values for this ratio.

Figure 4 presents relation between condenser heat load and evaporation temperature. The purpose of the condenser is to release heat and change the state of the refrigerant from vapor into liquid.

Even if values obtained for R-152a are closed to the one for R-134a, they resulted slightly lower. Values of condenser heat load are increasing with the increase of the evaporation temperature.

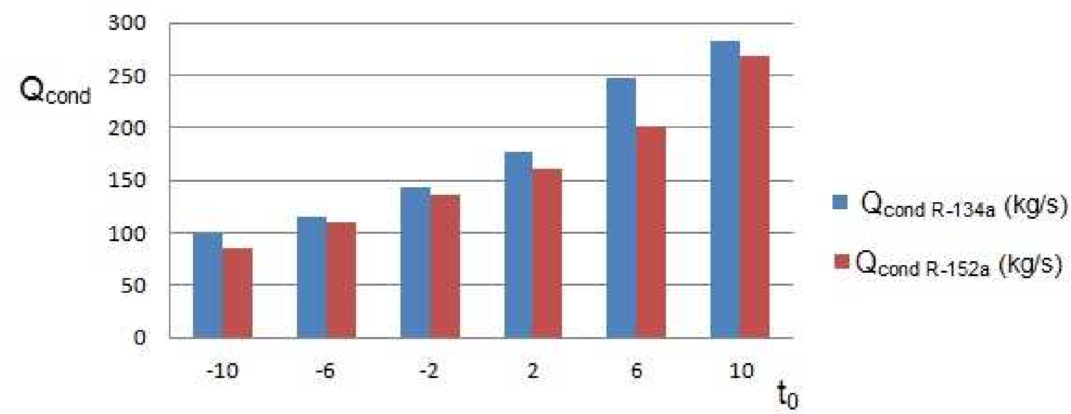

Fig. 4. Condenser heat load (Q_{cond}) versus evaporation temperature (t_0)

Figure 5 shows variation of the input power required by the compressor with the evaporation temperature. This is the input power required to run the compressor motor at a specific operating point. The compressor input power is a critical parameter which is recommended to be monitored continuously during operation. It is also important for the system efficiency determination.

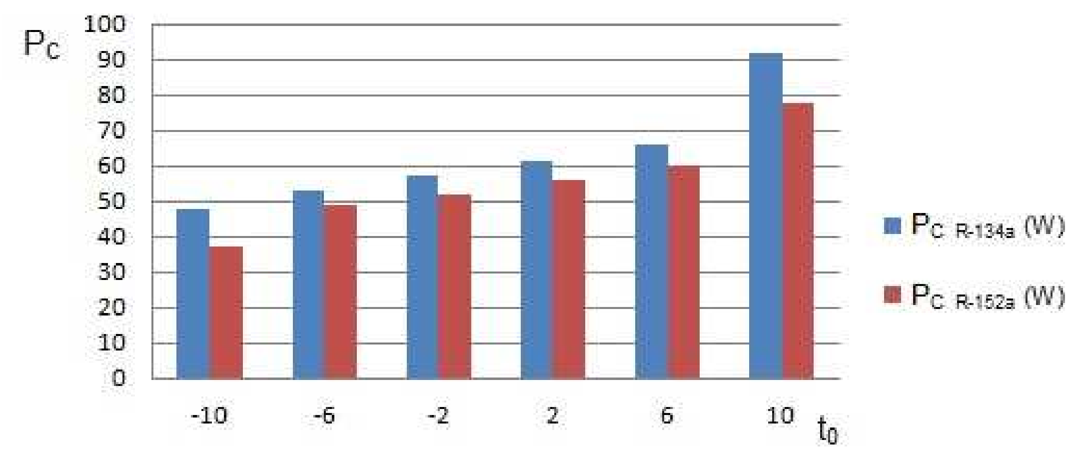

Fig. 5. Compressor input power (P_C) versus evaporation temperature (t_0)

Values of this power increase together with the increase of evaporation temperature, but the ones obtained for R-152a are lower than the ones belonging to R-134a.

Figure 6 shows variation of volumetric cooling capacity with evaporation temperature. These values increase with the increase of evaporation temperature. Values resulted for the two refrigerant are close. Similar VCC means no change in compressor size. Still, VCCs for R-152a are higher, an increase in VCC leading to a decrease in compressor size.

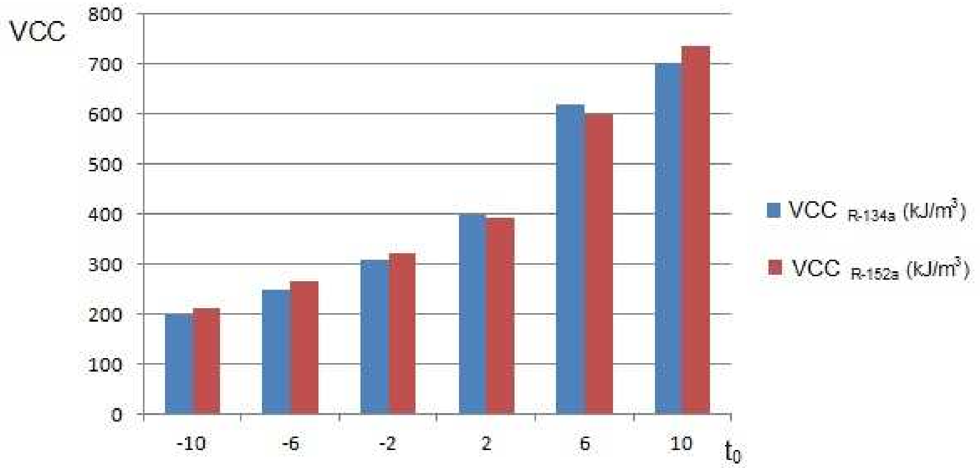

Fig. 6. Volumetric cooling capacity (VCC) versus evaporation temperature (t_0)

Figure 7 depicts relation between the performance of the system and evaporation temperature. The Coefficient of Performance increase with the increase of evaporation temperature. R-152a shows a better performance than R-134a.

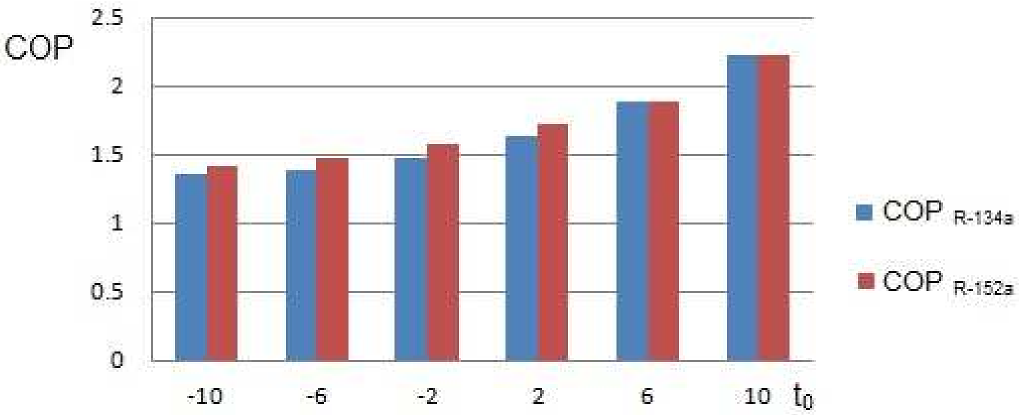

Fig. 7. Coefficient of Performance (COP) versus evaporation temperature (t_0)

4. CONCLUSIONS

The theoretical assessment developed in the paper showed that R-152a presents an environmental behavior; except its flammability, R-152a is a potential substitute of R-134a in vapor compression refrigeration systems. From operating pressure point of view, R-152a shows saturation pressures close to R-134a.

The thermodynamic comparison between R-134a and R-152a showed that R-152a presents lower values for the discharge temperature and pressure ratio, comparable values for the condenser heat load, but lower values for the compressor input power; volumetric cooling capacity values are similar. In the considered temperature range, R-152a shows a better energetic performance for lower evaporation temperatures.

REFERENCES

[1]. Bolaji B.O., Akitude M.A., Falade T.O. – ***Comparative analysis of performance of three ozone – friends HFC refrigerants in a vapour compression refrigerator,*** Journal of Sustainable Energy and Environment 2, pp 61-64, 2011

[2]. Gaurav, Kumar R. – ***Alternatives to R-134a (CF_3CH_2F) refrigerant – A review,*** Proc. Of the National Conf. On Trends and Advances in Mechanical Engineering, pp 73-77, 2012, Faridabad, Haryana

[3]. Ghodbane M. – ***An investigation of R-152a and Hydrocarbon refrigerants in mobile air conditioning,*** SAE Technical Papers, International Congress and Exposition, Detroit, pp 1-16, 1999

[4]. Mohanraj M., Jayaraj S., Muraleedharan C. – ***Comparative assessment of environment friendly alternatives to R-134a in domestic refrigerators,*** Energy Efficiency, No.1, pp 189-198, 2008

[5]. Paroche K., Gupta R.C. – ***Performance analysis of reciprocating compressor using eco-friendly refrigerants,*** VSRD Int. Journal of Mechanical, Automobile and Production Engineering, vol 2, No.9, pp 320-329, November 2012

[6]. Thangavel P., Somasundaram P., Sivakumar T., Kumar C.S., Vetriselvan G. – ***Simulation analysis of compression refrigeration cycle with different refrigerants,*** Int. Journal of Engineering and Innovative Technology (IJEIT), Vol 2, Issue 10, pp 127-131, April 2013

INDUCED MARITIME ACCIDENTS & SLOW SHIPPING

[1]MONTES DE OCA R, REYNALDO, [2]MARTÍNEZ MARÍN JESÚS E.

[1]Universidad Marítima del Caribe(Venezuela), [2]Universitat Politècnica de Catalunya & Rideport, Spain

Maritime accidents, share some factors already considered by the International Maritime Organization (IMO) and the researchers of the maritime world. The accelerated technological's changes, has allowed significant improvement of human activities, in many cases, improving the effectiveness and efficiency in the majority of the fields, of which marine transport is not the exception. Unfortunately in some cases, new technologies have led to relaxation in safety, so the idea to establish some minimum parameters, it is essential to ensure the safety of human life at sea, for increase the prevention of accidents and protection maritime environment.

***Keywords**:* Maritime Accident, Pollution Prevention, Induced accident, Slow shipping

1. INTRODUCTION

The International Maritime Organization, IMO, in Resolution MSC.255(84) (OMI, 2010) establish that a marine casualty means an event, or a sequence of events, that has resulted in any of the following which has occurred directly in connection with the operations of a ship:

1. the death of, or serious injury to, a person; .
2. the loss of a person from a ship; .
3. the loss, presumed loss or abandonment of a ship; .
4. material damage to a ship; .
5. the stranding or disabling of a ship, or the involvement of a ship in a collision;
6. material damage to marine infrastructure external to a ship, that could seriously endanger the safety of the ship, another ship or an individual;
7. severe damage to the environment, or the potential for severe damage to the environment, brought about by the damage of a ship or ships.

However, a marine casualty does not include a deliberate act or omission, with the intention to cause harm to the safety of a ship, an individual or the environment.

2. DISSEMINATION OF ACCIDENTS

In regard to the public knowledge of these accidents, previously, cases such as Titanic, took more time to be disclosed, however at the present time, cases such as Prestige or Costa Concordia, among others, they do so in real time, which promotes a reaction of the public opinion more swift and forceful, and that joined with the maritime transport system supports to a large extent the life forms of humanity, whose international trade is transported by more than 90 %, by sea (International Shipping and World Trade) some 8408 million tons of various loads transported in 2010 (UNCTAD Review of Maritime Transport 2011, p.7) on board of 104304 = >100 GT merchant propelled ships, highlights the fact that this is not a system of which we can dispense with, and therefore it is essential to know the causes that motivate the marine casualties to minimize its recurrence.

This core activity of the maritime transport has been adapting to commercial and technological requirements, transforming what it in the past it was considered by society as a safe activity, to an insecure and high-risk in the present. The modest size of the vessels of the past, in contrast to the enormous today, in themselves represent greater risk potential, either by the loss of lives and/or goods, environmental pollution, etc.

Upcoming major technological advances to the ships to reduce the consumption of fuel, the use of liquefied gas as fuel, the hull lubrication by air to decrease the friction with the sea and consequently reduce the fuel consumption. In the bridge is already normal the use of integrated systems ECDIS (Electronic Chart Display and Information System), AIS (Automatic Identification System), LRIT (Long-range identification and tracking of ships), to electronic navigational charts, new methods of tracking of vessels, among others.
These technological advances assumptions to improve maritime safety probably are activated, as they did in the past, the adaptation and balance of the safety margin accepted by the operator (Homeostasis of risk) which could compromise for a period of time, the safety.

3. FATAL STATISTICS & CASUISTRY

The maritime accidents have left huge amounts of dead, in 1820 during the winter of the North Sea, more than two thousand (2,000) ships foundered with the consequent loss of the lives of more than twenty thousand (20,000) people by then the United Kingdom (UK) adopted the Passengers Act, which led to the English Parliament to research on the causes of shipwrecks, focused on ten determinants, as the inadequate equipment, failures of construction, excess load or inappropriate assurance of the same, inadequate maintenance, incompetence of the Captain, etc. Boisson (op cit, p50). Later during 1848 France and the United Kingdom agreed to in writing the first regulating navigation at sea on the navigation lights, continuing with regulations to avoid collisions at sea. However, the reiteration of maritime accidents and multiple actions or regulations to minimize them, gender in the global maritime community, the need for their research and to identify causes and avoid as far as possible its recurrence. This has helped the international cooperation and the advent of the common ways to investigate them and in January 2010 came into force the Resolution MSC 255(84) that imposes mandatory internationally, the Code for the Investigation of Marine Casualties.

In spite of these efforts, however, the rate of losses of vessels has increased, from 1.3 in 2006 to 1.7 in 2010 (relation of ships lost/total number of vessels = >100GT) (IMO document CWGSP12/3) and the index of spills to the sea from 1970 to 2011, indicates that the 2% are product of fires or explosions, another 2% due to collisions, groundings 3 %, failure of the hull 7 %, equipment failures the 21% and surprisingly 64% of the causes of such spills, it is for another reason or the cause is unknown (annual statistics from the International Tanker Owners Pollution Federation, ITOPF's) and even more, from 1989 to 2010 were lost (totally) 4443 ships and 18189 lives as a result (UPC, 2012). (R. Montes de Oca, O.Marquez, Jesús Martínez, 2012)

4. ANALITICAL REVIEW & PROPOSALS

Faced with this concern in various branches of industry, the scientific world has produced alternating thoughts, among them as indicated by Charles Perrow in his book NORMAL ACCIDENTS (Living with High-Risk Technologies) (Perrow, 1999) which presents the theory of why accidents occur and some of them inevitably (the so-called Normal Accidents or System's Accident) due to the fact that the productive systems that builds society, are too complex and their components or parts can interact in unexpected ways by their designers or operators, thus leading to the accident. He also claims that with this new approach, it could be finalized with charges to persons and/or wrong factors, as commonly happens in the present, and also stop the attempts to repair the systems in a way that only make them more risky.

It is based on the fact that there isn't a good management of high-risk technologies, which the patient research of many disasters proves that in a certain time no one knew what was happening in reality, and even though they acted with the best practice, the results were worse. Highlights the gap between the human being and the technology (where the operator is left behind in the understanding of the given system). Perrow concludes, that the true cause of the Normal Accident is the complexity of the system because all the failures may be small in themselves and each to have a backup, but on the whole, it is their interaction (complex coordination of failures) that explains the accident, and these occur because the system is complex.

According to our interpretation of Perrow, (adding the risk homeostasis) develops this graph representing a possible sequence toward the accident (See Figure 1).

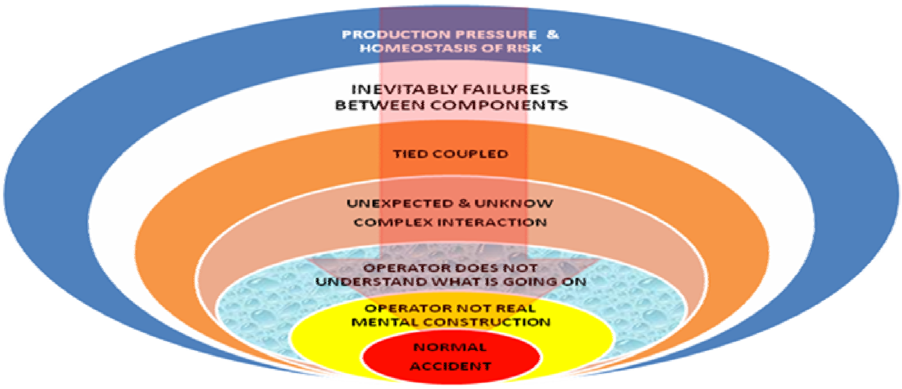

Fig. 1. Normal Accidents - Sequence Source: Author Reynaldo Montes de Oca R.

Another production of the scientific world that we might consider, in addition to Perrow, are failures of design raised by Henry Petroski (Design paradigms, case histories of error and judgment in engineering) (Petroski, 2010) or at the same time include on this vision of Petroski, modifications to the original design that might influence the failures, and negatively impacting on the couplings of some of the parts of the system before pointed out by Perrow, making them strongly bound or rigid, what would facilitate the generation of unexpected or unknown interactions. In order, we can assume the matrix of Perrow, enhanced by the vision of Petroski and this lead to the wrong mental construction of the operator and then take the wrong decision (although the operator was thought to be correct) and consequently detonate the sinister (See Figure 1).

Recalling the case of the collision in July of 1956 of passenger ships Stockholm and Andrea Doria, it might be clear to us that if the ships had not had radar, the Andrea Doria has sailed at a slower rate in the dense fog prevailing, and none of the two has produced such changes of course. In the meantime the presence of radars and detection of one each other, then the speed remained high, and in ships approximation both operators, of both bridges, generated mental images erroneous to the reality and consequently manoeuvred toward the collision, although they tried to avoid it. Resulting in loss of lives, the sinking of the Andrea Doria and considerable damage to the Stockholm.
In considering the catastrophic sinister happened to the oil tanker Torrey Canyon in March of 1967 that ran aground and break his hull with the consequent total loss of the ship and its cargo spill, generating this dreadful pollution in the waters around the semi-submerged reef Seven Stones, near the English coast.

With Dietrich Dörner´s theory (The Logic of Failure, Recognizing and Avoiding Error in Complex Situations) (Dörner) we could consider that there was the decisions of the Captain of the oil tanker, when taking an unusual route and not recommended in defeat toward the port of Milford Haven, besides accepting as true the position given by guard's Pilot in the approach to the reef, as the cause of the catastrophe.

With the theory of Henry Petroski, we might want to consider that was the modification of the physical characteristics of the ship's hull (lengthening of its length for greater load capacity) leading to this loss of manoeuvrability due to that the rudder is not restructured for the new size of the vessel, which in the end caused the incident to not be able to fall on the port side quickly and avoid the reef.

With the theory of Charles Perrow, we would consider that still so many commercial pressures and inaccuracy of the equipment that you've set up a gap in the dynamics of navigation that concluded in disaster.

It should be noted that in all theoretical scenarios of this case, the mental image wrong was present.

We can also infer that the operators of the bridge in the luxurious and ultra modern passenger ship Costa Concordia, generated, believed and decided according erroneous mental images, which allowed his ship will contact the submerged rock with the catastrophic consequences known.

Just thinking in the last three exposed cases, allows us to glimpse something prior to the act itself, had accumulated and inter linking in parallel and with the consequent reduction of the appropriate margin of safety, to the point of inducing decisions that led to the accident.
If focussing on this final phase (decision) we can get closer to the theory of Dietrich Dörner (The Logic of Failure, recognizing and avoiding error in complex situations) in which he said that we are so prone to make mistakes. Our brains are not fundamentally defective; quite simply, we have developed bad habits. When we fail to solve a problem, we do so by the tendency to make a mistake here, a small error beyond, and these accumulate, thus contributing to fail. Although he further maintains that the violation of safety standards by the operator, is due to the fact that frequently has already violated before (negative reinforcement) It is well that Dorner postulates the complexity and operational intelligence. In summary, Dorner argues that the causes of our mistakes when handling complex systems are: the slowness of our thinking and the small amount of information that we can process in a given time, our tendency to protect our sense of competence, the limited capacity of

income flow of information to our memory, and to our tendency to focus only on the immediate problems.

We have so that the human being is to some extent lags behind in the technological advances, and as a possible reaction the operator acts to balance its area of conformity / satisfaction (homeostasis of risk) which to my way of seeing is not another thing that modify the Risk (increasing), by the way of what I would call the Margin of Safety (downwards) (formerly did not have radar onboard and maintained highly careful attitude, while having them, increases the speed, or changes in direction, etc.) To this end, the proposal of the Slow Shipping to retrieve a greater margin of safety, lost through the rapid technological progress, the homeostasis of the risk in combination with the pressures of production, or in other words, keep the previous preventive attitudes (when the risk was greater without present technology) in conjunction with the positive technological advances in the decline of the risk. In this way avoiding failures (increasing the margin of safety by lowering the pressure of production with the Slow Shipping) could be generated sufficient time to adapt persons and systems to avoid errors in complex situations, which require that the design of such systems taking advantage of our natural talent of perception, presenting our attention to the precise information that we require at the exact moment.

5. THE THEORY OF THE INDUCED ACCIDENTS

This leads me to try to launch the configuration of a new theory, which I will call initially as Induced Accidents, based on the fact that accidents occur motivated to the infringement, decrease or absence of an acceptable margin of safety, generated among others due to the pressures of production, technological progress and the homeostasis of the risk. (See Figure 2).

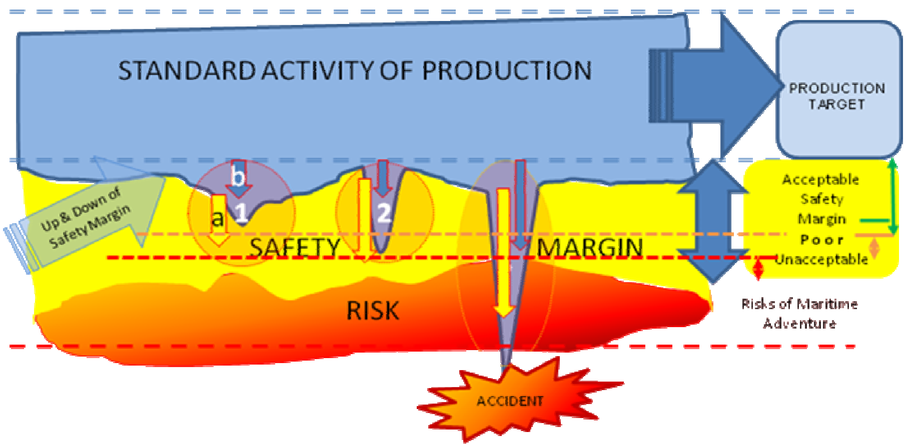

Fig. 2. Induced Accidents / Risk and Safety Margin Source. Author Reynaldo Montes de Oca R.

Margin of Safety up and down (Oscillating): Increase and decrease of margin of safety, because of technological progress and the Homeostasis to the risk of the operator, who perceive the higher margin due to technological progress, then decreases with his more risky actions.

a: Reduction of the Margin of Safety by homeostasis of the operator with the consequent increase of the Risk b: Reduction of the Margin of Safety by the increase in the pressure of production with the consequent increase of the Risk

In cases 1 and 2, the safety margin was enough to make the system will recover, while in case 3 the Homeostasis to the risk of operator in combination with a pressure increase of production, decreased the margin of safety to the point of deleting it thereby undermining the system causing the disaster.

We should increase the margin of safety, one way could be by the "SLOW SHIPPING" which means e.g. Not recklessly increase the speed or changes of heading course due to technological advances that provide us with better information than before, encourage our biological tendency to balancing our sensations, and in this case, the risk.
The technological progress makes us feel more safe and then the operator actuates until they reach the level of previous risk (highest), with the following consequences already known: Fatal Accidents, that cause damaged to the Human, to the Vessel, and very important also: To the Marine Environment.

To analyze, and open discussions on the academic's filed, having in mind the sail's experience, and also issue an study on board the vessels with the crews, will help to improve the maritime safety, knowing the human attitude with the new Technological advances.

REFERENCES

[1]. Dörner, D.-***The Logic of Failure, Recognizing and Avoiding Error in Complex Situations***. Metropolitan Books, Masachusets, USA, 211 pp, 1996
[2]. International Maritime Organization (IMO).- ***Code for the Investigation of Marine Casualties and Incidents (CIMC)***, London, 2010
[3]. International Maritime Organization (IMO).- ***Document GWGSP 12/3,*** AMSA - Meetings of the IMO Council, pp 16-17, London, 2011
[4]. Le Bureau Veritas, 1928. ***Edition du Centenaire*** , Paris, 1928
[5]. Perrow, C. -***Normal Accidents***. Princenton University Press New Jersey(NY), 1999
[6]. Petroski, H.-***Design Paradigms***. 14th ed. Cambridge University Press, New York, USA, 2010
[7]. R. Montes de Oca, O. Marquez, Jesús Martínez.- ***Inflatable Liferafts Servicing Station Maintenance Criteria***. Proc. of Maritime Transport V - Technological, Innovation and Research, Barcelona, 1298 pp, 2012
[8]. US Senate.- ***Titanic Disaster***, Government Printing Office, Washington. USA, 1912

WATER-OIL AND WATER-COAL DUST ARTIFICIAL FUELS: ITS ENERGETIC, ECONOMIC AND ECOLOGICAL BENEFITS

[1]SAJIN TUDOR, [2]BUZDUGA STEFANIA ROXANA, [3]ANITEI FLORIN

[1,2,3] *"Vasile Alecsandri" University of Bacau, Romania*

To stabilize the burning of heavy oils and coals with high content of water and reduce the pollution from the combustion installations, the fine emulsions of water in heavy oil and the fine suspensions of coal dust in water are prepared. Thus, from natural fuels with high water content are obtained artificial liquid fuels with water in excess, which improves some economic, energetic and ecological indicators of burning process. In principle, these fuels can be adapted for the utilization in the energetic installations off marine ships.This paper presents the economic, energetic and ecological indicators of combustion of water-oil emulsions and water-coal dust suspensions on a test installation.

Keywords*:* water-oil emulsion, water-coal dust suspension (water coal thick liquid), water content, energy, economic and ecological indicators of burning process.

1. INTRODUCTION

The burning of water-oil emulsions (WOE) in the stationary cauldrons of the thermo and thermo-electric plants has given positive results.

So, in Germany, on using the 82E ultrasonic emulgator they succeeded in obtaining a cauldron efficient 2,5-4,3% bigger than in its absence, the content of water in the fuel oil being of 4-5%. This has been possible based on the reduction of the excess air 1-2%, of the chemical imperfections of the burning with 0,1-0,5%, of the heat loss with the evicted gases and the deposits on the heating surface with 1,0-2,5% [1].

In Italy they are exploiting more than 1000 plants for the burning of WOE. The analysis of its functioning has proven that there is a reduction of 80-90% in the formation of incomplete burning products. Moreover there are fuel oil savings of up to 3-5% [2].

The carried out experiments at some thermo-electric plants in the Russian Federation have shown that using WOE with a water content of 15-20% allows an economic effect of 2 mil. ruble/year, taking into consideration the reduction of up to 30-35% in the a nitrid oxide emissions, with up to 70-80% of the black coal and with 80-90% of the benz (a) pyrene [2].

In the result of the study of the WOE burning in the cast iron cauldron, the annual economy of fuel per cast iron cauldron has been of 16 tons of conventional fuel [3].

Currently, internationally, many countries have provided a growing interest in water-coal dust suspension (WCDS), as a liquid type of fuel on base of coals, going up to commercially development of technology.

Thus, China a country rich in coal resources, but poor in oil, has the share of fuel consumption, about one third oil, which prompted a strong interest in research and in large-scale implementation of the WCDS in energy and metallurgy industries, build five installations for the WCDS with an annual capacity of 85,000 tons. WCDS was successfully tested and operated in different power plants for energy, and industrial furnaces used in petrochemical, chemical and metallurgical industries. However, during the handling and the storage, was found that WCDS stability is influenced by coal, leading to a limited use [4].

Russia is among the countries directly concerned by this technology and has a positive experience in production, transportation and burning of WCDS [5].

In the U.S., studies on the spraying and burning of WCDS at commercial level was started in 1980. Combustion of water-coal dust suspension was made in several coal combustion plants, one of the tests being conducted for 35 days in Memphis, in 1983, demonstrating that the WCDS can be used safely while watching and behavior the long-term use [6].

In Canada, the first significant research for the preparation and firing of WCDS were started in 1982 as a result of cooperation of two companies: New Brunswick Electric Power Commission and Cape Breton Corporation [6].

The Swedish company Svenska Fluidcarbon prepared and fed with WCDS three boilers, two with a capacity of 10 MWe and 6 MWe. WCDS has been used in a regional heating Sundyberg for 2,000 hours, thus proving its willingness to replace traditional fuels in combustion boilers [6].

2. ECONOMIC, ENERGETIC AND ECOLOGICAL INDICATORS OF THE WOE BURNING PROCESS

As compared to the traditional anhydrous fuel, the use of WOE as energetic fuel is conditioned by the following advantages:

1) at optimum values of the water content from the emulsion (10-15%) and of the finesse of the dispersion phase the energetic and economic factors of the burning process are improved: WOE burns faster; the increase of the effective power of the furnace or the cauldron is of over 4%; on burning WOE there can be obtained fuel savings of about 140 % the heat capacity remaining practically constant; the 30 to 35% reduction of the heat losses with the eviction gases through the air shafts by the reduction of the air excess; the reduction up to twice the average temperature of the gases after the cauldron; the efficiency of the heat transfer and of the reliability of the equipment in the cauldron or the furnace.

2) at optimum values of the water content from the emulsion and of the finesse of the dispersion phase the ecological indicators of the burning technology: the NO_X content in the burning gases is reduced; the deposits of carbon black on the heat exchange surfaces that on burning the anhydric fuel lead to an increase of 30-35 % of fuel consumption, are reduced by 3 to 4 times; the CO content in the burning gases is reduced with an average of 50%; the reduction of the benz(a)pirine 2 to 3 times; the high efficiency possibility of fixing the Sulphur from the low quality fuel-oil by adding the necessary additives to the WOE.

The study of WOE combustion in the experimental furnace of the Bucharest Institute of Metallurgic Studies, showed that starting with the 5% water content of WOE, furnace efficiency increases by 2.6 to 4.4% (Fig.1, *a*), air excess is reduced by 0.8 to 2.2% and the chemical imperfection of combustion process - with 0,2-0,4%. Heat losses with evicted gases and the depositions on the heating surface were reduced by 0.9 to 2.4% (Fig.1, *b*). In addition, are obtained the oil savings of up to 2.5-5.5%. By use of WOE with 15-20% water content is obtained a significant economic effect of the order of 51,400 Euro/year on an industrial furnace. The annual fuel economy on industrial furnace is 15 tons of conventional fuel.

As a result of study of WOE combustion in experimental furnace, at achieving of one of the most simple technologies of the emulsion preparation, were established some rules involved in changing economic and environmental indicators. Furnace efficiency increase (Fig.1, *a*) is determined by the intensification of burning process and by more complete

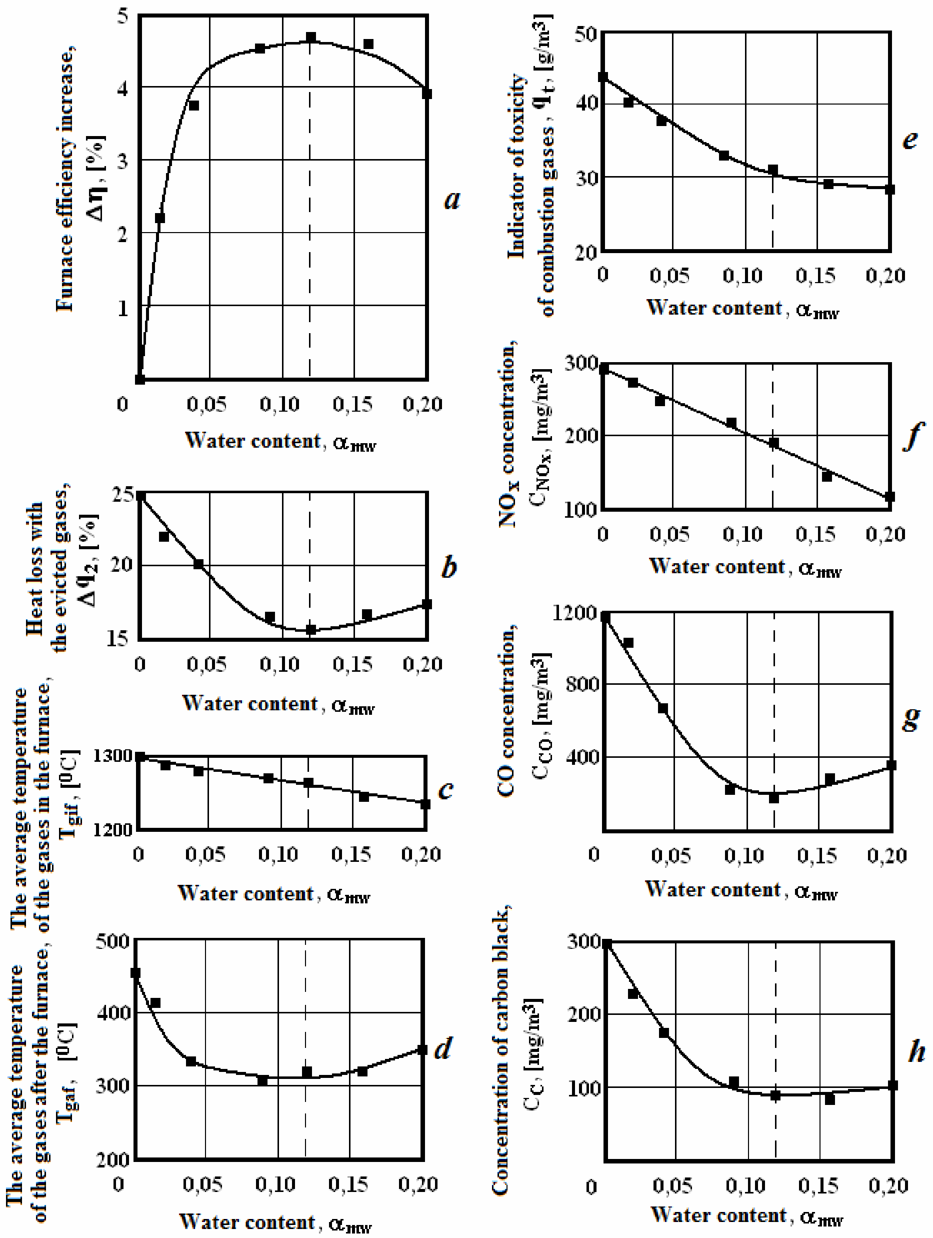

Fig. 1. Economic, energetic and ecological indicators of the WOE burning process

combustion of emulsified water-oil fuel. Increased of furnace efficiency was largely conditioned by a considerable drop of the gas temperature in the furnace of up to 70^{0}C

(Fig.1, *c*) and after furnace with 85-95^{0}C, or up to 185-195^{0}C (Fig.1, *d*). At temperature drop, the furnace efficiency increases with 3.0-4.5% and more, if the water content of WOE is fixed at optimal value (11-12%).

In terms of ecological aspect, the analysis of the furnace operation shows a 75-88% reduction of incomplete combustion products.

The experiments have shown that WOE use with water content of 15-20% reduces the indicator of toxicity of combustion gases from 44 to 28 g/m^3 (Fig.1, e), the emissions of nitrogen oxides with 29-34% (Fig.1, *f*), of carbon black with 68-80% (Fig.1, *h*) and of benz (a) pyrene with 79-88%.

The concentration of the nitrogen oxides in the composition of combustion products decreases with increasing of water content; this dependence is linear (Fig.1, f). If the emulsion is characterized by α_{mw} = 0.10, the concentration of NO_X in combustion products decreases by 35%.

The dependencies of carbon monoxide and soot concentrations by water content of WOE are more complicated. With increasing of humidity up to 11-12%, CO and carbon black contents decreases (Fig.1, *g* and *h*). Subsequent increase of WOE humidity leads to increase of CO and of black carbon in the products of combustion. The reducing of emissions of incomplete combustion products can be explained by the fact of complete combustion intensification provided by micro-fragmentation of the fuel droplets, by increase of partial pressure of water vapor and by other factors. At WOE humidity of 11-12%, the reducing of CO and soot emissions into the atmosphere reaches 48%. That stabilization and subsequent increase in concentration of incomplete combustion products, can be explained by the fact that for α_{mw} = 0.15, lower flame temperature begins to show a more pronounced influence on burning rate than the effect of micro-fragmentation of emulsion droplets.

These values of economic, energetic and ecological indicators are close to the values of those indicators obtained at test WOE firing on stationary boilers for power stations and plants [1,2], including the cast iron boilers [3].

Three functioning regimes of the plant have been tested: ***the natural gas heating regime*** (discontinuous), in which the plant is heated (the furnace and the water in the cauldron, used to pre-heat the fuel oil); ***the heating-burning regime*** (discontinuous), which begins the moment that the fuel oil is sufficiently pre-heated (70^{0}C) in order for it to be circulated through the plant, the burning continuing with fuel oil, until the furnace reaches a thermal balance (at a 1280^{0}C temperature);

the burning regime(continuous) represents the functioning of the plant only with WOE at a constant temperature in the furnace (1280^{0}C).

Based on the experimental results obtained from the plant functioning with WOE, there have been made out on computers the energetic balances of the plant and the Sankey diagrams have been drawn up (Figs.2-4).

These results show that there are critical values for the ecological indices of the burning process of WOE not only in relation to the humidity (Fig.1, b), but also in relation to the air and fuel debits.

The character of these dependences is

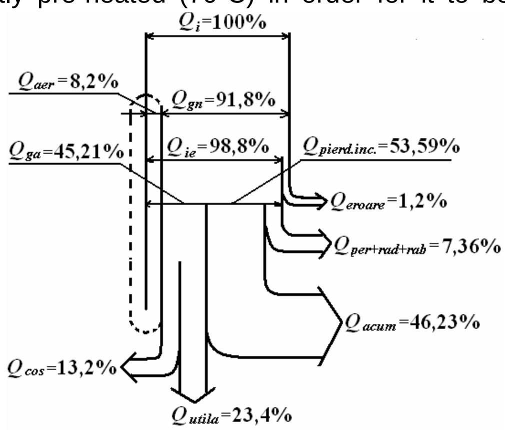

Fig. 2. Sankey diagram for the pilot plant on functioning with natural gas in heating regime

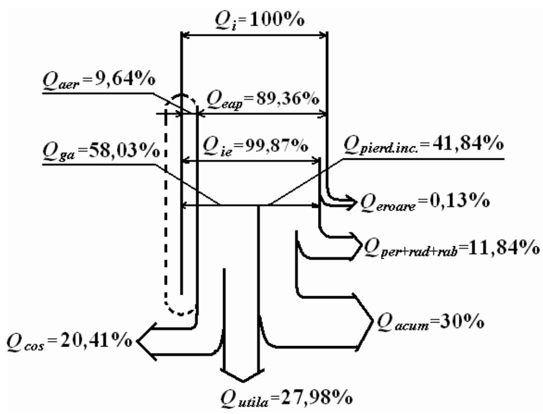

Fig. 3. Sankey diagram of the pilot plant on functioning with WOE-10 in heating-burning regime

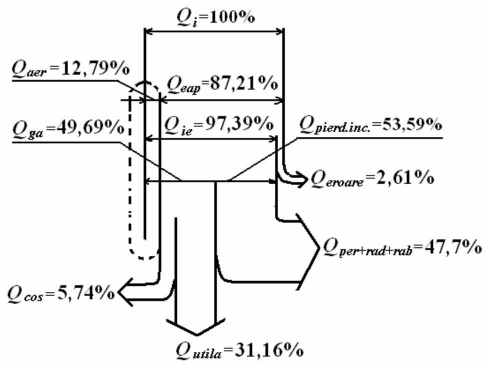

Fig. 4. Sankey diagram of the pilot plant on functioning with WOE-10 in burning regime

strongly influenced by the competition of the burning mechanisms, micro-fragmentation and dissociation of the water globules from WOE.

While using WOE, the effective heat rises from 27,98% in the heating drive (Fig 4) and exceeds its value equal to 23,40 % in the natural gas heating drive (Fig.2). Even if in the ca case of using WOE the heat losses also grow, the effect of the increase in the effective heat is explained by the more significant share in the energetic balance of the enthalpy of the burning gases formed on burning the WOE as compared to the burning of the burning of natural gas.

3. ECONOMIC, ENERGETIC AND ECOLOGICAL INDICATORS OF THE WCDS BURNING PROCESS

From analysis of existing publications is determined that the advantages of WCDS using, as compared to coals, are:

1) ***ecological***: it is not dangerous ecologically in any stages of production; transportation and usage; allows the reduction of 1,5 to 3,5 times of the polluting emulsions in the atmosphere (dust; nitric oxides and Sulphur, benzopyrene); allows the efficient usage of the ash formed during the burning;

2) ***technological***: just as with liquid fuels, the setting of the generating plants for usage for WCFS does not require any essential modification in the construction of the equipment, it allows for mechanization and automation without any difficulty in the taking delivery, alimentation and burning of the fuel; the technology for turbinionary burning at temperatures of 950-1050^{0}C allows reaching of the utilization efficiency of fuel more than 97% (from coal burning in layer the utilization efficiency do not exceeds 60%); there can be used four lighting systems for the ignition of WCDS; with the help of the plasmotrone, with natural gas, with liquid fuel and with solid fuel;

3) ***economic***: the price for 1 *t* of WCDS is by 2-3 times lower than for a tone of coal from which is prepared suspension; operating costs for storage, transport and combustion are with 15-30% lower; The capital expenditures for upgrading of thermo and thermo-electric plants in order of transition from gas and oil operation to WCDS operation are reduced by 3 times. The recovery time of implementation expenses of WCDS is 1.0-2.5 years.

To determine the influence of water content of WCDS on pilot plant efficiency and the average flue gas temperatures in the combustion chamber and out of it, were drawn the maximum value at water content α_{mw} = 0.35 (Fig.5, *a*).

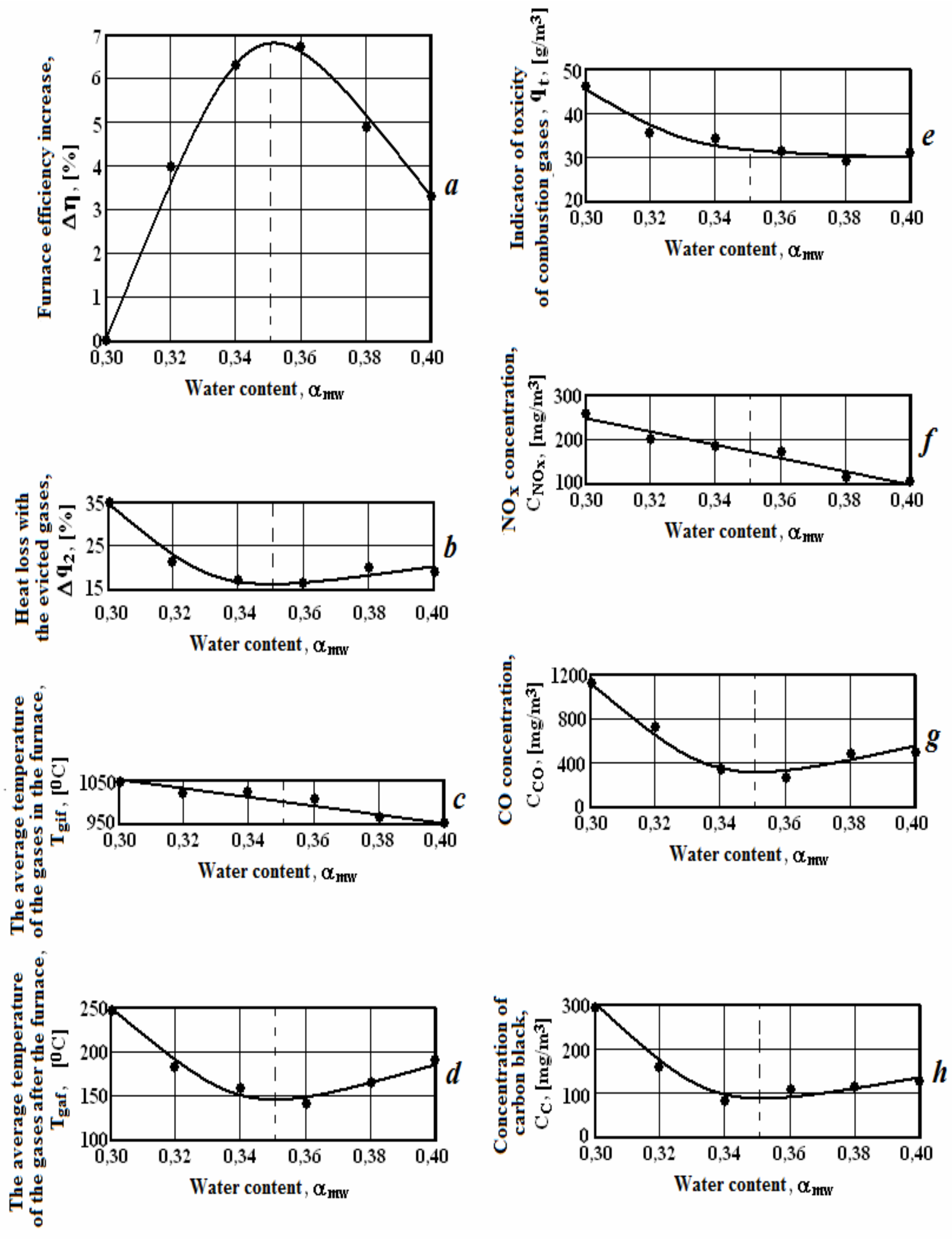

Fig. 5. Economic, energetic and ecological indicators of the WCDS burning process

Increase of efficiency is determined by the intensification of combustion, by more complete fuel combustion and by reduce of heat losses of exhaust gases (Fig.5, *b*). To a large extent the efficiency increase was due to the significantly reduction of exhaust gases temperature with 95-105℃ (Fig.5, *c*). The maximum reduction in the average temperature of gases after the combustion chamber is achieved also at α_{mw} = 0.35 (Fig.5, *d*).

At WCDS burning is achieved a reduction by 1.5-3.5 times of air pollutant emissions (dust, the nitrogen and the sulfur oxides, benz (a) pyrene). It is also possible to use effectively the fly ash during combustion. The summary indicator of toxicity of exhaust gases is reduced by 1.5 times (Fig.5, *e*), the concentration of nitrogen oxides by 2.8 times (Fig.5, *f*), the concentration of carbon monoxide by 3.5 times (Fig.5, *g*) and the concentration of carbon black by 3.2 times Fig.5, *h*).

In this case the maximum degree of emission reduction occurs at α_{mw} .= 0.35

The Figs.5, *c* and *d*, shows that with increasing of WCDS water content up to 0.35, the CO and carbon black contents decreases. Subsequent growth of α_{mw} leads to increased the CO and soot contents in the flue gas composition.

The reducing of emissions of incomplete combustion products can be explained by the fact of complete combustion intensification provided by increase of partial pressure of water vapor and by other factors [2, 3].

That stabilization and subsequent increase in concentration of incomplete combustion products, can be explained by the fact that for α_{mw}>0.35, lower flame temperature begins to show a more pronounced influence on burning rate than the growth effect of partial pressure of water vapor.

Emissions from WCDS burning are lower, since the WCDS combustion was realized at lower temperatures (~950-1050^{o}C) than fluidized bed combustion of coal (1200-1400^{o}C); the nitrogen oxides emissions (NO_X), are also reduced.

The ash obtained from burning is a finely divided powder, having a density of 330...360 kg/m^3. The ash particles are porous and different in comparison with the ash particles produced by burning of coal in a fluidized bed.

Developers of a diverse assortment of alternative liquid fuels manufacturing plants are currently on the sidelines waiting to initiate commercially viable projects, but the risk of market manipulation by OPEC and others is keeping them from committing. The oil market risk insurance program described here provides a self-funding means to overcome a significant barrier to the rapid development of a new and needed domestic liquid fuel industry [7].

China has not only recognized the strategic significance of its coal resources, it is acting aggressively to realize the full potential of this low cost, multi-use fuel and feedstock. 0 decade develop a kind of coal base clean generation the new fuel of oil and acting coal, is state committee of science and technology accredited high new technology, develop new product for national focal point, is also present world research hot point - the important branch in clean coal technology [8]. So, the water coal technology of thick liquid may be not only used to also have energy saving and environmental benifit for coal used in acting oil. According to acting oil user recent intention, the price of thick liquid that may be accepted does not be lower than 350-380 first/ton in which only, a ton of coal and the coal of 70% may be made 1.4 tons of thick liquid. Also namely a ton of coal processing after may form 490-532 first output value, have better economic benefits for coal enterprise; two is to use mining area, is low-priced the difficult slime of sale abroad simple process water coal thick liquid, burn for boiler and self-provided power station use, raise economic benefits.

A serious problem arising during burning fuel oil and coals is high sulfur content. Sulphides fly away together with smoke fumes and pollute the air. When using fuel oil in the metallurgy, the sulfur containing in the fuel oil in colloid form, usually transfers into the liquid metal melt and lowers the metal's quality, due to what in its turn costs for the sulfur localization raise in the further processing of the furnace charge obtained. Sulfur neutralization in fuel in the metallurgical industry, is obligatory if high-Sulphur fuel oil or coal are used.

The method of the highest efficiency in this problems resolving is additives introduction, that will bind sulfur on the stage of the fuel preparation for burning, namely on WOE and WCDS preparation stage. It is the most effective method on the point of view of economizing, as the most of the additives applied is water-soluble.

4. CONCLUSIONS

On testing the plant the fuel oil has been mixed with water in 10% 20% and 30% for the preparation of WOE-10, WOE-20, respectively WOE-30 it has been established that the optimal water content for WOE in relation to the economical and energetic parameters but also that of the ecological indices is of 12-15%.

The tests have lead to the obtaining of thermo powers of over 100 *kW* for WOE with a 5-30% water content. The experimental dates have been treated anf used for the calculation of the energetic balances of the plant in three functioning drives: heating; heating-burning and burning.

There are optimal values of humidity content of water-oil emulsion (0.11-0.12) and of water-coal dust suspension (~0.35) at which the increase of thermal plant efficiency is maximal and the heat loss with evicted gases, gases temperature, C and CO contents in the flue gas are minimal.

The average temperature of gases in the combustion chamber decreases, and accordingly the NO_X content decreases linearly with increasing of water content of WOE and WCDS fuels and the toxicity summary indicator of evicted gases is reduced.

The coal that it controls from 70%, the water of 30% and few chemical additive are made, are a kind of body fuel of thick liquid, may like oil the same pump send , atomization, storage and steady combustion. Its calorific value is equivalent to the half of fuel oil; may replace fuel oil is used in boiler, power station, industrial stove and kiln stove; burn used in substitute coal use, have combustion efficiency is, load adjustment high convenient, reduce environmental pollution and improvement labour condition with save with coal etc. advantage.

REFERENCES

[1] Piero Barbieri - ***Emulsione: nuovo combustibile***, Perito Ind. Vol. 45 (1), pp. 5-7,1983

[2] Krivonogov V. A. - ***Повышение эффективности сжигания газа и охрана окружающей среды***, Изд-во Недра, Ленинград, [in Russian], 1986

[3] Volikov A. N. - ***Сжигание газового жидкого топлива в котельных малой мощности***, Изд-во Недра, Ленинград, [in Russian], 1989

[4] Li Y. and Li B. - ***Study on the ultrasonic irradiation of coal water slurry***, Fuel, Vol. 79, , pp. 235-241, 2000

[5] Burdukov A. P., Popov V. I., Tomilov V. G. and Fedosenko V. D. - ***The theodynamics and combustion of coal-water mixtures***, Fuel, Vol. 81, pp. 927-933, 2002

[6] Yavuz R., Küçükbayrak S. - ***Preperation and Combustion of Coal-Water Mixtures***, Coal, editor Kural O., pp. 435-451, 1998

[7] http://www.americanenergysecurity.org/AES%20 Appendices.pdf

[8] http://www.tyboiler.com.cn/english/news.asp?news_id=60

MATHEMATICAL MODELING OF THE NEW SYSTEM FOR CAPTURE OF WAVE ENERGY

[1]SAJIN TUDOR, [2]NEDELCU DRAGOS-IULIAN
[1,2]"Vasile Alecsandri" University of Bacau, Romania

The paper presents the mathematical modeling of the wave energy capture process. The wave energy is transformed into torque by a plant composed of multiple floating cylinders, which perform oscillating motions according to the wave parameters and to the constructive elements of a new patented plant.

***Keywords**:* waves, conversion, potential energy, floating cylinders, damped oscillations, elongation, angular speed, linear speed, useful power, efficiency, mathematical modeling, computer simulation.

1. INTRODUCTION

Lately the utilization of the wave energy is much publicized, due to high energetic potential of seas and oceans, which cover over 70% of the Earth.

The first patent in the field of wave energy capture systems was released in 1799 by Parisians Girard [1], for an installation using direct mechanical action to drive pumps, wood cutting cells and other machines. Methods for wave energy conversion date back to 1890, but few of them were reliable and had a successful finalization.

A first significant project was realized in 1907 in California, where with the Starr Wave Motor, which was assembled on the Redondo Beach, was hoped to ensure six counties with electric energy, the infrastructure resisting only two years, until the papyrus dam was destroyed [2].

The conversion technologies of wave energy were increased worldwide in the last 35 years. Significant contributions were registered in countries like Argentina, Australia, Canada, China, Denmark, France, India, Ireland, Japan, United Kingdom, Norway, Portugal, Russia, Scotland [3,4]. All competitive technological installations converts the wave action into mechanical or electrical energy, using four basic principles [5]: by means of submerged turbines; waves channeling in tanks for increase of water level in comparison with sea level; installation of floating systems with buoys on ocean or sea surface; air turbines driven by water oscillating columns.

Between the installations, which have been designed or are in research stage, we will mention the following [6]: plant firm SDE shore Energy Ltd., Israel; LIMPET (company Wavegen, UK); WECA (Daedalus Informatics Ltd, Greece); SSG and TAPCHAN (Norwave AS, Norway); ANACONDA (Checkmate Sea Energy, UK); McCABE WAVE PUMP (Hydam Technology Limited, Ireland); Pelamis (Ocean Power Delivery Pelamis Wave and Power, UK); Salter Duck (University of Edinburgh, UK); Kaimei and Mighty Whale (group JAMSTEC, Japan), OWC (Sanz and Haramachi localities, Japan), Wave Star (Denmark); DECM (company Trident Energy Limited, England); Seabased AB (company Seabased, Sweden), Wave Energy Buoy (Oregon State University, USA); AquaBuoy (Finavera Renewables Limited Wind Energy ESS later, Ireland, Canada, Scotland); Bristol Cylinder, OWEC IPS Buoy (corporations Interproject Service AB (IPS) and Technocean (TO)); WaveDragon (Erik Friis-Madsen, Wave Dragon Ltd, Denmark).

In this paper is theoretically studied a new plant for capture of wave energy, in which is developed the principle of setting of floating buoy systems on the sea or on the ocean surface.

2. FORMULATION OF PHYSICAL AND MATHEMATICAL MODELS

According to the patent [7], the plant for capture of wave energy [8] is built from a structure of floating cylinders, which is anchored in the centre of symmetry to the sea bottom. The floating cylinders are mounted so they can rotate relative to longitudinal axes and are connected to each other in parallel at both ends using connecting rods perpendicular to the longitudinal axes. Thus, one end of the connection rod is rigidly connected to the end of a floating cylinder and the other end of the connection rod is rigidly connected to the longitudinal axis of the neighboring floating cylinder.

Mathematical modeling about the behavior of floating bodies of the different shapes under the wave action have been developed by Newman and Evans [9,10].

The schematics to compute an element of the plant for wave energy capture [11,12] is

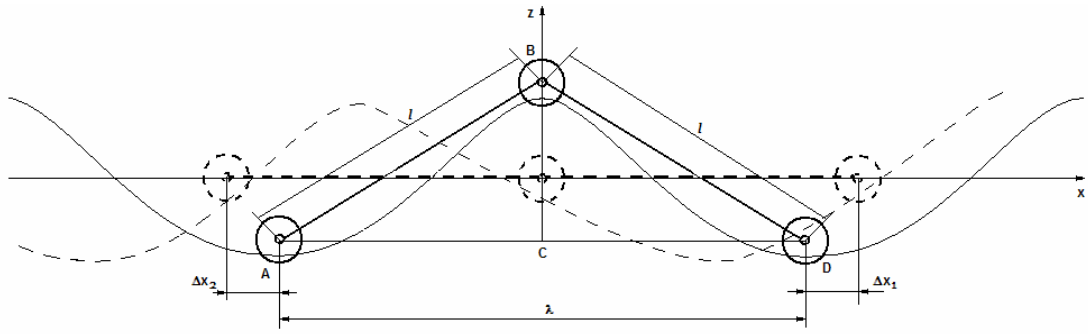

Fig. 1. The schematics to compute the motion dynamics of an element to capture wave energy

presented in Fig. 1.

The system has three degrees of freedom: vertical and horizontal translation and rotation around the axis of the considered floating cylinder.

The computing element of the plant for capture potential wave energy is built out of three floating bodies: a central one, which is the considered floating cylinder and two peripheral floating cylinders, which interact with the central floating cylinder using rods of length l.

The following wave parameters are known: wave length λ and the oscillation period T. Using these parameters we can calculate the waves' amplitude [12] a, the oscillation frequency (angle speed) Ω and phase speed C.

We also know the constructive characteristics for the capture plant: diameter for the floating cylinders D, length of the floating cylinders L, length of the connection rods between the floating cylinders l, thickness of the floating cylinder wall δ, weight of the constructive elements (transmissions, electric generator, arresters, bearings, etc.) compared to the weight of the floating cylinder m_0.

The sea water density is ρ and the average density for the constructive materials of the elements incorporated inside the floating cylinders is ρ_{cm}.

We have to determine: the phase-shift times of the oscillations for the peripheral floating cylinders $\tau_1(t)$ and $\tau_2(t)$; the vertical elongations for the central floating cylinder $z(t)$ and for the peripheral floating cylinders $z_1(t)$ and $z_2(t)$; the angle variation $\theta(t)$ between the rods which connect the central floating cylinder to the peripheral floating cylinders; the angular speed $\omega(t)$ of rotation for the central floating cylinder in contrast to its body; the forces $F_1(t)$ and $F_2(t)$ through which the peripheral floating cylinders act on the connection rods l, the linear speeds $v_1(t)$ and $v_2(t)$ of the peripheral floating cylinders around the rotation axle for the central floating cylinder; the mechanical power extracted from wave energy $P(t)$, the efficiency $\eta(t)$ of the plant to transform the wave energy into mechanical energy. Also, we have to determine the dependency between the plant efficiency and the ratio l/λ, the diameter of the force F_0 which performs the oscillations, as well as the dependency between the reported weight m_0 and the amplitude of the force F_0 to the floating cylinder diameter D.

3. MATHEMATICAL MODEL

We will draw the horizontal axis *X* through the centers of mass of the floating cylinders in the initial position (balance position) when the surface is plain (this position is shown in figure 2 with dotted lines). Axis *Z* will be oriented perpendicular to the *X* axis. The origin for the *X-Z* axes can be chosen randomly. For example, we can choose the origin to be in the center of mass of the central floating cylinder in the balance position.

Through the developing of the model [11], we will examine the forced oscillations of the central floating cylinder under the action of the periodical excitation force [13],

$$F = F_0 \cos \Omega t, \tag{1}$$

exerted by the waves on the cylinder.

The differential equation for the oscillation of the central floating cylinder on the *Z* axis can be written as [11,13]:

$$m\frac{d^2 z}{dt^2} = -kz - c\frac{dz}{dt} + F_0 \cos \Omega t, \tag{2}$$

or

$$\frac{d^2 z}{dt^2} + 2b_a \frac{dz}{dt} + \omega^2 z = \frac{1}{m} F_0 \cos \Omega t, \tag{3}$$

where *k* is the elastic constant, [kg/s^2]; *c* – water resistance coefficient, [*kg/s*]; b_a – damp coefficient, [s^{-1}]; ω_p – frequency of own oscillations for floating cylinder without damping, [s^{-1}]; F_0 – excitation periodic force amplitude, [*N*]; Ω – wave oscillation frequency, [s^{-1}]; t – time, [*s*]. The following relations exist between these values [11,13]:

$$\omega_p^2 = \frac{k}{m}; b_a = \frac{c}{2m}; m = m_0 \cdot L\left[\left(L + \frac{D+\delta}{4}\right)\cdot \pi\delta(D+\delta)\cdot \frac{1}{V_{mc}} + 1\right];$$

$$F_0 = \left[\frac{\pi D^2}{4}(L - 2\delta) - V_{mc}\right]\cdot \rho g - mg. \tag{4}$$

The values of m_0 and V_{cm} are chosen in a way that they satisfy the relation [11,12]:

$$mg = \frac{1}{2}\left[\frac{\pi D^2}{4}(L - 2\delta) - V_{cm}\right]\cdot \rho g, \tag{5}$$

which states that the amplitude of the excitation force on the oscillation period remains constant and at a value equal to half of the Archimedes force.

The general solution of the differential Eq.(3) with the right side is composed of the general solution of the homogenous equation (without the right side), and a specific solution of the complete equation.

We will obtain the general solutions for the homogenous equation:

$$\frac{d^2 z}{dt^2} + 2b_a \frac{dz}{dt} + \omega_p^2 z = 0, \left(z = z_1^0\right). \tag{6}$$

The general solution of this equation is known as the solution for the damped oscillations:

$$z_1^0 = c_1 e^{v_1 t} + c_2 e^{v_2 t}, \left(v_1 \neq v_2\right), \tag{7}$$

where $v_{1,2} = -b_a \pm \sqrt{b_a^2}$ are the roots for the characteristic equation $v^2 + 2b_a v + \omega$ [13].

There are three cases, according to the values of the roots $v_{1,2}$ of the characteristic equation, which can be complex conjugates, real and distinct or identical [13]:

1. If $b_a < \omega_p$, which means that the damping coefficient is low enough ($c < \sqrt{2mk}$), the roots $v_{1,2}$ are complex. We have real solutions if the constants c_1 and c_2 are complex conjugates of each other:

$$c_1 = \frac{1}{2} A_0 e^{i\alpha}, \quad c_2 = \frac{1}{2} A_0 e^{-i\alpha}, \tag{8}$$

where A_0 and α α are other two real arbitrary constants.

The solution can be written, considering Euler's equations, as such:

$$z_1^0 = A_0 e^{-bt} \cos(\omega' t + \alpha) = A\cos(\omega' t + \alpha),$$

$$A = A_0 e^{-bt} \cos(\omega' t + \alpha) = A_0 e^{-\frac{c}{2m}t},$$

$$\omega' = \sqrt{\omega_p^2 - b_a^2} = \sqrt{\frac{k}{m} - \frac{c^2}{4m^2}} < \omega_p = \sqrt{\frac{k}{m}}, \tag{9}$$
$$z_1^0 = A_0 e^{-\frac{c}{2m}t} \cos\left(\sqrt{\frac{k}{m} - \frac{c^2}{4m^2}} \cdot t + \alpha\right),$$

where ω' is the frequency of the free damped oscillations, also known as pseudo-frequency or pseudo-pulsation.

In this case, the damped oscillations (9) are sinusoidal, with an exponentially decreasing amplitude and the relaxation time $\tau = 1/b_a = 2m/c$.

2. If $b_a > \omega_p$ (or $c > 2\sqrt{mk}$), which means that the damping coefficient is high enough, the roots $v_{1,2}$ are real and negative and the general solution is:

$$z_1^0 = c_1 \exp\left[-\left(b_a + \sqrt{b_a^2 - \omega_p^2 t}\right)\right] + c_2 \exp\left[-\left(b_a - \sqrt{b_a^2 - \omega_p^2 t}\right)\right] = \tag{10}$$
$$e^{-bt}\left[c_1 \exp\left(-\sqrt{b_a^2 - \omega_p^2 t}\right) + c_2 \exp\left(-\sqrt{b_a^2 - \omega_p^2 t}\right)\right]$$

which means that the elongation converges to zero and based on the initial conditions, the body can pass at least one time through the balance position. The motion is called aperiodic dampened.

3. If $b_a = \omega_p$, the roots $v_{1,2}$ have the same value and the general solution is:

$$z_1^0 = (c_1 + c_2)e^{-b_a t}. \tag{11}$$

This is a particular case of aperiodic dampened motion, called critical aperiodic motion.

The dampened oscillations after a transitory condition passes will relax and the permanent conditions will set in, where the floating cylinder will perform oscillations at constant amplitude and the frequency Ω of the exterior periodical force, called forced oscillations.

The particular solution of the differential equation (3) is obtained applying the composition method of the sinusoidal oscillations.

Because the right side is periodic and has Ω frequency, it is imperative that the left side is periodic with the same frequency, thus we search the particular solution like $z_2^0 = B\cos(\Omega t + \beta)$, where:

$$\frac{dz_2^0}{dt} = \Omega B \cos\left(\Omega t + \beta + \frac{\pi}{2}\right), \tag{12}$$
$$\frac{d^2 z_2^0}{dt^2} = -\Omega^2 B \cos(\Omega t + \beta).$$

By replacing Eq.(12) in Eq.(3) we have:

$$-\Omega^2 B\cos(\Omega t+\beta)+2b\Omega B\cos\left(\Omega t+\beta+\frac{\pi}{2}\right)+\omega_p^2 B\cos(\Omega t+\beta)=\frac{1}{m}F_0\cos\Omega t\,,$$

$$B\left(\omega_p^2-\Omega^2\right)\cos(\Omega t+\beta)+2B\Omega b\cos\left(\Omega t+\beta+\frac{\pi}{2}\right)=\frac{1}{m}F_0\cos\Omega t\,.$$

On the left side of the last equation we apply the composition formula for the sinusoidal oscillations and we obtain:

$$B\sqrt{\left(\omega_p^2-\Omega^2\right)^2+4\Omega^2 b_a^2}\cdot\cos(\Omega t+\alpha)=\frac{1}{m}F_0\cos\Omega t\,, \tag{13}$$

where the resulting phase α has to be zero as on the right hand side:

$$0=\sin\alpha=\frac{B\left(\omega_p^2-\Omega^2\right)\sin\beta+2B\Omega b_a\sin\left(\beta+\frac{\pi}{2}\right)}{B\sqrt{\left(\omega_p^2-\Omega^2\right)^2+4\Omega^2 b_a^2}}$$

$$1=\cos\alpha=\frac{B\left(\omega_p^2-\Omega^2\right)\cos\beta+2B\Omega b_a\cos\left(\beta+\frac{\pi}{2}\right)}{B\sqrt{\left(\omega_p^2-\Omega^2\right)^2+4\Omega^2 b_a^2}}$$

where results:

$$B=\frac{F_0}{m\sqrt{\left(\omega_p^2-\Omega^2\right)^2+4\Omega^2 b_a^2}}=\frac{F_0}{\Omega\sqrt{c^2+\left(\Omega m-\frac{k}{\Omega}\right)^2}}\,, \tag{14}$$

$$\sin\beta=\frac{-2\Omega b}{\sqrt{\left(\omega_p^2-\Omega^2\right)^2+4\Omega^2 b_a^2}}=\frac{-c}{\sqrt{c^2+\left(\Omega m-\frac{k}{\Omega}\right)^2}}<0\,, \tag{15}$$

therefore $\beta\in(0,-\pi)$;

$$\cos\beta=\frac{\omega_p^2-\Omega^2}{\left(\omega_p^2-\Omega^2\right)^2+4\Omega^2 b_a^2}=\frac{\frac{k}{\Omega}-\Omega m}{\sqrt{c^2+\left(\Omega m-\frac{k}{\Omega}\right)^2}}\,, \tag{16}$$

for $\Omega<\omega_p, \cos\beta>0,$ therefore $\beta\in\left(0,-\frac{\pi}{2}\right)$;

$$\tan\beta=\frac{2\Omega b_a}{\omega^2-\Omega^2}=\frac{c}{m\Omega-\frac{k}{\Omega}}\,, \tag{17}$$

for $\Omega > \omega_p, \cos\beta < 0,$ therefore $\beta \in \left(-\frac{\pi}{2}, -\pi\right)$;

Considering the Eqs.(14) and (17) the particular solution of the equation for the forced oscillations will be written such as:

$$z_2^0 = \frac{F_0}{\Omega\sqrt{c^2 + \left(\Omega m - \frac{k}{\Omega}\right)^2}} \cdot \cos\left(\Omega t + \arctan\frac{c}{m\Omega - \frac{k}{\Omega}}\right). \tag{18}$$

The complete general solution of the differential equation (2) will be given by the superposition of the own oscillations with the forced oscillations:

$$z(t) = z_1^0 + z_2^0 = A_0 e^{-bt}\cos(\omega' t + \alpha) + B\cos(\Omega t + \beta), \tag{19}$$

where *ω'* is calculated using Eq.(9), and

$$B = \frac{F_0}{\Omega\sqrt{c^2 + \left(\Omega m - \frac{k}{\Omega}\right)^2}}, \tag{20}$$

$$\beta = \arctan\frac{c}{m\Omega - \frac{k}{\Omega}}. \tag{21}$$

According to the definition, the elastic constant *k=F/x*, where *F* is the module of the force which acts on the spring, and *x* represents the movement of the force application force compared to the balance position of the spring. In case of the interaction between the floating cylinder and the water

$$k = \frac{F_0}{\psi \cdot D}, \tag{22}$$

where F_0 is the amplitude of the sinusoidal excitation force for the oscillations, *D* – exterior diameter of the floating cylinder, *ψ* – part of the cylinder diameter which represents the immersion of the mass center into calm waters compared to the balance position for F_0 = 0. The frequency of the own oscillations will be calculated using the first relation of Eqs (4).

From the $B = a$ condition, we obtain

$$c = \sqrt{\left(\frac{F_0}{a \cdot \Omega}\right)^2 - \left(\Omega \cdot m - \frac{k}{\Omega}\right)^2}. \tag{23}$$

After a period of time equal to the relaxation time

$$\tau = \frac{1}{b_a} = \frac{2m}{c}, \tag{24}$$

the first term of Eq.(19), which dictates the own oscillations, becomes ignorable. Thus, after the damped own oscillations stop, the permanent oscillation conditions for the floating cylinder remain. Next we will analyze only this type of forced oscillations conditions.

Being connected to the central floating cylinder with rods of length l (Fig.1), the peripheral floating cylinders will oscillate out of sync:

a) the left peripheral floating cylinder,

$$z_1(t) = a\cos\left[\Omega\left(t - \frac{l}{\lambda}T\right) + \arctan\frac{c}{\Omega m - \frac{k}{\Omega}}\right]. \quad (25)$$

b) the right peripheral floating cylinder,

$$z_2(t) = a\cos\left[\Omega\left(t + \frac{l}{\lambda}T\right) + \arctan\frac{c}{\Omega m - \frac{k}{\Omega}}\right]. \quad (26)$$

In any position of the floating cylinders Pitagora's theorem will be respected for the *ABC* or *BCD* right angled triangles (Fig.1):

$$\left[z_i(\tau_i) - z(t)\right]^2 + \left[(\tau_i - t)\cdot\frac{\lambda}{T}\right]^2 = l^2 \text{, (i=1,2),} \quad (27)$$

where τ_i are the respective times for conjugating the wave angle profile with the elongations z_i of the peripheral bodies.

Times $\tau_i(t)$ are determined from the transcendent Eq.(27), which has two real roots, the lowest being $\tau_1(t)$, and the highest being $\tau_2(t)$.

Using the values t, τ_1 and τ_2, we calculate the elongations of the floating cylinders oscillations, central $z(t)$ and peripheral $z_1(t)$ and $z_2(t)$:

$$z(t) = a\cdot\cos\left[\Omega\cdot t + \arctan\left(\frac{c}{\Omega m - \frac{k}{\Omega}}\right)\right]; \quad (28)$$

$$z_1(t) = a\cdot\cos\left[\Omega\cdot\tau_1(t) + \arctan\left(\frac{c}{\Omega m - \frac{k}{\Omega}}\right)\right]; \quad (29)$$

$$z_2(t) = a\cdot\cos\left[\Omega\cdot\tau_2(t) + \arctan\left(\frac{c}{\Omega m - \frac{k}{\Omega}}\right)\right]. \quad (30)$$

The angle of rotation for the rod on the left hand side of the central floating cylinder around its axis is determined using the relation

$$\theta_1(t) = \arccos\left[\frac{z(t) - z_1(t)}{l}\right], \tag{31}$$

and the angle of rotation for the rod on the right hand side of the central floating cylinder, with the relation

$$\theta_2(t) = \arccos\left[\frac{z(t) - z_2(t)}{l}\right]. \tag{32}$$

The variation of the angle between the rods is equal to the algebraic sum of the angles $\theta_1(t)$ and $\theta_2(t)$:

$$\theta(t) = \theta_1(t) + \theta_2(t). \tag{33}$$

The angle speed for the rotation axis of the central floating cylinder in contrast to its body is given by the relation:

$$\omega(t) = \frac{d}{dt}\theta(t) = \frac{d}{dt}\theta_1(t) + \frac{d}{dt}\theta_2(t). \tag{34}$$

The variation of the modules of the forces exerted by the peripheral floating cylinders on the rods is determined using:

$$F_1(t) = F_0 \cos[\Omega \tau_1(t)], \tag{35}$$

$$F_2(t) = F_0 \cos[\Omega \tau_2(t)]. \tag{36}$$

The linear speeds of rotation for the centers of mass of the peripheral cylinders around the axis of the central floating cylinder are given by the relations:

$$\mathrm{v}_1(t) = l \cdot \frac{d}{dt}\theta_1(t), \tag{37}$$

$$\mathrm{v}_2(t) = l \cdot \frac{d}{dt}\theta_2(t). \tag{38}$$

The mechanical power extracted by the plant for capture wave energy is determined using the formula [11]:

$$P(t) = F_1(t) \cdot \mathrm{v}_1(t) + F_2(t) \cdot \mathrm{v}_2(t). \tag{39}$$

The available power for the wave on the length *L* of the floating cylinders is given by the relation [11]:

$$P = \frac{1}{2} \cdot \frac{\rho g a^2 \cdot L \cdot \lambda}{T}. \tag{40}$$

The useful power $P_{us}(t)$ is considered to be the positive part of the Eq.(39).

Using the values of the powers in according with Eqs.(39) and (40) we can calculate the efficiency for the plant to convert the wave energy, at a given moment [11],

$$\eta(t) = \frac{P_{us}(t)}{P} \cdot 100, \tag{41}$$

and the average value for the wave period [11],

$$\eta_m = \frac{\int_0^T P_{us}(t)}{\frac{1}{2}\rho g a^2 L \lambda} \cdot 100 . \qquad (42)$$

4. COMPUTER SIMULATION

Using the relations (25)–(42) we draw the charts $\tau_1(t/T)$, $\tau_2(t/T)$, $z(t/T)$, $z_1(t/T)$, $z_2(t/T)$, $\theta(t/T)$, $\omega(t/T)$, $F_1(t/T)/L$, $F_2(t/T)/L$, $\mathrm{v}_1(t/T)$, $\mathrm{v}_2(t/T)$, $P(t/T)/L$ and $\eta(t/T)$.

By modifying the length of the rods l, the diameter of the floating cylinders *D*, the amplitude of the excitation force for the oscillations F_0 we draw the charts $\eta_m(l/\lambda)$, $\eta_m(D)$ and $\eta_m(F_0/L)$.

To simulate the mathematical model used to extract the potential wave energy using the proposed energetic plant, we designed a computing program using Mathcad 14 software.

The base values were used: D=1.25 *m*, L=10 *m*, δ=3·10^{-3} *m*, l=0.5·λ, m_0=567.99 *kg*, for waves with the following characteristics λ=10 *m*, T=3.5 *s*. Sea water density is ρ=1150 *kg/m*^{3}. With fixed values for the other base measures we varied *D* in the 0.2 -2.0 *m* interval and the ratio l/λ inside the 0.1–1.0 interval. When varying D, m_0 and V_{cm} are chosen in such way that they satisfy the Eq.(5) and F_0 is determined using Eq.(4).

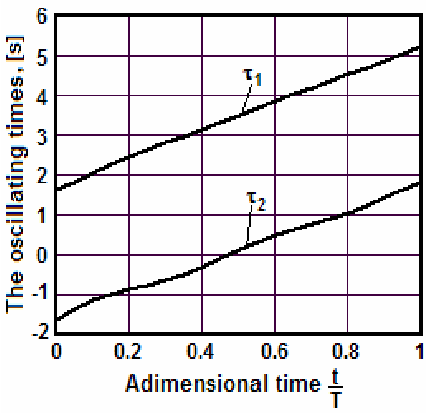

Fig. 2. Chart for the oscillating times for the peripheral cylinders during one wave period

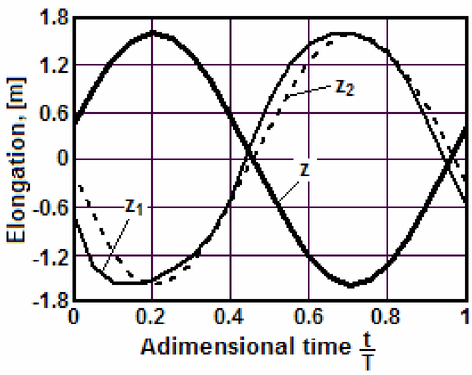

Fig. 3. Elongation variation z_1 and z_2 of the peripheral cylinders and the elongation of the wave during one period

The oscillating times $\tau_1(t/T)$ and $\tau_2(t/T)$ for the peripheral floating cylinders are phase-shifted with the same value one towards each other on the entire wave period T (Fig.2).

There is a certain phase-shift between the oscillations of the peripheral cylinders (Fig.3), in average these being in counter phase with the oscillations of the central floating cylinder, which is good for the efficiency of the wave conversion process.

The intersection between the elongations of the floating cylinders happens in the same points on the time axis (z = 0).

The angle θ between the rods oscillates during one period in the interval 110 - 250°, meaning that it varies by 140° (Fig.4). The oscilla tion for the angle θ is sinusoidal.

The angular speed $\omega(t/T)$ of the rotation axle for the central floating cylinder has a sinusoidal variation and has lag in report with the elongation of the central cylinder by approximately (1/4)·T, varying in the interval -1.2…+1.2 *rad/s* (Fig.5).

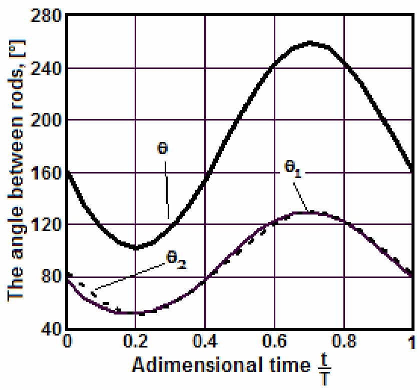

Fig. 4. Variation of the angle θ between the peripheral cylinder rods and the angles θ_1 and θ_2 of the rods during one period

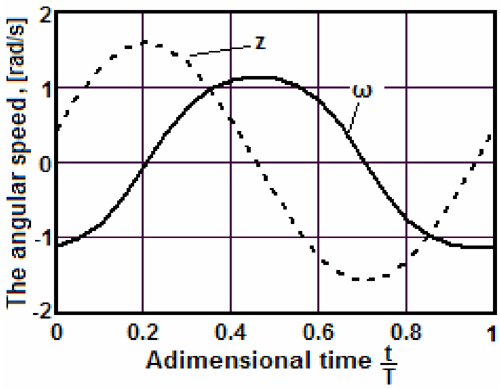

Fig. 5. Variation of the angular speed ω of the rotation axle of the central cylinder and the phase-shift in report to the elongation z during one wave period

The forces between the peripheral cylinders and the rods have different variations, but they coincide at the beginning, the middle and the end of the wave period (Fig.6) [11]. There are time frames when both forces have the same orientation (the most benefic case for the wave conversion process) and there are time frames when the forces have opposite orientation. In the latter case, where the modules of the forces are equal the plant will not produce energy.

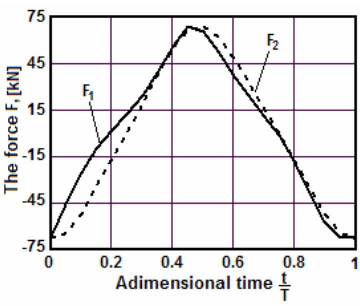

Fig. 6. Variation of the forces between the peripheral cylinders and the rods during one wave period

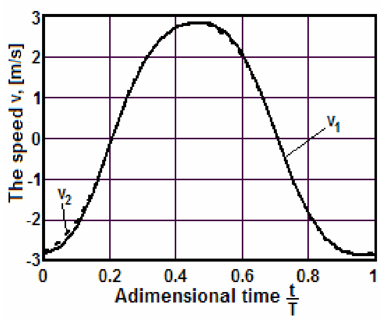

Fig. 7. The variation of the linear speeds for the peripheral cylinders during one wave period

The linear speeds of the centers of mass for the cylinders vary sinusoidal and are equal, which proves the existence of symmetry in the dynamics of the peripheral cylinders motion (Fig.7).

The useful mechanical power has an oscillating period equal to half the wave period, and it's maximum value is reached at the beginning and at half the period *T* and it's minimal value is reached at 0.3·*T* and 0.8·*T* (Fig.8) [11].

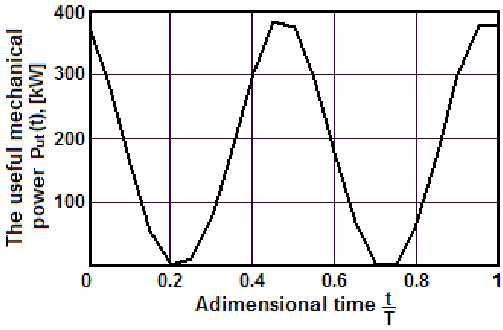

Fig. 8. Chart of the useful mechanical power extracted by the cylinders

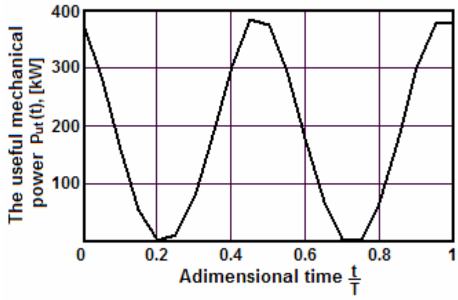

Fig. 9. Chart for the efficiency at a certain moment in time

The chart for the efficiency at a certain moment in time *η(t/T)* has the same character as the chart for the mechanical torque (Fig.9).

The variation of the average efficiency during the wave period reaches maximum value for *l/λ<0.5*, (Fig.10) [11].

The average efficiency increases with the increase of the diameter of the cylinders and has a tendencv to stav level at values for *D* >1.8 *m* (Fig.11) [11].

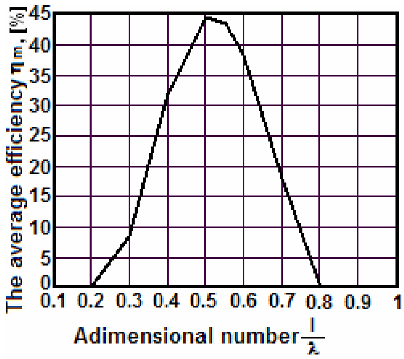

Fig.10. Chart for average efficiency depending on the wave length

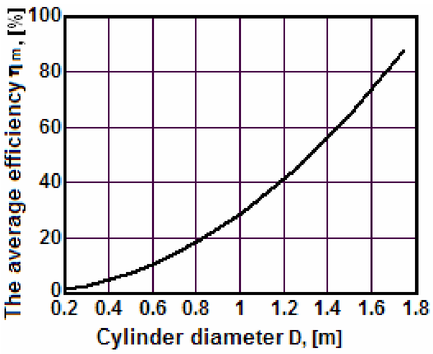

Fig.11. Chart for average efficiency depending on the cylinder diameter

The increase in the average efficiency is sustained by the increase in the excitation force F_0 of the forced oscillations for the floating cylinders by increasing their diameter (Fig.12), which is confirmed by the chart $\eta_m(F_0/L)$ from Fig.13.

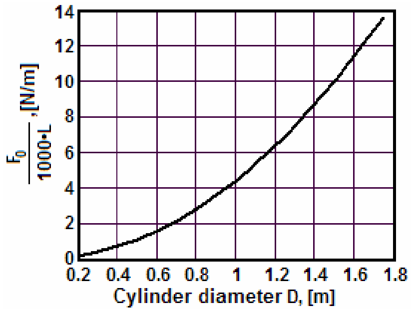

Fig.12. Chart for the dependency between the cylinder diameter and the force which is exerted on the length unit

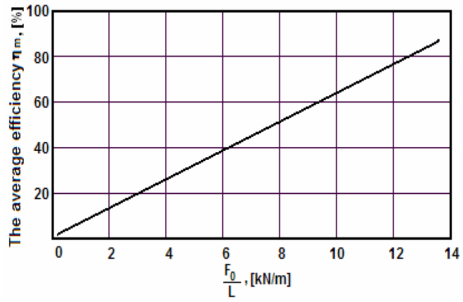

Fig.13. Chart for the average efficiency depending on the excitation force

With the increase in diameter of the floating cylinders also increases the mass of the constructive elements reported to the cylinder mass m_0 (Fig.14).

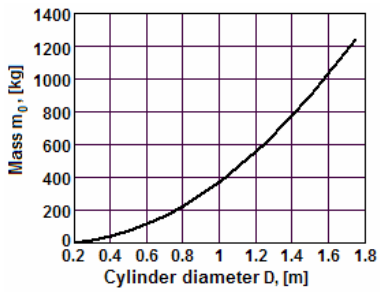

Fig.14. Chart for the dependency between the cylinder diameter and the mass reported to the length unit m_0

The proposed mathematical model proves the functionality of the patented plant for capture of potential wave energy with good efficiency.

5. CONCLUSIONS

The mathematical model of the process to capture potential wave energy using floating cylinders articulated with connection rods was developed. Using this model we simulated the process of capturing potential wave energy and determined the variations on the oscillating period for elongations, deviation angles, angular and linear speeds, forces, power extracted and efficiency.

It was determined that the oscillation times for the floating cylinders are phase-shifted at the same angle based on the connection rod length.

The elongations and the deviation angles for the rods vary based on the ratio between the rod length and the wavelength l/λ.

The angular speeds for the rods have sinusoidal variations which are lagging in report with the central cylinder elongation.

The linear speeds for the centers of mass for the floating cylinders vary sinusoidal and are equal, which proves the existence of symmetry in the dynamics of the peripheral cylinders.

The forces which act on the peripheral cylinders joints based on the ratio l/λ, the elastic constant k and the resistance coefficient *c* can be oriented in the same way as the speeds or in the opposite way. There are cases when the bodies are in counter-phase.

The useful power becomes maxim when the linear speeds and the forces have the same phase, but is zero when they oscillate in counter-phase. The maximum value for the power was obtained for the ratio $l/\lambda = 0.5$.

The plant efficiency has the same variation degree as the useful power.

The average absorption efficiency for potential wave energy increases with the rise in diameter D of the cylinders and the efficiency tends to have the same values for $D > 1.8$ *m*. The increase in efficiency is sustained by the increase in the excitation force of the oscillations.

REFERENCES

[1] Leslie F. R. - ***Renewable Energy in (and above) the Oceans***, 2002

[2] Blair Fox S. - ***Ocean Wave Generators for Southern California***, Information on http://www.laprogressive.com/the-environment/ocean-wave-generators-for-southern-california/

[3] Bostan I., Dulgheru V., Sobor I., Bostan V., Sochireanu A - ***Sisteme de conversie a energiilor regenerabile***, Ed. Tehnica-Info Chişinău, [in Romanian], 2007

[4] Craig J. - ***Country notes***, Tidal Energy, AEA Technology. U.K., 2003

[5] Boyle G.: Renewable Energy: Power for a sustainable future, Oxford University Press/The Open University, ISBN 0-19-856451-1, 2004

[6] ***Prezentarea sistemelor de conversie a energiei valurilor*** Information on http://www.crses.sun.ac.za/oen/images/pdf/WaveEnergyConvertors.pdf [in Romanian]

[7] Nedelcu D. Iu., Sajin T., Vernica S., Aniței F., Marian M., Birsan C., Ostahie C. N. - ***Plant for wave energy conversion***, RO ***patent no.125676,*** 2009

[8] Sajin T., Nedelcu D. Iu. - ***The study of waves energy capture process by mechanical and electrical analogy***, Journal of Marine Technology and Environment, Vol.2, pp. 99-104, 2012

[9] Newman J. N. - ***Interaction of waves with two-dimensional obstacles: a relation between the radiation and scattering problems***, J . Fluid Mech., 71, pp. 273-282, 1975

[10] Evans D. V. - ***A theory for wave-power absorption by oscillating bodies***, Journal Fluid Mech., Vol. 77, part 1, Great Britain, pp.1-25, 1976

[11] Nedelcu D. Iu., Sajin T. - ***Efficiency analysis of waves energy conversion system with floating cylinders***, Journal of Marine Technology and Environment, Vol.2, pp. 93-98, 2012

[12] Nedelcu D. Iu. - ***Contribution to the study of wave energy conversion process***, Phd thesis in Mechanical Engineering, "Vasile Alecsandri" University of Bacau, Romania, 2011

[13] Hristev A. - ***Mecanică şi acustică***, Editura Didactică şi Pedagogică, Bucureşti, 1982

SOCIO-ECONOMIC & ENVIRONMENTAL IMPACT OF THE PORT EFFICIENCY IN THE TRANSPORT LOGISTIC CHAIN.

[1]SALAMA BENAZAR. ROSANA, [2]MARTINEZ MARIN. JESUS E.

[1]Universidad Marítima del Caribe, Venezuela
[2]Universitat Politècnica de Catalunya & Rideport, España

Port efficiency and productivity are two of the most important factors in defining the competitiveness of a port. Lately it has been shown that while the ports are more developed and more competitive, have a greater tendency to respecting the environment, because that same competitiveness, are encouraged to apply at their facilities to international quality standards such as ISO14000, including measures that represent respect for the environment and corporate policies designed for that purpose. Moreover the socio-economic implications of logistics undoubtedly affect the social development of cities. So, the aim of this paper is to open a discussion in this regard, and analyze with a real situation and the economical , social & Envinmental impact on the venezuelan society.

***Keywords**:* Port's Eficiency, Port's Productivity, Environmental Policy of the Port, Port's Pollution Prevention, Christmas Port's Congestion in Venezuela.

1. INTRODUCTION

A global distribution channel with a reliable transport system is essential in the modern world economy (Siu Lee Lam, 2011), where the main mode of transport is the maritime one, since more than 90% of the total commerce is moved by sea (United Nations Conference on trade and Development, 2010).

The manufacturing industry in global supply chains depends on maritime transport services. Therefore, shipping is a vital component in global supply chain management (Siu Lee Lam, 2011). When logistics fails, not only production fails, but also products distribution, not satisfying the products peak seasons demand.

Since its advent in the mid – 1960s, containerization has been responsible for integration within the transport chain (Brooks, 2000). Nevertheless, traditionally, maritime transport comprised a well defined service of related but separate activities, with each participant being responsible for a limited part of the process (Siu Lee Lam, 2011). The maritime transport business is characterized by fragmentation of operating units and a requirement for an intensive network control (Graham, 1998).

2. PORT'S EFICIENCY. CASUISTRY

Port efficiency is a special component of that network, and an important criterion for a country in international competitiveness (Tongzon, 1989). The productivity of container ports/terminals depends on the efficient use of land, labor, and capital (Dow & Leschine, 1990), and for sure is a very strog attractive to the shippowners at the time to select a port as a base for it's operations.

In terms of land, the literature has often used terminal area as a variable. As for equipment, the number of quayside gantries, yard gantries and straddle carriers are often selected, while the number of berths and the total length of terminals are frequently used as infrastructure variables. (Jim Wu & Goh, 2010) On the measurement of capital, Liu (1995) used the net value of fixed capital, including land, buildings, docks, berths, roads, storage, and equipment as the input variable for capital, while Cullinane and Song (2003) chose the net book value of fixed equipment, buildings, land, and cargo handling equipment as the input variable.

Measuring labor inputs, broadly speaking, are taking into account stevedoring, port authority employees, container terminal labor and other labor expenditures (Jim Wu & Goh, 2010).

Referring to the output variables of the port system, most researches use the number of containers or cargo throughput to measure efficiency or assess port operation performance (Jim Wu & Goh, 2010).

Several other input variables have been proposed, for example, (Tongzon, 2001) proposed the number of tugs and the amount of delay time as inputs. Taking into account the variables to measure efficiency, the nowadays ports should be prepared for the increasingly demand of the containerized cargo.

Figure 1 shows the rate increase of containerized cargo capacity in the last 23 years.

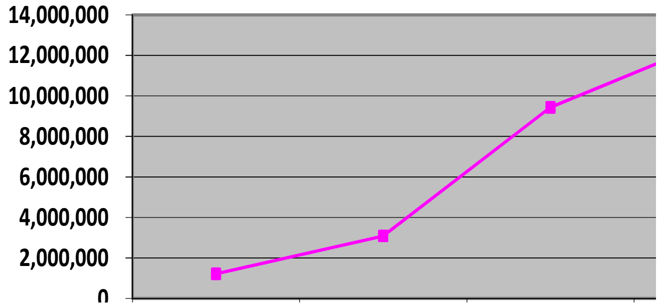

Fig. 1. Long term cellular ships capacity in TEU´s. Ships Bigger than 100 GT

Source: (United Nations Conference on trade and Development, 2010)

Figure1 shows that the total of TEU´s moved worldwide in 1987 was 1.215.215, while in 2010 was 12.824.648 TEU´s, which represents a remarkable increase in quantity and volume. For this reason, improving port efficiency or productivity has become a critical yet challenging task in the development of many countries (Turner, et al., 2004).

Ports develop a public interest activity, thus, the State to which they belong should participate in its regulations, and it is mainly the State who defines how the port ´s system of each country should be, establishing its management policies (Estrada, 2007).

3. CASE OF STUDY: VENEZUELA

In Venezuela, by a presidential order, central government took over control of the ports from regional governments. Private handling companies were nationalized, so far without compensation. The ports are now jointly run by a State company, Bolipuertos (with a 51% stake), and an outfit called Asport (with a 49% stake), owned by the Cuban government. Curiously, Cuba-hardly the Singapore of the Americas-is also paid to “advise” Venezuela on port operations (The Economist, 2012).

Business people say that port infrastructure has deteriorated since the nationalization, thanks to poor maintenance and inexperienced management, adding to the time that ships must wait offshore. In the past year (November 28) 10 ships were anchored outside of the Port of La Guaira and 18 off the country’s main port, Port of Puerto Cabello. Since then, the Bolipuertos web page that gives such figures has been off-line “for maintenance”. To add to the problem, Port of La Guaira is operating at only two-thirds of its normal capacity while the port builds a new container terminal, intended to handle trade with MERCOSUR, the trade bloc which Venezuela recently joined (The Economist, 2012).

Venezuela signature to MERCOSUR (Mercado Común del Sur), was in order to reduce tariff and rates of products commercialized with member countries (Brasil, Chile, Argentina, Uruguay and Paraguay), but this will not be an enough measure to increase commerce between countries if the Venezuelan ports do not insert themselves into modernization of its infrastructures, hinterlands and ways of access to the port (Lam, 2006).

According to Rusvel Gutierrez, president of the Venezuelan Custom Agents Chamber, only 4 wharfs of 24 are operatives in La Guaira Port, using only 30% of its capacity. He says there is not a reasonable explanation for such situation, since the expansion works made at the port, just affects section 8, but not the terminal areas where vessels arrive (López, 2012)
Red tape has proliferated in Venezuelan ports. In addition to the lack of wharfs and customs and sanitary inspections, cargoes must be separately checked for adherence to foreign-exchange and other controls and examined for drugs by the National Guard. It can be weeks before a container is released. In all, goods can take longer to get from the port of La Guaira to Caracas, 25 kilometers (16 miles) away, than from China to Venezuela (The Economist, 2012).

4. LOGISTICS & ECONOMICAL’S EFFECTS

In Venezuela, the failure in port efficiency, an essential link of the logistic chain, brought a summer Christmas in some cases; in others, Christmas did not arrive.

Natural Canadian Christmas trees, used to decorate homes in December, had more than three weeks of delay in the Port of La Guaira, waiting for nationalization. Dealers assure they waited the trees to arrive as lately as November 16, since if they don’t sale them, they don’t sale the ornaments to decorate it either (Sojo, 2012).

Yiannis Assimakopoulos, Manager of Florandes, a store located in the town called La Hoyada (a place in Caracas city), says that “products delays more in arriving from La Guaira (the port) to our store, than from China to La Guaira”. Likely, she assures that failures in supplies are a constant, but last weeks it has been even worst (Sojo, 2012).

The Venezuelan Chamber of Toys, Sports and Entertainment is also worried about the arrival of its merchandise. It denounces that the slow imports legalization processes, changes in licenses and the priority it ensures the port offers to the governmental cargoes, have contributed to port congestion, delaying more than 60% of toys that arrive to the country. Elizabeth Rama, the Chamber´s president, notes that charging and discharging time have been duplicated comparing it to prior years, which affects its associates in storage costs, merchandise guard, payments to carriers and even more, the merchandise lost because of legal abandonment (Sojo, 2012).

Fig. 2. ***Port of La Guaira- Venezuela (With the Vessels anchoraed waiting for berth)***
Source: (Web of the Ministery of Information of Venezuela)

On November 15, there were 30 vessels in the Port of Puerto Cabello´s shore, waiting for a wharf to go to berth. In an interview made to Neidy Rosal, member of a Commission in the Carabobo State (where the port is located), said, based on a port movement inform made by that entity, that 14 of those 30 vessels contain food such as yellow and white corn, rice and sugar (needed to prepare traditional Christmas food) and that according to the information they manage, vessels are spending an average of 12 days in bay waiting for a wharf to be assigned. Furthermore, when that happens, the discharge time delays as much as 72 hours (Romero, 2012).

Fig. 3. Port of Puerto Cabello- Venezuela (With the Vessels anchoraed waiting for berth)
Source: (www.google.es)

According to the President of the Custom Agents Chamber, Gutierrez, R., on December 11, there were still containers with Christmas trees and other season products, and 10 vessels waiting for a berth to go to. Importers are requested with about 5.000 Bs. (833 EU at the official rate) to arrange containers movements from wharf to container yard, in order to get the reception act needed to proceed with nationalization. (López, 2012). Christmas trees sales decreased 30% relating to the same period in 2011 (Rodríguez, 2013).

In addition to governmental problems in Puerto Cabello, "there has been a lack of light (power) almost every day, paralyzing administrative work since it does not have electric plants. If there is no power, there is not bank, not tariffs payments, which brings an additional delay", says the governmental worker Neidy Rosal. She also notes that nationalization time last as much as 18 days, since there is not a unique consignment window or a unique revision process (Romero, 2012).

Martínez de Oses & Velásquez Correa, (2012) when referring to the unique consignment window, they say it benefits Port´s communities and Cargo Transport, since it reduces administrative procedures that implies documents creation, interchange and verification. A documental management that difficult efficiency and could block the goods flow. Since in both communities work different actors, places, ambits and domains, the unique windows should be interconnected with official data, private and public, that allows making the usual verifications of:

a. Ships and other modes of transport

b. Merchandise

c. Services and supplies

d. Port controls and flags permissions

e. Phytosanitary controls

f. Custom

g. Terminal

h. Port´s authorities

i. Traffic Control Systems

j. Safety and Security systems controls

k. Commercial rules

l. Insurances

It could be said that information flow should occur simultaneously or previously to the passengers and goods flow, which would ensure administrative procedures simplification at the unique window, under the premise One Stop Shop (Martínez de Oses & Velásquez Correa, 2012).

In La Guaira and Puerto Cabello port, in addition to the lack of a unique consignment window, there are also all the problems already mentioned, which affect all the logistic chain when the link port fails due to a failure in input and output variables to measure port efficiency, such as wharf availability, its dimension, the labor force, the equipment available to charge, discharge and move merchandise and the number of containers through the port. That explains why those dealers who imported Christmas goods since August 2012, where those who could sale it on time for the season celebration.

Up to January 04, there were still containers with Christmas products at the port, as well as vessels ride at anchor, waiting for going to berth. Dealers ensure that imported goods nationalization goals were not accomplished, and that there are still many containers with Christmas and other products repressed at La Guaira port. Vessels keep coming, since the Venezuelan economy is a port economy where at least 70% of goods are imported. According to Quintana, the Vargas Fedecamara´s vice president, on January 03, there were 5 vessels ride at anchor in La Guaira port waiting for berth, 8 at wharf waiting to discharge containers and 6 in discharge plans" (Rodríguez, 2013).

Among the containers stuck at port, there are some with olives, one of the main ingredients to prepare the national season dish, called Hallaca, and the ham Bread (typical season accomplishment). There is not an estimated time to deliver those containers. (Rodríguez, 2013).

Also, is very curious to know that, according to the actual port's practices, there is not any specific environmental's policy, only the national & international regulatios, adopted by the country (MARPOL), but there is a lack of implication in this regard, i.e. the application of the ISO14000 or something in relation with, or others initiative with the idea of prevent the Port's Pollution.

Also, having in mind the usual electrical blackouts, this miss can be also relationed with the warranty of “safe operation”, so the stardard policies, usually applied on the majority of the ports, are not reflexed on the daily port’s practices, due to are not fosued to the port’s operations & port’s Facilities, so, this is a very complex problem to study and developed, on future investigations.

Not only the Christmas ornaments that were at stores since August where those that fulfill the seasonal Venezuelan spirit, but also toys and food that came in vessels arrived in summer. Particularly, I consider that the Venezuelan typical dish should have change its name this year, since its name “Hallaca” comes from the union of two words, “allá” (there) and acá (here) due to the origin its ingredients, from there: Spain; and from here: Venezuela. Nevertheless, this year the only products in supermarkets were those from here “aca”, so this year we did not have “hallacas”, but just “acas”. Seems like, also in this case, global logistics growth is back to society, and even approaching it from the standpoint of preserving the environment, society has every interest in preserving it, because the survival of the species depends mainly on the existence of the planet (Martínez J, 2011).

As possible solutions, rethink the theoretical foundation of logistics today, brings a change of consciousness that allows us to address sustainable, economic growth and social development (Martínez J, 2011) and, in order to elaborate a special plan for the development of better post’s systems, to make an analytical review of all the port’s functioning with the aim to find the best local solution to find the Port’s Eficiency and Port Development with a real good ecological & socio-economical’s impact.

REFERENCES

[1]. Brooks, M. - **Sea *Change in Liner Shdipping***. Pergamon, Oxford, s.n., 2000

[2]. Cullinane, K. & Song, D.-W. - ***A stochastic frontier model nof the productive efficiency of korean container terminals***. Journal of Applied Economics, 35(3), pp. 251 - 267, 2003

[3]. Dow, T. & Leschine, T. - ***Container terminal productivity: a perspective***. Journal of Maritime Policy and management, 17(2), pp. 107 - 112, 1990

[3].Estrada, L. - ***Mejora de la competitividad de un puerto por medio de un nuevo modelo de gestión de la estrategia aplicando el cuadro de mando integral***, Doctoral Thesis, Universidad Politécnica de Madrid. [Online], 2007

[4]. Graham, M. - ***Stability and competition in intermodal container shipping: finding a balance***. Journal of Maritime Policy and Management, 25(2), pp. 129 - 147., 1998

[5]. Jim Wu, Y., C. & Goh, M. ***- Container port efficiency in emerging and more advanced markets***. Journal of Transportation Research, 46, pp. 1030 - 1042, 2010

[6]. Lam, J. - ***Managing container shipping supply chains***. In: Proceedings for the International Association Of Maritime Economists Annual Conference, Melbourne: CD-Room, 2006

[7]. Liu, Z, - ***The comparative performance of public and private enterprises: the case of British ports***. Journal of Transport, Economics and Policy, 29(3), pp. 263 – 274, 1995

[8]. López, L. - ***20 muelles siguen inoperativos en el puerto de La Guaira***. El Nacional, 24 12, p. Economía 5, 2012

[9]. López, L. - ***Continúa Represada Mercancía Navideña***. El Nacional, 11 12, p. Economía 6, 2012

[10]. Martínez de Oses, X. F. & Velásquez Correa, S.- ***“e” a New Paradigm in Navigation and Maritime Transport: “ELECTRONIC – ENHANCED - ENVIRONMENTAL***”. Rideport, 1(1), pp. 10 - 14., 2012

[10]. Martínez Marín, Jesús E. - ***Impact of Logistics and Shipping In The Sustainable Development of Societies***. Journal of Marine Technology and Environment- Vol-II, 2011 , pp 55-61, 2011

[11]. Rodríguez, D. M. - ***Aceitunas y juguetes permanecen en contenedores. Mercancía de Navidad continúa en los puertos***. El Nacional, 04 01, p. Economía y Negocios 4, 2013

[12]. Romero, T. - ***30 buques permanecen en muelle de Puerto Cabello***. El Nacional, 16 11, p. Ciudadanos 8,2012

[13]. Siu Lee Lam, J. - ***Patterns of Maritime Supply Chains: Slot Capacity Analysis***. Journal of Transport Geography, Issue 19, pp. 366 – 374, 2011
[14]. Sojo, M. F., - ***Sin llegar pinos y juguetes por congestionamiento en los puertos***. El Nacional, 17 11, p. Ciudadanos 1, 2012
[15]. The Economist, - ***Venezuela's ports Cancelling Christmas***. [Online] Available at: http://www.economist.com/news/americas/21567381-inefficiency-promoting-autarky-perhaps-design-cancelling-christmas [Accessed: 09 12 2012
[16]. Tongzon, J. - ***The impact of wharfage costs on Victoria´s export oriented industries***. Journal of Economic Papers, 8, pp. 58 – 64, 1989
[17]. Tongzon, J. - ***Efficiency measurement of selected Australia and other international ports using data envelopment analysis***. Journal of Transportation Research, 2(35), pp. 107 – 122, 2001
[18]. Turner, H., Windle, R. & Dresner, M. - ***North American container port productivity***: 1984 - 1997. Journal Transportation Research Part E: Logistic and Transportation Review, 4(40), pp. 339 – 356, 2004.
[19]. Web of the Ministery of Information of Venezuela http://www.minci.gob.ve/2012/08/modernizan-puerto-de-la-guaira/ [Accessed: 09 12 2012].
[20]. United Nations Conference on Trade and Development, U.,. Secretary´s Office Report, Geneva: United Nations, 2010

NUMERICAL CALCULATION OF HYDROCARBON SEPARATION PROCESSES IN BILGE INSTALLATIONS USING VOLUME OF FLUID METHOD

[1]SCUPI ANDREI-ALEXANDRU, [2]DINU DUMITRU, [3]DOBRE ANDREI-MIHAI

[1,2,3]*Constanta Maritime University, Romania*

The ballast-bilge installation on board of a commercial ship has many purposes (correction of the position of the center of mass of the vessel, transferring and disposal of liquid ballast overboard, discharging overboard the water bilge collected). These installations are extremely important for transport efficiency and environmental protection.
The paper presents the use of numerical computation for studying the hydrocarbon separation process in bilge installations. The separation process is significant because we must assure that all the hydrocarbons are well isolated so no environmental damage will be done. In the simulation process we were able to visualize all the parameters participating that characterize the process (density, pressure, velocity, turbulent kinetic energy, and turbulent intensity). The volume of fluid was discretized into a structured mesh using uniform quad methods of discretising.
These installations are used by both commercial and leisure ships and on on-shore and on off-shore structures. The process of hydrocarbon separation is done in various branches of industry.

***Keywords**:* bilge installation, CFD, hydrocarbon separation, volume of fluid method, mixture of fluids.

1. INTRODUCTION

Ships are equipped with on-board facilities for navigation security, integrity of transported goods, conditions necessary for living and for work of crew and passengers.
Ships are generally equipped with a large variety of plants that perform specific functions can be classified according to several criteria: purpose, applicability to various ships, working fluid, and the degree of participation in maintaining the vitality of the ship.

One of the most important installations is the ballast-bilge installation. It has many purposes such as: it is used to correct the position of the center of mass of the vessel by boarding, to transfer and disposal of liquid ballast overboard and to discharge overboard of bilge water collected; these facilities consist of ballast enclosures and circuit drainage pumps interdependent with each other that can have common and shared portions of pipelines.

This grouping of two different installations is allowed by common fluid agent the sea water, and the location of both facilities in the ship's bottom. Also, this association imposes a use of a smaller number of pumps, pipes of smaller length and hence reduces the weight and volume of the system. Generally a bilge installation consists of the following elements: collection boxes (for bilge wells collector drainage); the main drainage pipe and branches; boxes maneuver with caution; sludge filters; bilge pumps; bilge separator; main pipe for discharging overboard [2].

To avoid waste discharged overboard a separation of hydrocarbons accumulated bilge is necessary. Hydrocarbon separation can be done in several ways; the most commonly used way is the gravitational separation and centrifugal-gravitational separation. This paper focuses on gravitational separation processes of hydrocarbons in bilge installations using numerical computation.

The main objective of the paper is to understand how the separation takes place, how much time does it take to complete the process and how numerical programs can can help in for a better comprehension of the installation utilization. Because a full-scale experiment is difficult to perform, we used a numerical program ANSYS-Fluent v.13.

With the help of Ansys program, we were able to determine how much time it took for the fluids to separate for a certain volume and what value had the parameters at a certain time. Analytically, if we consider a particle volume V and the density of hydrocarbon ρr located at the bottom of a water box of density ρw. We have an Archimedes force acting on the particle F1 pointing upward and a force F2 opposing called the drag. When the particle velocity reaches a value large enough the force F2 is equal to the force F1. From the equality of the two forces results a sedimentation velocity W_g [1,2].

$$F_1 = (\rho_w - \rho_r) \cdot V \cdot g[N] \tag{1}$$

$$F_2 = \frac{\xi \cdot A \cdot \rho_w \cdot W_g^{\ 2}}{2}[N] \tag{2}$$

$$F_1 = F_2 \Leftrightarrow W_g = \sqrt{\frac{2 \cdot g \cdot V \cdot (\rho_w - \rho_r)}{\xi \cdot A \cdot \rho_w}} \tag{3}$$

2. NUMERICAL SIMULATION

2.1 Geometry characteristics

Since gravitational separation of hydrocarbons is usually done in rectangle boxes, we have chosen a rectangle box with the following dimensions 0.05x 0.02x0.001 m. (Fig. 1).

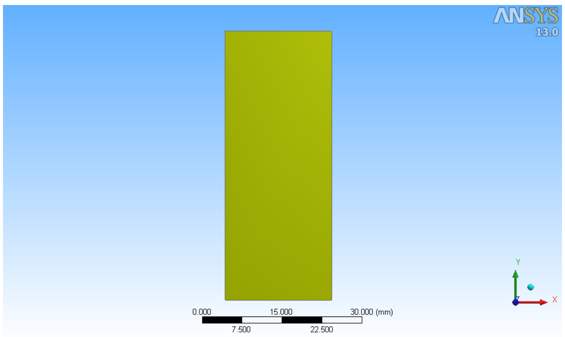

Fig. 1 Geometry design

2.2 Geometry discretization

After the representation of the geometry, we went to its discretization. In mathematics, discretization concerns the process of transferring continuous models and equations into discrete counterparts. This is done using quantization. Quantization is the process of mapping a large set of input values to a smaller set – such as rounding values to some unit of precision. A device or algorithmic function that performs quantization is called a quantizer. The error introduced by quantization is referred to as quantization error or round-off error [3].

A structured grid was created using the automatic method. In total it was made of 1 x 10^3 cells with 1.4 x 10^3 nodes (Fig. 2).

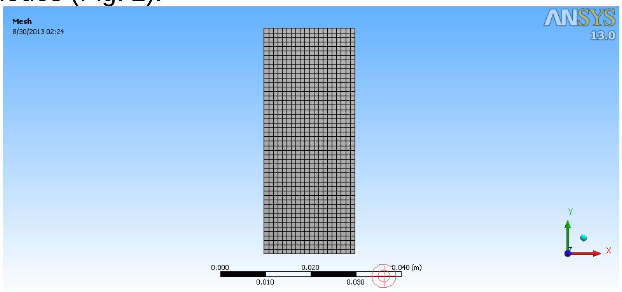

Fig. 2 Domain discretization

2.3 Calculation of the studied case

We have chosen 2 main fluids: water with a density of 1000 kg/m^3, a dynamic viscosity equal to 0.001003 kg/ms, a cinematic viscosity equal to 0.1003x$10^{-5}$$m^2$/s, and diesel oil with a density of 730 kg/m^3, a dynamic viscosity equal to 0.0024 kg/ms, a cinematic viscosity equal to 0.3287x$10^{-5}$$m^2$/s. Both fluids were put together in the box in the same time, and then over time the fluids gravitationally separate. We have chosen representatively a 0.8 volume fraction of water and 0.2 volume fraction of diesel oil.

The flow was numerically computed using Fluent. We have chosen k-ε model and the SST subgrid-scale model. The case was run for about 20000 iterations, Fluent allowing us to visualize and export the graphics that show the variation of density, volume fraction, pressure, velocity, kinetic energy etc.

To calculate the two-phase transportation (air and wheat) we have used the volume fraction method. The volume fraction method relies on the fact that two or more fluids are not interpenetrating. For each additional phase that is added to the model, a variable is introduced: the volume fraction of the phase in the computational cell. In each control volume, the volume fraction of all phases sum to unity. Thus, the variables and properties in any given cell are either purely representative of one of the phases, or representative of a mixture of the phases, depending upon the volume fraction values [4].

$$\frac{1}{\rho_q}\left[\frac{\partial}{\partial t}\left(\alpha_q\rho_q\right)+\nabla\cdot\left(\alpha_q\rho_q\right)=S_{\alpha_q}+\sum_{p=1}^{n}\left(\dot{m}_{pq}-\dot{m}_{pq}\right)\right] \tag{4}$$

where: $\dot{m}_{qp}$ is the mass transfer from phase q to phase p and $\dot{m}_{pq}$ is the mass transfer from phase p to phase q; α_q is the volume fraction of the phase q and S_{α_q} is a specific constant.

For turbulent model k-epsilon: the program used the equation for turbulent kinetic energy k (5), disipation epsilon (6) and the energy equation (7) [4]:

$$\frac{\partial}{\partial t}\left(\rho_m k\right)+\nabla\cdot\left(\rho_m\bar{v}_m k\right)=\nabla\cdot\left(\frac{\mu_{t,m}}{\sigma_k}\nabla k\right)+G_{k,m}-\rho_m\varepsilon \tag{5}$$

$$\frac{\partial}{\partial t}\left(\rho_m\varepsilon\right)+\nabla\cdot\left(\rho_m\bar{v}_m\varepsilon\right)=\nabla\cdot\left(\frac{\mu_{t,m}}{\sigma_\varepsilon}\nabla\varepsilon\right)+\frac{\varepsilon}{k}\left(C_{l\varepsilon}G_{k,m}-C_{2\varepsilon}\rho\varepsilon\right) \tag{6}$$

$$\frac{\partial}{\partial t}(\rho E)+\nabla\cdot\left(\bar{v}(\rho E+p)\right)=\nabla\cdot\left(k_{eff}\nabla T-\Sigma_j h_j \bar{J}_j+\left(\bar{\tau}_{eff}\bar{v}\right)\right)+S_h \tag{7}$$

where:

$$\rho_m=\sum_{i=1}^{N}\alpha_i\rho_i\ , \tag{8}$$

$$\bar{v}_m=\frac{\sum_{i=1}^{N}\alpha_i\rho_i\bar{v}_i}{\sum_{i=1}^{N}\alpha_i\rho_i}\ , \tag{9}$$

$$\mu_{t,m}=\rho_m C_\mu\frac{k^2}{\varepsilon}\ , \tag{10}$$

$$G_{k,m}=\mu_{t,m}\left(\nabla\bar{v}_m+\left(\nabla\bar{v}_m\right)^T\right):\nabla\bar{v}_m\ , \tag{11}$$

where k_{eff} is effective conductivity; J_j fluid diffusion flux j; S_h heat due to chemical reaction. In the equation (7) we have:

$$E=h-\frac{p}{\rho}+\frac{v^2}{2}\ , \tag{12}$$

where h – enthalpy; for ideal fluids (13) and for real fluid (14):

$$h=\Sigma_j Y_j h_j\ , \tag{13}$$

$$h=\Sigma_j Y_j h_j+\frac{p}{\rho}\ , \tag{14}$$

$$h_j=\int_{T_{ref}}^{T}c_{p,j}dT\ . \tag{15}$$

3. RESULTS AND DISCUSSION

It is important to visualize the variation of the parameters mentioned above because each one of them has a key role in understanding who the process develops.

At the beginning of the process (t=1s) the mixture of fluids starts to separate (Fig. 3) and we can see that the velocity values are not negative which implies a motion of the particles of the fluids (Fig.4). It is also represented by figure 5 which also shows that in the middle of the box we have the maxim kinetic energy. On the other hand figure 6 presents the variation of turbulent intensity. We can see that the maxim turbulent intensity only reaches 2.5 % which implies that we are dealing with a stationary fluid.

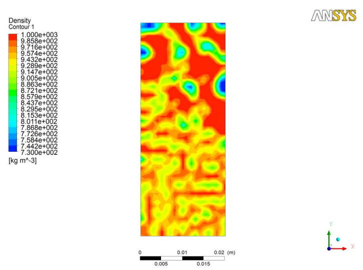

Fig. 3 Density of fluid mixture at t=1s

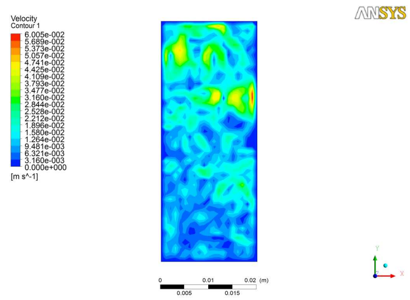

Fig. 4 Velocity of fluid mixture at t=1s

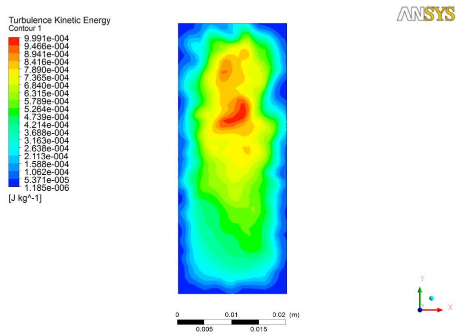

Fig. 5 Turbulent kinetic energy at t=1 s

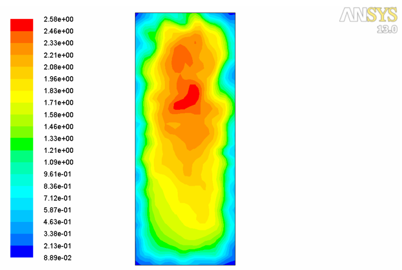

Fig. 6 Turbulent intensity at t=1s

Close to the end of the process the fluids have fully separated (Fig. 7 and Fig. 8).

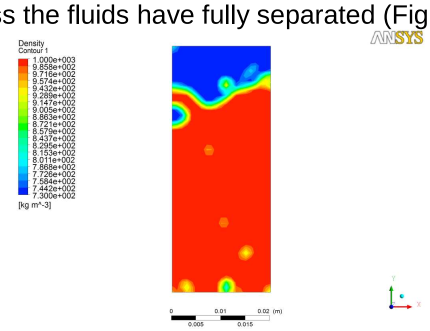

Fig. 7 Density of fluids at t=4s

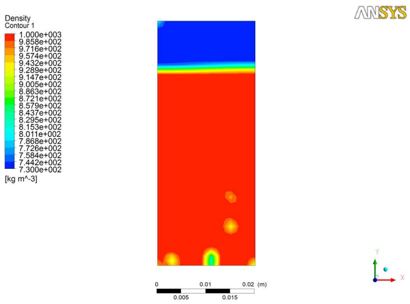

Fig. 8 Density of fluids at t=5s

The graphic of pressure variation (Fig. 9) shows the fact that fluid with the lower density acts as a load on top of the fluid with higher density.

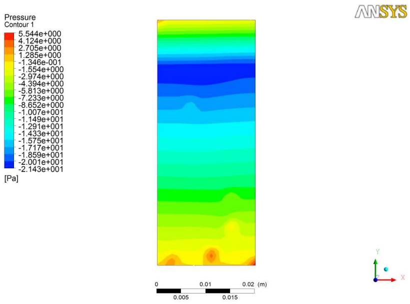

Fig. 9 Pressure of fluids at t=5s

The total time duration of the process was around 5 seconds, for a volume of 1000 mm^3.

4. CONCLUSIONS

Numerical computation represents a way to solve a mathematical model and to simulate physical complex phenomena. Therefore the person who uses a computational program to simulate a real physical phenomenon must well understand the physical processes that take place, must know how the software operates so that he can correctly interpret the data that the computer has to offer [3].

The data represented in Figures 3 to 9 present the gravitational separation process that generally takes place in a bilge installation. If we have two or more fluids mixed together we have to know how much time it takes for the fluids to separate. Numerical computational programs offer us the answer and not only this. They will also show us how the parameters involved in the process develop over time.

REFERENCES

[1]. Dinu D. - ***Mecanica fluidelor pentru navalisti***, Ed. Nautica, Constanța, 2010
[2]. Ioniță I.C., Apostolache J. - ***Instalații navale de bord-Construcție şi exploatare***, Editura Tehnică Bucureşti, 1986
[3]. Scupi, A., Dinu, D. - ***Unsteady Flow Over A Bluff Body With Application In Unconventional Propulsion System***, 6th WSEAS International Conference on Manufacturing Engineering, Quality And Production Systems (MEQAPS '13), Braşov, 2013
[4]. Ansys-Fluent v.12, ***Theory guide***, 2007

STATION KEEPING STUDY OF OFFSHORE AQUACULTURE OCEANIC FARMING SYSTEM

[1]SULAIMAN O., [2]WAN NIK, W.B., [3]SAMAN AB.,

[1,2]Maritime Technology Department, University Malaysia Terengganu, [3]Marine Technology Department, University Teknologi Malaysia

Offshore aquaculture system require reliable structural integrity and mooring system design for ultimate state limit, fatigue state limit and accidental and progressive state limit against environmental loading and accidental loading. To avoid mooring system failure, selecting an appropriate breaking strength and limit state for mooring system components is necessary. Suitable mooring system has been designed by group of researchers at Universiti Malaysia Terengganu. Valuable information was obtained from Technip and BV. The system has been tested in towing tank in Universiti Teknologi Malaysia. This paper describes mooring system design that account for forces and environmental loadings. The paper describes evaluation of optimum mooring performance in wave, wind and current loadings on mooring components anchor buoy and riser elements that are involved the mooring system dynamics.

***Keywords**:* aquaculture, dynamic loading, marine, offshore, structure

1. INTRODUCTION

Floating offshore aquaculture farms drift at the mercy of ocean currents, wind and waves. They are designed to move easily up and down in a vertical motion that can range up to several meters under normal sea conditions and tens of meters during a storm. Although these systems can be positioned at depths that avoid storm damage, a major challenge of such floating systems is the uncertainly of where the farms may end up after a storm. There has been renewed interest in floating farms in recent years as platforms and technologies have improved to withstand open ocean conditions. Almost all that were moderately successful have combined a floating platform with a tethered or anchored component (Buck et al, 2006). Most aquaculture systems are tethered to the sea floor through anchors, floats and lines.

Recently, large scale cultivation of seaweed have been develop to meet the increasing market demand and at the same time to provide alternative livelihood schemes for local populations. The large farming expansion near onshore is likely to bring so much problem. In some cases, unfavorable environmental factors such as near shore pollution from sewage is pushed marine farming sites further offshore to water depths of 50 m or greater. Thus the need to move operations into more exposed sites and in totally unprotected open sea may have to face devastating natural disasters caused by tropical storms is becoming necessary. In moving offshore, wave, current and wind forces increase rapidly (North, 1987). This means that maximum wave heights of 5-10 m, current speed of 2-3 knots and wind speed of 35 m s-1. This situation can occur at the same time and in the same direction. A requirement is, therefore, that the farming unit may be able to withstand conditions like these. Mooring system design is a trade-off between making the system compliant enough to avoid excessive forces on the farming platform, and making it stiff enough to avoid difficulties, such as damage to , caused by excessive horizontal excursions of the farming platform. This study use South China Sea, Terengganu as a case study (Naylor, 1996). Figure 1 shows the location of research area.

Fig. 1. Location of research area (Google Earth, 2011)

2. MOORING GEOMETRY

Design criteria specific for the site in the coast of setiu were established prior to the engineering analysis and specification of components. It necessary that the new mooring be able to accommodate 100M x 1000M planting block shape, the Block had to be able to withstand the waves and currents that occur at the site, especially those associated with extreme storms. The mooring system also needed to be designed to minimize entanglement of seaweed planting. The design constraint required that the mooring system be deployed in the existing permitted site approximately 200 meter from the shore. The site is 10-50 meter of water depth and the bottom composition consists of relatively heterogeneous materials, which include bedrock outcroppings, gravel and muddy sands. Figure 2 showing the top view of the mooring system (O.O. Sulaiman et al).

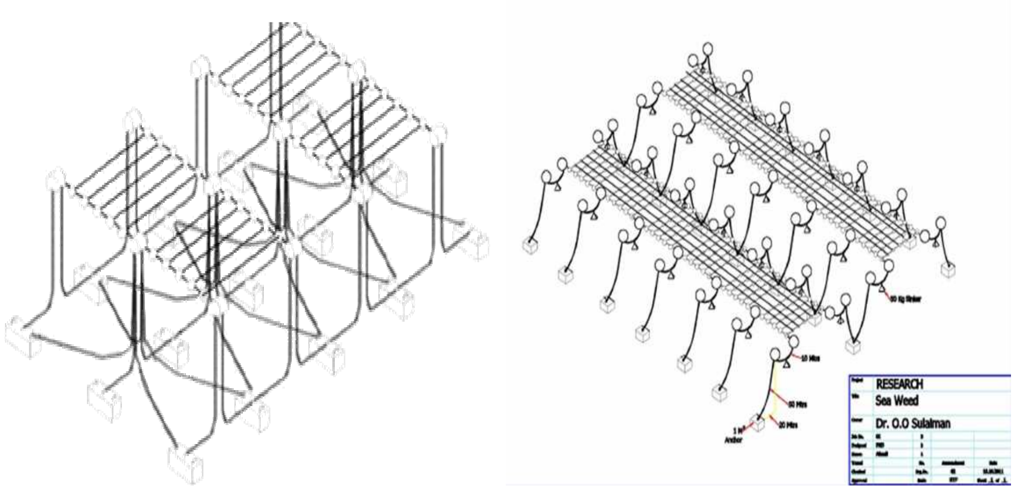

Fig.2: Mooring geometry

3. DATA ACQUISITION PROCESS

Mooring Analysis

For this study, current are considered because of the dominant contribution of load compared with wave and wind. Static current loads are discussed in detail below. Static loads due current are separated into longitudinal load, lateral load. Flow mechanisms which influence these loads include main rope drag, main buoy drag, seaweed drag, and planting lines drag (Chakrabarti, 2005).

Total load is determined using the following equation,

$$F_{total} = F_{main\ rope} + F_{buoy} + F_{loadlines} + F_{seaweed}. \quad (1)$$

Total load is determined using the following equation,

$$F_{total} = F_{main\ rope} + F_{buoy} + F_{loadlines} + F_{seaweed}. \quad (2)$$

The analysis of cables, or mooring lines that maintain surface and subsurface platform on station, is the study of the loads exerted on the lines by gravitational and time-invariant current fields and of their resulting effects. This study allows one to predict the geometry of the line between the structure and its anchoring point and the distribution of stresses from top to bottom. The study of mooring cable address the two-dimensional cases where the line and the current can be assumed to be coplanar (Skop, 1988). Forces that need to be considered are the immersed weight or the resultant gravity force per unit of cable length is usually defined as

$$P = B_c - W_{c\,1} \quad (3)$$

Where: B_c =is cable buoyancy per foot that is the weight of the water displaced by one foot of cable, W_c= is "air weight" of one foot of cable.

The hydrodynamic resistance due to current passing a cable element of diameter and the length, when normal to the flow as shown in the Figure 3.5 is given by

$$Rds = \frac{1}{2}\rho\ C_{DN} dV^2 ds \tag{4}$$

where : C_{DN}= Normal drag coefficient, V = Current speed

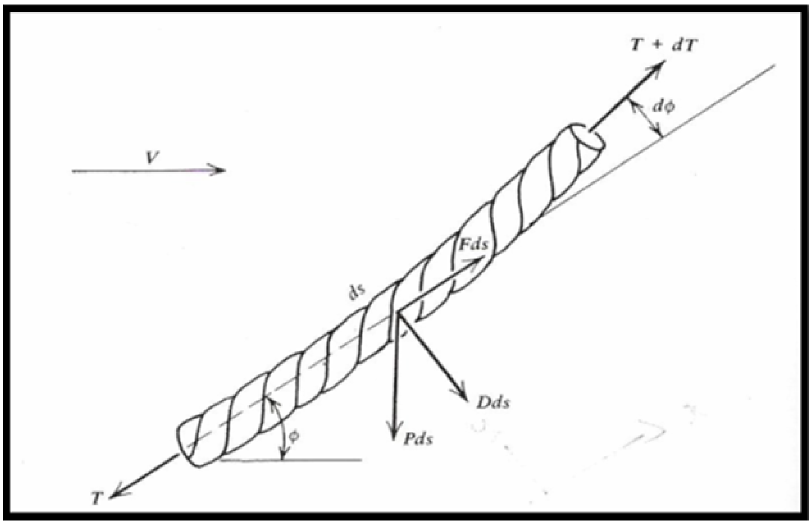

Fig. 3. Forces on cable element

If the cable element is at an angle φ from the current horizontal direction, its resistance can be considered to be made of two components: one normal and one tangential to the cable.
The normal component is given by

$$Dds = \frac{1}{2}\rho\ C_{DN} dV^2 \sin^2\varphi\ ds = R \sin^2\varphi\ ds \tag{5}$$

and tangential component given by

$$Fds = \frac{1}{2}\rho\gamma\ C_{DN}(\pi d)V^2\cos^2\varphi\ ds = \pi\gamma\ \cos^2\varphi\ ds \tag{6}$$

where : D γ C_{DN}= the tangential drag coefficient , $(\pi d)ds$ = the "skin" or longitudinal area of the cable element

For equilibrium to prevail the tension, T_1, in the segment must be

$$T_1 = \left[R_{X(0)}{}^2 + R_{Z(0)}{}^2\right]^{\frac{1}{2}} \tag{7}$$

Knowing that this segment is in line with the tension vector at its upper end, its inclination is given by

$$\theta_1 = \tan^{-1}\left[\frac{R_{z(o)}}{R_{x(o)}}\right] \tag{8}$$

Under the action of the pull T_1 the segment stretches to a length $s_{(1)}$

$$s_{(1)} = L_{(1)} + \Delta L_{(1)} \tag{9}$$

Where: $L_{(1)}$= segment original length, $\Delta L_{(1)}$ = elongation resulting from the applied ension

To determine the hydrodynamic coefficient of the design, the rows of seaweed are held using ropes separated by about 2.6 m between rows. A frame consisting of aluminium channel sections attached to the towing carriage is used. The seaweed clumps then attached to a rope line. Tension load cells will be attached between the line and the frame and the measured forces recorded on the model basin's data acquisition system. Figure 4 shows the aluminium test frame to hang the seaweed0 (API, 1997).

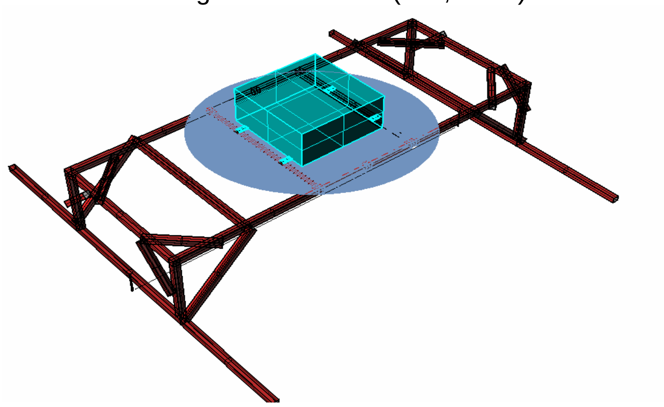

Fig. 4. **The aluminium test frame**

Fig. 5. **Test frame with seaweed attached**

Table 1 shows the data of the structure component used in this study. The full scale data were used to calculate the environment load on one block structure. Normal drag coefficient is used for the longitudinal load on the structure which is 90 degree. This is because 90 degree is considered maximum load. Tangential drag coefficient is used for the lateral load on the structure which is 0 degree. 0 degree is considered minimum load on the structure.

Table 1: Component properties

	Length (m)	Diameter (m)	Effective area (m^2)	Normal drag coefficient (cdn)	Tangential drag coefficient(cdt)
Main bouy	-	0 16	2 2	0 8	0 8
Main rope	100	0 022	0 8	1 3	0 008
Load line rope	100	0 008	0 020114	1 3	0 008
Seaweed plant	100	-	0 125	0 18	-

In this study, basic equation that will be used to estimate harbour vessels emissions is:

$$\text{Emission} \quad (E) = MCR \times Act \times LF \times EF \times FCF \tag{10}$$

Where;E = emission in (g/year) but converted to (tons/year) by dividing by 453.6 g/pound and 2000 pounds/ton, MCR = maximum continuous rated engine power, (kW), Act = activity, (hr/year),LF = load factor, (unitless),EF = emission factor, (g/kW.hr),FCF = fuel correction factor

4. RESULTS AND DISCUSSIONS

Mooring Line Properties

Table 2 shows the mooring line data used in this research. Type of mooring line used is the polyester rope. Other type of mooring line that normally used for moored platform is chain and wire rope. Water depth value is 50 meters from the seabed.

Table 2: Mooring Cable data

Mooring Line Data	Value	Units
Effective area of mooring line	0.001520531	m2
Diameter of mooring line, Dc	0.022	m
Length of mooring line	50	m
Mean sea level	50	m
Young modulus of mooring line	13200000000	N/m2
Segment length, Ln	1	m

Figure 6 shows that the drag current coefficient of tow two lines transverse across the basin is more higher than other four test case. This is because tow line transverse across the basin has more resistance compared to tow two lines longitudinally and tow two lines diagonally across the basin. Furthermore, for tow one line, tow one line transverse across the basin has more drag current coefficient compared to tow one line diagonally across the basin. It can be concluded that, at the transverse direction the drag current coefficient is higher than longitudinally and diagonally direction. Hence, the transverse direction should highly considered.

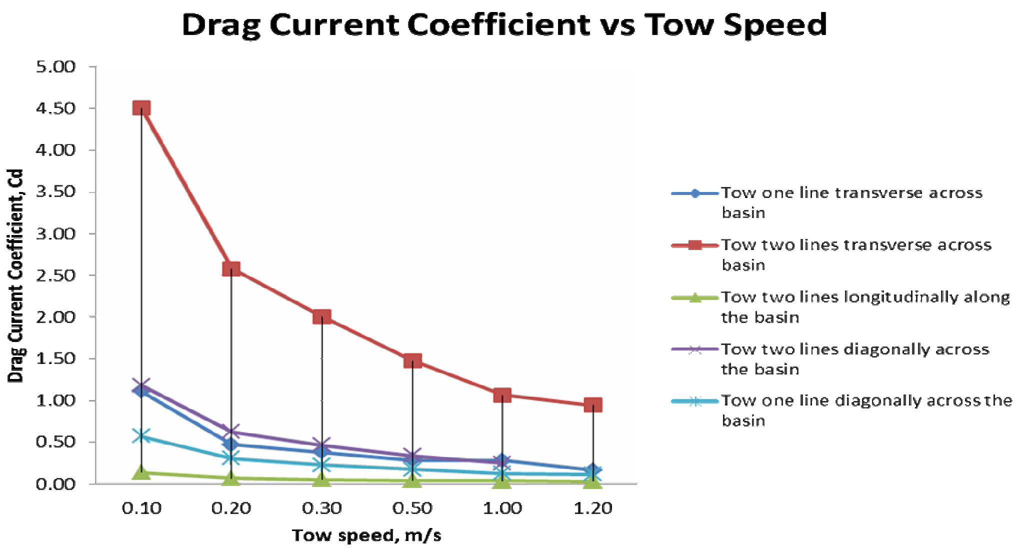

Fig. 6. Drag current coefficient at the tow test

Current Load Analysis

From the Table 3, four sample of current speed are taken. The current speeds start with 0.1 m/s, 1 m/s, 1.5 m/s and 2 m/s. The maximum longitudinal current load occur when the structure facing 2 m/s of current speed which has the value of 24916.61 Newton.

Table 3 Longitudinal current load

	No	Speed (m/s)	Longitudinal			
			0.5	1	1,5	2
Main rope	2	-	266.5	1066	2398.5	4264
Main buoy	4	-	902	3608	8118	14432
Load line rope	30	-	100.50	402.02	904.56	1608.11
Seaweed plant	1	-	288.28	1153.12	2594.53	4612.5
Total load	-		1557.28	6229.15	14015.59	24916.61

Table 4 Lateral current load

	No	Speed (m/s)	Lateral			
			0.5	1	1,5	2
Main rope	2	-	266.5	1066	2398.5	4264
Main buoy	4	-	902	3608	8118	14432
Load line rope	30	-	0.6185	2.474	5.5665	9.8960
Seaweed plant	30	-	86.48	345.93	778.359	1383.75
Total load	-		1255.60	5022.41	11300.42	20089.64

From the Table 5, four sample of current speed are taken. The current speeds start with 0.1 m/s, 1 m/s, 1.5 m/s and 2 m/s. The maximum lateral current load occur when the structure facing 2 m/s of current speed which has the value of 200.89.64 Newton.

5. CONCLUSIONS

Station keeping analysis is performed to determine the suitable mooring component to be equipped on the seaweed farming. Model test is carried out to determine environmental loading requirement of the system. Mooring behavior and it performances is determined for the feasibility of deploying floating structure for offshore aquaculture in exposed sites. The analysis serves as the basis for comparing and evaluating mooring systems tension.

REFERENCES

[1]. American Petroleum Institute - ***Recommended Practice for Design and Analysis of Station Keeping Systems for Floating Structures***, Recommended Practice 2SK, 2nd Edition, 1997

[2]. Buck, B. H. And Smetacek, V.- ***Aquafarm Roter Sand***, Vol. 2007, Alfred-WegenerInstitut fur Polar- und Meeresforschung, 2007

[3]. Naylor, J.- ***Production, trade and utilization of seaweeds and seaweed products***, FAO Fisheries Technical Paper No. 159. Food and Agriculture Organization of the United Nations. Rome, 1976

[4]. North, W. J. ***Oceanic farming of Macrocystis, the problems and non-problems***, In Seaweed Cultivation for Renewable Resources, Ed. Benson, K. T. B. a. P. H., pp. 3967, Elsevier, Amsterdam, 1987

[5]. O. O Sulaiman, Allan Magee, M Ilham A Razak, W.B. Wan Nik- ***Preliminary Design And Prototype Scale Model Of Offshore Acquaculture Floating Structure For Seaweed Ocean Farming***, ICSOT: Developments In Fixed & Floating Offshore Structures, 23 – 24 May, Busan, Korea, 2012

[6]. S.Chakrabarti- ***Handbook of Offshore Engineering**,* Vol 1, Elsevier, 2005

[7].Skop RA- ***Mooring system: a state of the art review***. J. Offshore Mechanical Arctic Eng; 110: 365-72, 1988

CONSTANTA TOMIS HARBOR ECOTOXICOLOGICAL ASSESSMENT USING MARINE ALGALTOXKIT BIOTEST

SUNDRI MIRELA-IULIANA

Constanta Maritime University, Romania

An ecotoxicological assessment of Constanta Tomis harbor aquatic area was done using Marine Algaltoxkit, a 72 h algal growth inhibition biotest. A toxicity of the samples less than 20% and a tendency of test species *Phaeodactylum tricornutum* to adapt to aquatic conditions were found.

Keywords*:* ecotoxicological assessment, microbiotests, Constanta Tomis harbor.

1. INTRODUCTION

Coastal zones, especially such ecosystems as cities areas or seaports, receive toxic inputs of various chemicals. Usually the management of contaminated water is based on the results of chemical analysis of a few substances.

Ecotoxicological risk assessment of polluted areas is difficult to do because a lot of substances can not be detected (analysis is limited) and the bioavailability and often synergic effects of substances can not be predicted.

The usefulness of applying bioassays as tools in evaluating damage to the health of marine ecosystems has been demonstrated in the last periods of time [1], [2].

Aquatic toxicity tests (bioassays) are used to assess the potential for damage to an aquatic environment and to provide qualitative and quantitative data on toxic effects on organisms from different chemicals [3].

The interest in biological testing is growing rapidly and small-scale bioassays have been developed. These miniaturized toxicity tests used test species, which are independent of the sourcing, the culturing and/or the maintenance of live stocks of test biota. Toxkits are microbiotests in kits containing all necessary materials including the test organisms to perform simple, rapid, sensitive and reproducible tests at low costs.

This study presents the results of the ecotoxicological evaluation of the aquatic ecosystem of the Constanta Tomis Harbor using Marine Algaltoxkit. This marine algal growth inhibition bioassay has been developed by the MicoBioTests Inc., Belgium, and has been modeled on and follows the prescriptions of the ISO guidelines.

2. METHODS

In March 2012 water samples were collected at 2 m depth from Tomis Harbor area using a Schindler- Patalas device.

A dilution series (100%, 50%, 25%, 12.5% and 6.25%) of the effluent sample was prepared by serial dilution. For ecotoxicological assessment we used a 72 h algal growth inhibition biotest performed in long cell test vials with the marine diatom *Phaeodactylum tricornutum*. The Algaltoxkit technology is bassed on the rapid measurement of the optical density of algal cell suspensions in special long cells (10 cm). Measurement of optical density was performed with a Jenway 6300 spectrophotometers a 670 nm filter, equipped with a holder for 10 cm cells. Optical density was converted into algal numbers with the aid of the special sheet included in Algaltoxkit. For growing algal cells an incubator with 20^0C temperature controlled and a 10000 lux constant illumination supplied by cool white fluorescent lamps was used. The test was performed with batch PT240811, according "Marine Algaltoxkit standard operational procedure" [4].

Optical density was converted into algal numbers on each cell using the special equation corresponding to the batch work (sheet included in Algaltoxkit). In this case was used the relation:

(1) $y = (1685849\ x - 105857)$

(y = cells number and x = optical density)

For calculated the average specific growth we used the equation:

(2) $\mu = (\ln N_2 - \ln N_1) / (t_2 - t_1)$

where

t_1 time of test start;

t_2 time of test finish

N_1 initial number cell density;

N_2 cell density at t_2;

The percentage inhibition to each test concentration is calculated from the following equation:

(3) $I_\mu = 100\ (\mu_c - \mu_t) / \mu_c$

3. RESULTS

Starting with the same cells number, algal populations growing was different depending on the concentrations of the harbor sea water sample. After 72 h test, the differences between algal population from control vials and 100% Tomis Harbor water sample concentration, the differences were not more than 40%.(Figure 1).

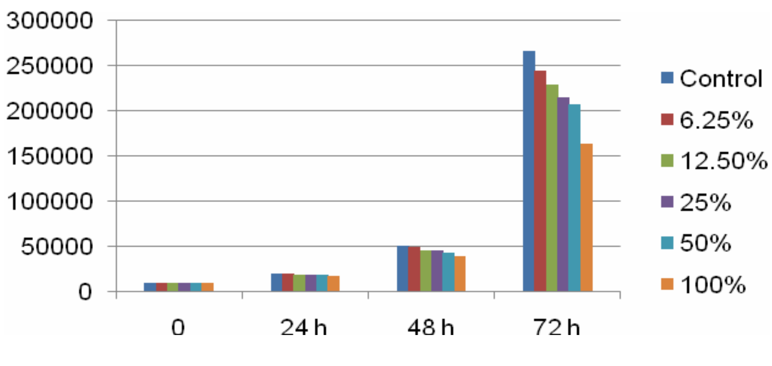

Fig.1. Algal concentration (cell number/mL)

For each Tomis Harbor water concentration, algal growth rate is greater than the day to day of testing (tab.1). In samples with 100% Tomis harbor water concentration, on the first day of testing algal growth rate was 82.23% of the algal growth rate in control group; on the third day of testing this percentage was 85.26%.

These behaviors suggest an adaptation of algal populations at the stress factor.

Tabel 1. Algal growth rate [%]

Time (h)	Control	Effluent concentration				
		6.25%	12.50%	25%	50%	100%
0 - 24 h	0.02802	0.02741	0.02619	0.02572	0.0244	0.02305
24 - 48 h	0.03818	0.03728	0.0362	0.03626	0.03458	0.03308
48 - 72 h	0.06872	0.06677	0.06633	0.06405	0.06254	0.05859
0 - 48 h	0.0331	0.03234	0.03119	0.03099	0.02949	0.02806
0 - 72 h	0.04497	0.04382	0.04291	0.04201	0.04151	0.03824

The largest percentage of algal cells growth inhibition was found for 100% Tomis Harbor water concentration: 17.7% after 24 h; 15.22% after 48 h and 14.97% for the whole period of testing (72 h). The algal growth inhibition was less then 10% for other concentrations (Figure 2).

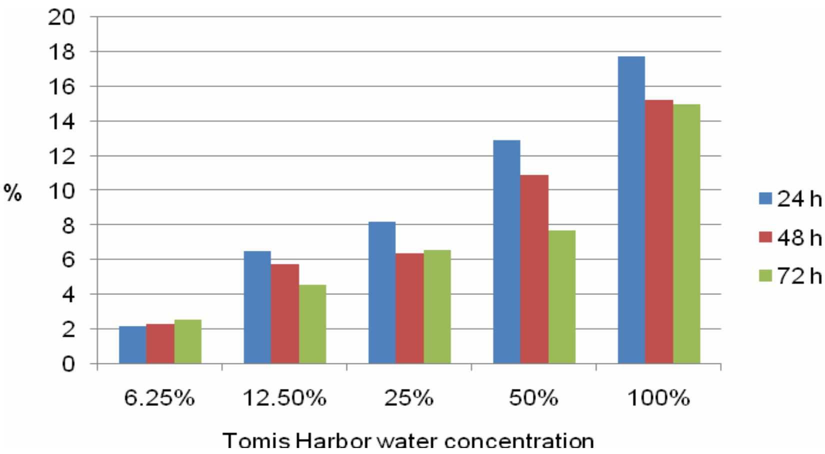

Fig. 2. Algal growth inhibition

We can consider that the sample taken from the Constanta Tomis Harbor does not have significant toxicity for *Phaeodactylum tricornutum* growth.

4. CONCLUSIONS

Testing conducted with the Marine Algaltoxkit allowed us to highlight the following:

- The ability to assess in the short time (72 hours) toxicity in the aquatic environment of Constanta.
- The toxicity of the sampled water of the harbor was less than 20% on the diatom *Phaeodactylum tricornutum* growth.
- A tendency of test species *Phaeodactylum tricornutum* to adapt to the conditions of the Constanta harbor aquatic environment, expressed through a reduction in inhibition of growth through generations of algal origin.

REFERENCES

[1]. Committee on Toxicity Testing and Assessment of Environmental Agents, Board on Environmental Studies and Toxicology, Institute for Laboratory Animal Research, Division on Earth and Life Studies, National Research Council *of the National Academie,* - ***Toxicity Testing in the 21st Century: A Vision and a Strategy,*** http://www.nap.edu/catalog/11970.html, 2007
[2] Persoone, G. and Vangheluwe, M.L. - ***Toxicity determination of the sediments of the river Seine in France by application of a battery of microbiotests***. In *New Microbiotests for Routine Toxicity Screening and Biomonitoring*, Persoone, G, Janssen, C. and De Coen, W. (eds), pp. 427-439, Kluwer Academic/Plenum Publishers, New York, 2000
[3] Persoone, G., Marsalek, B., Blinova, I., To¨ro¨kne, A., Zarina, D., Manusadzianas, L., Nalecz Jawecki, G., Tofan, L., Stepanova, N., Tothova, L. and Kolar, B. - ***A practical and userfriendly toxicity classification system with microbiotests for natural waters and wastewaters.*** *Environmental Toxicology*, 18(6), 395–402, 2003
[4] Microbio Test Inc. - ***Algaltoxkit. Toxicity test with microalgae. Standard operational procedure***.

ONE WAY TO IMPROVE GSP ACCURACY USING LOCAL METEOROLOGICAL DATA

[1]TSVETKOV MIROSLAV, [2]GROZDYU GROZEV, [3]CHAVDAR ALEXANDROV

[1,2,3]*"Nikola Vaptsarov" Naval Academy, Varna, Bulgaria*

This paper represents an approach for improving the accuracy of global positioning systems (GPS) measurements using local meteorological data. The current status of GPS accuracy is analyzed. The use of the data generated by the suggested model increases considerably the accuracy of GPS measurements.

Keywords: GPS, GNSS, DGNSS, Radio beacons, Troposphere

1. INTRODUCTION

Since their development, GNSS have passed a long way of transformation. They have been constantly subjected to modernization and improvement in order to provide maximum accuracy in positioning the users. Presently the accuracy of GNSS Navstar is 36 meters of horizontal accuracy (2drms) and 77 meters of vertical accuracy (2drms), the accuracy of GNSS GLONASS is similar and sometimes better. The accuracy requirements of various countries and organizations are different, but the common is that, the accuracy must be higher as possible.

Different kinds of augmentation systems have been developed for increasing the GPS measurement accuracy. There are wide area (WAAS, EGNOS, MSAS), regional (SkyFix, StarFix, Eurofix, GRAS) and local (maritime, aeronautical, geodetical) augmentation systems. The best accuracy is achieved when using data from a local reference station situated near the user.

Table 1 summarizes the quantity estimation of error sources, derived from the relevant information, their typical values and elimination of some of them by using data from reference station (differential technique). The typical values are represented in meters and corresponding percentage values.

Table 1 shows that the sum of errors on account of Ionosphere refraction, Troposphere refraction and Ephemeris and Clock errors of Space Vehicle, known as User Range Error (URE) is approximately 82,35 % of the User Equivalent Range Error (UERE).

In other words, if we reduce or eliminate the user range error, we will increase the accuracy of GPS measurements up to approximately 82,35 %. User Equivalent Range Error is defined as formula 1:

$$UERE = \sqrt{(URE^2 + UEE^2)} \,, \tag{1}$$

where UEE is the User Equipment Error, that depends on technical characteristics of user receiver and its antenna. The User Equipment Error includes multipath and receiver noise errors.

Table 1: GPS error budget

Error Source	**Symbol**		**Without differential reference station**	
			Value (1-sigma)	**Value [%]**
Ionosphere refraction	URE	Δ_{ION}	7 m	45.75
Ephemeris and clock errors of Space Vehicles		Δ_{SV}	3.6 m	23.53
Troposphere refraction		Δ_{TRO}	2 m	13.07
Multipath	UEE	Δ_{MP}	1.2 m	7.84
Receiver noise		Δ_{R}	1.5 m	9.81
Total		Δ_{PR}	15.3 m	100

The horizontal Estimated Position Error (EPE) at 95 % confidence level (2drms) can be defined using the following equation 2:

$$EPE_{(2drms)} = 2.HDOP.UERE \, , \tag{2}$$

where HDOP is the Horizontal Dilution of Precision, that depends on the actual constellation from navigational satellites (space vehicles) with respect to user's position only.

In summary, reducing or fully eliminating the User Range Error decreases the Estimated Position Error and respectively increases the accuracy of the GPS measurements.

2. OUR APPROACH

In order to reduce the User Range Error with approximately 13÷15 percent, the value of component Δ_{TRO} has been calculated in accordance with Table 1 using local meteorological data.

For calculating the value of error caused by troposphere refraction (Δ_{TRO}) and obtaining the best result, various combinations of different troposphere models and troposphere mapping functions have been used. The magnitude of Troposphere error can be defined by using the following equation:

$$\Delta_{TRO}[m] = ZHD.MF_H + ZWD.MF_W \, , \tag{3}$$

where ZHD is the Zenith Hydrostatic Delay caused by the "dry" troposphere, ZWD is the Zenith Wet Delay caused by the "wet" troposphere, MF_H and MF_W are the mapping functions respectively, used to transform vertical delay to equivalent delay, that depend on zenith angle z to the navigation satellite.

To provide meteorological data (temperature, relative humidity and surface total pressure) for the troposphere models and the mapping functions, automatic ships meteorological station or databases of the World Meteorological Organization (WMO) can be used.

3. VERIFICATION

An experiment has been conducted for verification and validation of proposed model efficiency. Figure 1 illustrates the experiment. The experiment was carried out on 22 and 23 of February 2013 with duration of 24 hours, using meteorological data from weatherstation La Crosse, model WS 3500, two identical GPS receivers u-bloxAntaris AEK-4P and one laptopwith installed MatLab, u-center and Heavy Weather Pro software.

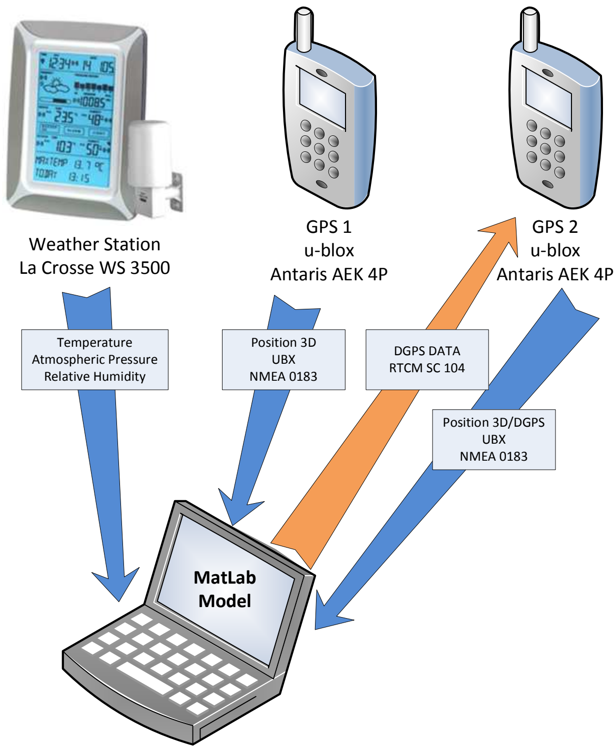

Fig.1. Experiment Diagram

The laptop ensured monitoring and recording of all data from the GPS receivers and weather station. Table 2 and figure 2 illustrate the data recorded from weather station and used for computation of troposphere errors. MatLab Model is used for calculation of the troposphere errors; transform it to DGPS corrections (PRC – pseudo range correction) in RTCM SC-104 format and sending to GPS receiver number two (GPS 2) every second. As a result the GPS receiver number two is putted in DGPS regime. The GPS number one (GPS 1) is used for reference receiver.

Table2 – Data from weather station (3 hours interval)

Local Time and Date	Temperature[℃]	RH [%]	Absolute pressure[hPa]
09.55 22.02.2013	6.7	74	998.2
13.0022.02.2013	8.0	75	1011.7
16.0022.02.2013	7.7	78	1010.4
19.0022.02.2013	7.0	82	1010.5
22.0022.02.2013	7.2	82	1010.9
01.0023.02.2013	7.2	82	1011.2
04.0023.02.2013	7.0	83	1012.2
07.0023.02.2013	7.0	84	1014.2
10.0023.02.2013	7.2	83	1016.1

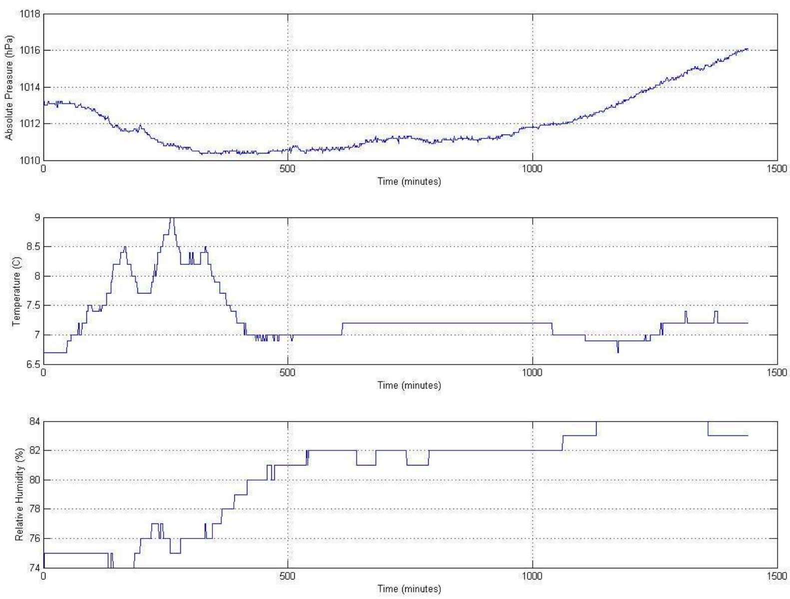

Fig. 2. Data collected from weather station (every one minute)

4. RESULTS

During the experiment, 1440 position reports from each GPS receiver have been recorded. The data is collected using ASCII NMEA 0183 format and UBX binary data format, especially NAV-POSLLH message (see figure 3).This massage carries information about horizontal accuracy estimate (hAcc).

Diagrams of the horizontal accuracy alternation during experiment are shown on Fig. 4. Time (t) in minutes is plotted on the abscissa from the beginning of the experiment and on the ordinate is plotted the value of horizontal position accuracy in meters.

Message	**NAV-POSLLH**				
Description	**Geodetic Position Solution**				
Type	Periodic/Polled				
Comment	This message outputs the Geodetic position in the currently selected Ellipsoid. The default is the WGS84 Ellipsoid, but can be changed with the message CFG-DAT.				
	Header	*ID*	*Length (Bytes)*	*Payload*	*Checksum*
Message Structure	0xB5 0x62	0x01 0x02	28	*see below*	CK_A CK_B
Payload Contents:					

Byte Offset	*Number Format*	*Scaling*	*Name*	*Unit*	*Description*
0	U4	-	iTOW	ms	GPS Millisecond Time of Week
4	I4	1e-7	lon	deg	Longitude
8	I4	1e-7	lat	deg	Latitude
12	I4	-	height	mm	Height above Ellipsoid
16	I4	-	hMSL	mm	Height above mean sea level
20	U4	-	hAcc	mm	Horizontal Accuracy Estimate
24	U4	-	vAcc	mm	Vertical Accuracy Estimate

Fig. 3 UBX(u-blox) binary data protocol, NAV-POSLLH message

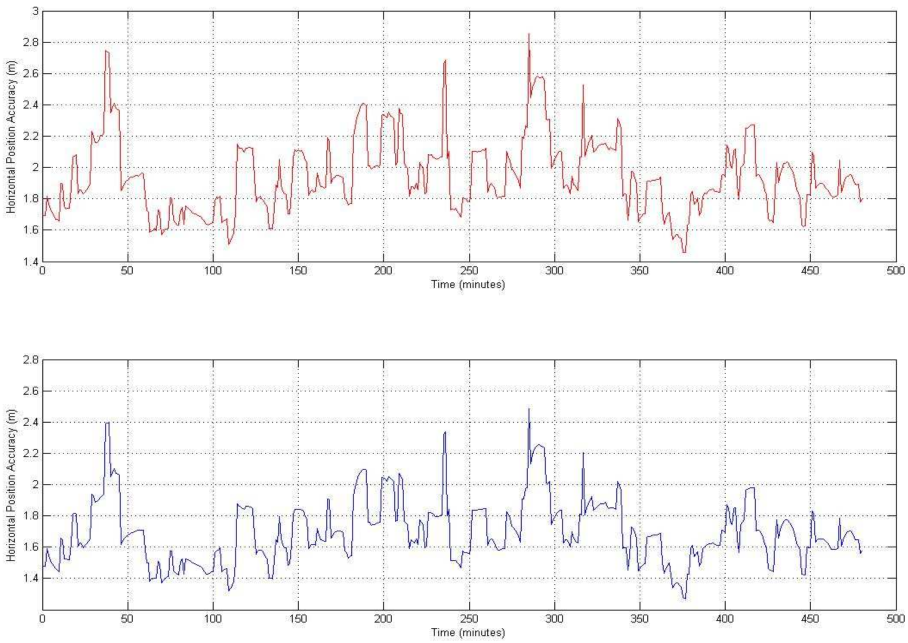

Fig. 4 Horizontal Position Accuracy of GPS 1 (red curve),
Horizontal Position Accuracy of GPS 2 (blue curve) in DGPS regime

The parameters of horizontal position accuracy of GPS 1 at 50%confidence level are: minimal value –1.4564 meters, maximal value – 2.8528 meters, average – 1.9412 meters, standard deviation – 0.2373 meters.

The parameters of horizontal position accuracy of GPS 2 (in DGPS mode)at 50%confidence level are: minimal value – 1.2700meters, maximal value – 2.4880 meters, average – 1.6956 meters, standard deviation – 0.2070 meters.

The comparison between homonymous parameters of GPS 1 and GPS 2 shows that minimal value of GPS 2 is better than minimal value of GPS 1 with 12.786 %, maximal value – 12.787 %, average – 12.651 % and standard deviation – 12.768 %.

In other words horizontal accuracy increases in approximately 12.6÷12.8 %.

5. CONCLUSIONS

The proposed model is capable to generate pseudorange corrections in real time using local meteorological data. Using the pseudorange corrections generated from the proposed model, the accuracy of GPS measurements in horizontal plane is increased in about 12÷13%. During the experiment, for a period of 24 hours the worst horizontal accuracy at 50% confidence level was 2.49 meters.

REFERENCES

[1]. Department of The Army - ***Engineering and Design NAVSTAR GLOBAL POSITIONING SYSTEMS SYRVEYING***, Manual No. 111-1-1003, 2003

[2]. Hofmann-Wellenhof B., Lichtenegger H., Collins J.–**Global Positioning System: Theoryland Practice**

[3]. NMEA, UBX Protocol Specification, u-blox 5 GNSS Receiver, Public Release

[4]. RTCM RECOMMENDED STANDARDS FOR DIFFERENTIAL GNSS SERVICE VER.2.2

[5]. US Department of Defense and US Department of Transportation “2001 Federal Radio navigation Systems”, 2001

SOFTWARE MODULE FOR GNSS NAVSTAR RADIO EFEMERIS PROCESSINGS

TSVETKOV MIROSLAV

"Nikola Vaptsarov" Naval Academy, Varna, Bulgaria

This paper represents the developed with MatLab algorithms for extracting radio ephemeris from the receiver to the global satellite navigation system NAVSTAR and handling in order to realize the possibility of calculating the reference orbits of navigation satellites. The results can be used to extrapolate the location of navigational satellites, determining the exact location in ECEF coordinate system to a point in time or to a period of time.

Keywords: GPS, Navstar, Radio ephemeris, Errors

1. INTRODUCTION

Global satellite radio navigation system Navstar (GPS) has been designed and deployed in order to allow for the determination of position, velocity and time to their customers in a common reference system.

The principle is based on the idea that the position of point (user) can easily be calculated using the distance to at least four navigation satellites with known coordinates.

Radioephemeris data is called data with precise orbit information for every one navigation satellite. They determine satellite orbits as short sectors in the orbital plane. Ephemeris parameters are required to be used in an algorithm to calculate at any time the location of the navigation satellite.

In accordance of Interface control document the radioephemerisdata consistsof the following componentslisted in Table 1.

Table 1 – Radioephemeris data

Symbol	Definition	Units
M_0	Mean Anomaly at Reference Time	semi-circles
Δn	Mean Motion Difference From Computed Value	semi-circles/sec
e	Eccentricity	dimensionless
$\sqrt{a}$	Square Root of the Semi-Major Axis	√meters
Ω_0	Longitude of Ascending Node of Orbit Plane at Weekly Epoch	semi-circles
i_0	Inclination Angle at Reference Time	semi-circles
ω	Argument of Perigee	semi-circles
Ω	Rate of Right Ascension	semi-circles/sec
IDOT	Rate of Inclination Angle	semi-circles/sec
C_{us}	Amplitude of the Cosine Harmonic Correction Term to the Argument of Latitude	radians
C_{us}	Amplitude of the Sine Harmonic Correction Term to the Argument of Latitude	radians

C_{rc}	Amplitude of the Cosine Harmonic Correction Term to the Orbit Radius	meters
C_{rs}	Amplitude of the Sine Harmonic Correction Term to the Orbit Radius	meters
C_{ic}	Amplitude of the Cosine Harmonic Correction Term to the Angle of Inclination	radians
C_{is}	Amplitude of the Sine Harmonic Correction Term to the Angle of Inclination	radians
t_{oe}	Reference Time Ephemeris	seconds
IODE	Issue of Data (Ephemeris)	

Table 2 provides more detailed information about the location of the components of the ephemeris data, their length in bits, range of variation, scale and number of bits in subframe and Figures 2 and 3 depict graphically the form and content of subframes number 2 and 3

Table 2 - Location of the components of the ephemeris data

Symbol	subframe	word	bits	Length	ScaleFactor
M_0	2	4 и 5	107-114;121-144	32	3^{-31}
Δn	2	4	91-106	16	2^{-43}
e	2	6 и 7	167-174;181-204	32	2^{-33}
$\sqrt{a}$	2	8 и 9	227-334;241-264	32	2^{-19}
Ω_0	3	3 и 4	77-84;91-114	32	2^{-31}
i_0	3	5 и 6	137-144;151-174	32	2^{-31}
ω	3	7 и 8	197-104;211-234	32	2^{-31}
Ω	3	9	241-264	24	2^{-43}
IDOT	3	10	279-292	14	2^{-43}
C_{uc}	2	6	151-166	16	2^{-29}
C_{us}	2	8	211-226	16	2^{-29}
C_{rc}	3	7	191-196	16	2^{-5}
C_{rs}	2	3	69-84	16	2^{-5}
C_{ic}	3	3	61-76	16	2^{-29}
C_{is}	3	5	121-136	16	2^{-29}
t_{oe}	3	5	137-144;151-174	32	2^{-31}
IODE	2;3	3;10	61-68;271-278	8;8	

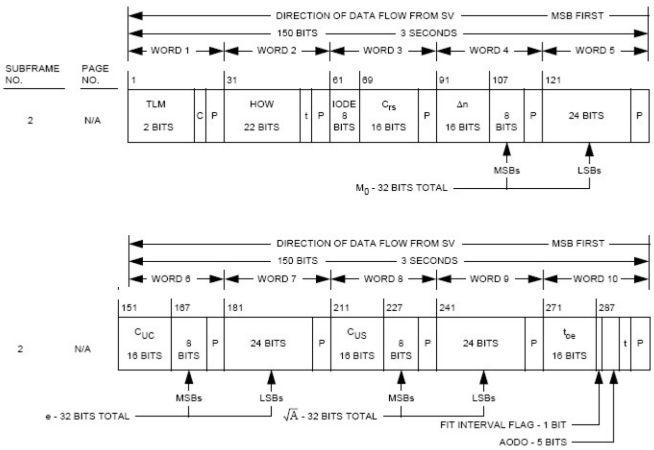

Fig. 1 Subframe 2

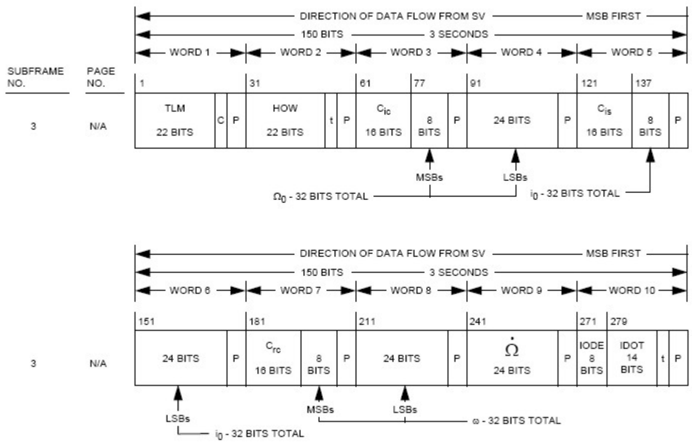

Fig.2 Subframe 3

2. EXTRACTING RADIOEPHEMERIS DATA

One way to obtain radioephemeris data is to download it from memory of the GPS receiver. I have used GPS receiver u-blox, model AEK-4P. In addition to supporting the approved format ASCII data in GPS, namely the NMEA-0183 standard, the GPS device is embedded processor that allows for the transmission of data in binary code. Protocol for transmitting data in binary code developed by the manufacturer and is called "UBX Binary Protocol". This protocol supports over 100 different messages, divided into classes and types.

For transmitting ephemeris data "UBX Binary Protocol" defined message class AID type EPH. The format of AID-EPH message is shown on Figure 3.

GPS Aiding Ephemeris Input/Output Message

Message	**AID-EPH**				
Description	**GPS Aiding Ephemeris Input/Output Message**				
Type	Input/Output Message				
Comment	• SF1D0 to SF3D7 is only sent if ephemeris is available for this SV. If not, the payload may be reduced to 8 Bytes, or all bytes are set to zero, indicating that this SV Number does not have valid ephemeris for the moment. • SF1D0 to SF3D7 contain the 24 words following the Hand-Over Word (HOW) from the GPS navigation message, subframes 1 to 3. See IS-GPS-200 for a full description of the contents of the Subframes. • In SF1D0 to SF3D7, the parity bits have been removed, and the 24 bits of data are located in Bits 0 to 23. Bits 24 to 31 shall be ignored.				
	Header	ID	Length (Bytes)	Payload	Checksum
Message Structure	0xB5 0x62	0x0B 0x31	(8) or (104)	see below	CK_A CK_B
Payload Contents:					
Byte Offset	Number Format	Scaling	Name	Unit	Description
0	U4	-	svid	-	SV ID for which this ephemeris data is (Valid Range: 1 .. 32).
4	U4	-	how	-	Hand-Over Word of first Subframe. This is required if data is sent to the receiver. 0 indicates that no Ephemeris Data is following.
Start of optional block					
8	U4[8]	-	sf1d	-	Subframe 1 Words 3..10 (SF1D0..SF1D7)
40	U4[8]	-	sf2d	-	Subframe 2 Words 3..10 (SF2D0..SF2D7)
72	U4[8]	-	sf3d	-	Subframe 3 Words 3..10 (SF3D0..SF3D7)

Fig. 3 AID-EPH message format

According to the specification of "UBX Binary Protocol" message AID-EPH is non-recurrent, i.e. receiver needs to be submitted request message generation and transmission of AID-EPH. Request message is also class AID type EPH. The formats of request AID-EPH message is shown on Figure 4.

Poll GPS Aiding Ephemeris Data

Message	**AID-EPH**				
Description	**Poll GPS Aiding Ephemeris Data**				
Type	Poll Request				
Comment	**This message has an empty payload!** Poll GPS Aiding Data (Ephemeris) for all 32 SVs by sending this message to the receiver without any payload. The receiver will return 32 messages of type AID-EPH as defined below.				
	Header	*ID*	*Length (Bytes)*	*Payload*	*Checksum*
Message Structure	0xB5 0x62	0x0B 0x31	0	*see below*	CK_A CK_B
No payload					

Poll GPS Aiding Ephemeris Data for a SV

Message	**AID-EPH**				
Description	**Poll GPS Aiding Ephemeris Data for a SV**				
Type	Poll Request				
Comment	Poll GPS Constellation Data (Ephemeris) for an SV by sending this message to the receiver. The receiver will return one message of type AID-EPH as defined below.				
	Header	*ID*	*Length (Bytes)*	*Payload*	*Checksum*
Message Structure	0xB5 0x62	0x0B 0x31	1	*see below*	CK_A CK_B
Payload Contents:					

Byte Offset	*Number Format*	*Scaling*	*Name*	*Unit*	*Description*
0	U1	-	svid	-	SV ID for which the receiver shall return its Ephemeris Data (Valid Range: 1 .. 32).

Fig. 4 Request AID-EPH message formats

3. MATHEMATICAL DATA PROCESSING

To calculate the coordinates of the navigational satellites (x, y, z) in Eart-fixed coordinate system, using radioephemeris data the following mathematical apparatus are used.

Constants:

$\mu = 3.98600 \cdot 10^{14}\ m^3/s^2$ — WGS 84 value of the earth's universal gravitational parameter for GPS user;

$\Omega_e = 7.292115167.10^{-5}\ rad/s$ — WGS 84 value of the earth's rotation rate;

Formulas:

$a = \left(\sqrt{a}\right)^2$ — Semi-major axis;

$n_0 = \sqrt{\mu / a^3}$ — Computed mean motion;

$t_k = t - t_{0e}$ — Time from ephemeris reference epoch;

$n = n_0 + \Delta n$ — Corrected mean motion;

$M_k = M_0 + n.t_k$ Mean anomaly;

$M_k = E_k - e.\sin E_k$ Kepler's Equation for Eccentric Anomaly;

$f_k = \cos^{-1}\left(\frac{\cos E_k - 1}{1 - e.\cos}\right)$ True Anomaly;

$f_k = \sin^{-1}\left(\frac{\sqrt{1-e}\ .\sin E_k}{1 - e.\cos E_k}\right)$ True Anomaly;

$E_k = \cos^{-1}\left(\frac{e + \cos f_k}{1 + e.\cos f_k}\right)$ Eccentric Anomaly;

$\varphi_k = f_k + \varpi$ Argument of Latitude;

$\delta \mu_k = C_{uc}.\cos 2\varphi_k + C_{us}.\sin 2\varphi_k$ Argument of Latitude Correction;

$\delta r_k = C_{rc}.\cos 2\varphi_k + C_{rs}.\sin 2\varphi_k$ Radius Correction;

$\delta i_k = C_{ic}.\cos 2\varphi_k + C_{is}.\sin 2\varphi_k$ Inclination Correction;

$\mu_k = \varphi_k + \delta \mu_k$ Corrected Argument of Latitude;

$r_k = a\ (1 - e.\cos E_k) + \delta r_k$ Corrected Radius;

$i_k = i_0 + \delta i_k = (IDOT).t_k$ Corrected Inclination;

$x_k^{'} = r_k.\cos\ \mu_k$ Positions in orbital plane;

$y_k^{'} = r_k.\sin \mu_k$ Positions in orbital plane;

$\Omega_k = \Omega_0 + \left(\Omega - \dot{\Omega}_0\right).t_k - \dot{\Omega}e.\ t_{0e}$ Corrected longitude of ascending node;

$x_k = x_k^{'}.\cos\Omega_k - y_k^{'}.\cos i_k.\sin\Omega_k$ Earth-fixed coordinates;

$y_k = x_k^{'}.\sin\Omega_k - y_k^{'}.\cos i_k.\cos\Omega_k$ Earth-fixed coordinates;

$z_k = x_k^{'}.\sin i_k$ Earth-fixed coordinates;

4. THE SOFTWARE MODULE

The block diagram of the software module is shown in Figure 5. The software module is MatLab scripts that sequential algorithms and formulas set. The module is consisting of:“communication block” – open, set, close and transferring data thru communication link with GPS receiver; “message coder/decoder” block – generate requests for poll messages and decode downloaded messages from GPS; the blocks “request/poll message” and "ephemeris output massage" support the "message coder/decoder" block; "controller and data processor" block – synchronizes work of all units and performs all calculations to obtain the coordinates of navigation satellites; "data transformation and communication block" - if necessary, carry out additional transformations of initial data and transmit them for use by other modules; "visualization block" - displays the output in the form of figures and graphs; "storage data block" - recorded output data in the output text files. The text files contents is illustrated on Figures 6 and 7.

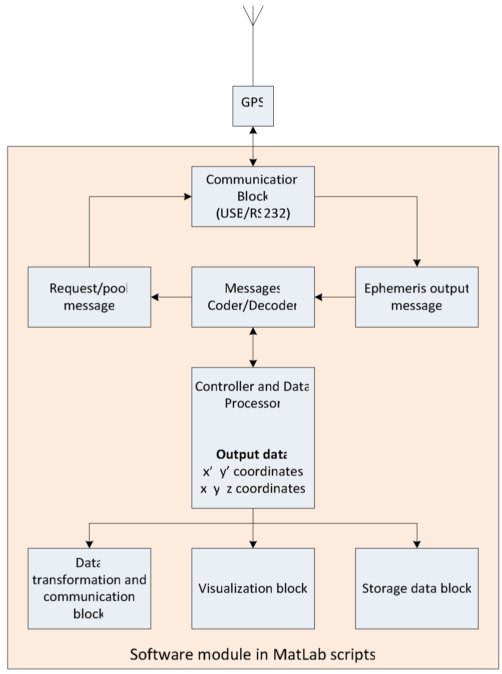

Fig. 5 Software module block diagram

Figure 6 depicts the coordinates in Earth-fixed coordinate system, and Figure 7 depicts the coordinates in orbital plane. Coordinates of the two figures are given in meters and time in seconds.

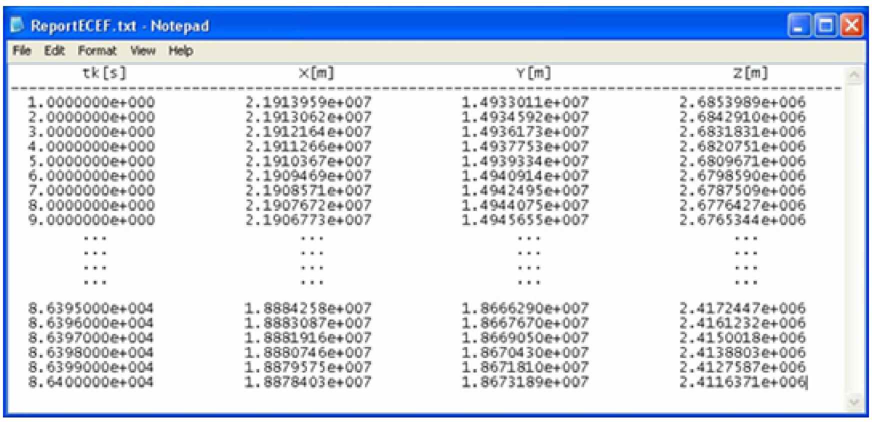
ReportECEF.txt - Notepad

File Edit Format View Help

tk[s]	x[m]	Y[m]	z[m]
1.0000000e+000	2.1913959e+007	1.4933011e+007	2.6853989e+006
2.0000000e+000	2.1913062e+007	1.4934592e+007	2.6842910e+006
3.0000000e+000	2.1912164e+007	1.4936173e+007	2.6831831e+006
4.0000000e+000	2.1911266e+007	1.4937753e+007	2.6820751e+006
5.0000000e+000	2.1910367e+007	1.4939334e+007	2.6809671e+006
6.0000000e+000	2.1909469e+007	1.4940914e+007	2.6798590e+006
7.0000000e+000	2.1908571e+007	1.4942495e+007	2.6787509e+006
8.0000000e+000	2.1907672e+007	1.4944075e+007	2.6776427e+006
9.0000000e+000	2.1906773e+007	1.4945655e+007	2.6765344e+006
...	...	...	...
...	...	...	...
...	...	...	...
...	...	...	...
8.6395000e+004	1.8884258e+007	1.8666290e+007	2.4172447e+006
8.6396000e+004	1.8883087e+007	1.8667670e+007	2.4161232e+006
8.6397000e+004	1.8881916e+007	1.8669050e+007	2.4150018e+006
8.6398000e+004	1.8880746e+007	1.8670430e+007	2.4138803e+006
8.6399000e+004	1.8879575e+007	1.8671810e+007	2.4127587e+006
8.6400000e+004	1.8878403e+007	1.8673189e+007	2.4116371e+006

Fig. 6 Output text file with x, y, z coordinates and time

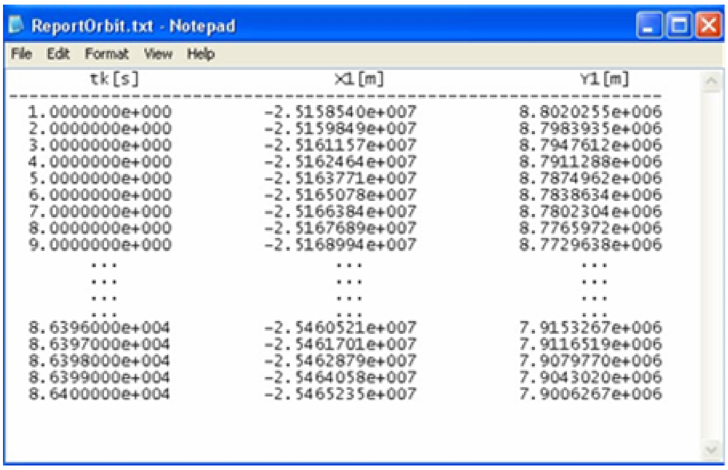

ReportOrbit.txt - Notepad

File Edit Format View Help

tk[s]	X1[m]	Y1[m]
1.0000000e+000	-2.5158540e+007	8.8020255e+006
2.0000000e+000	-2.5159849e+007	8.7983935e+006
3.0000000e+000	-2.5161157e+007	8.7947612e+006
4.0000000e+000	-2.5162464e+007	8.7911288e+006
5.0000000e+000	-2.5163771e+007	8.7874962e+006
6.0000000e+000	-2.5165078e+007	8.7838634e+006
7.0000000e+000	-2.5166384e+007	8.7802304e+006
8.0000000e+000	-2.5167689e+007	8.7765972e+006
9.0000000e+000	-2.5168994e+007	8.7729638e+006
...	...	...
...	...	...
...	...	...
...	...	...
8.6396000e+004	-2.5460521e+007	7.9153267e+006
8.6397000e+004	-2.5461701e+007	7.9116519e+006
8.6398000e+004	-2.5462879e+007	7.9079770e+006
8.6399000e+004	-2.5464058e+007	7.9043020e+006
8.6400000e+004	-2.5465235e+007	7.9006267e+006

Fig. 7 Output text file with x' and y' coordinates and time

5. RESULTS

Figure 8 illustrate the output of a visualization block. Center of the coordinate system coincides with the center of the sphere (the earth). A red solid line depicts the extrapolated trajectory of navigation satellite for 24 hour period. On it with blue markers are mapped locations of navigation satellite in time intervals of one hour counted from the starting point.

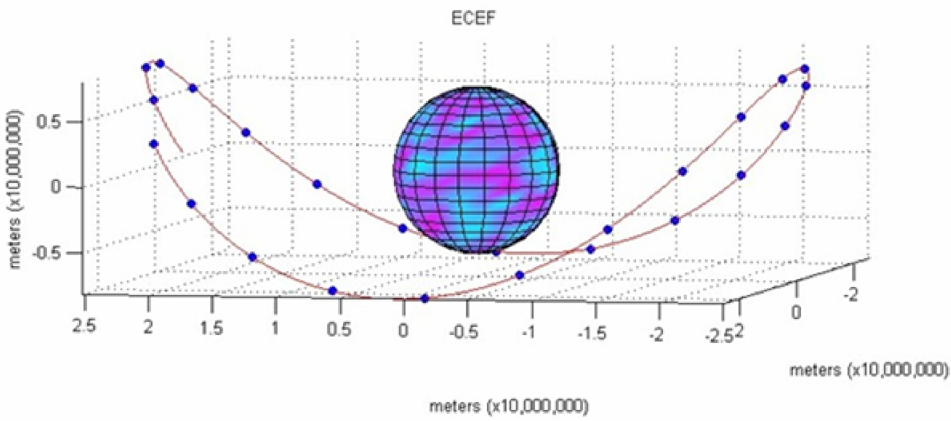

Fig. 8 Extrapolated radioephemeris data of navigational satellite

As shown in Figure 8, it is not appropriate to extrapolate out the location of the navigational satellite for 24 hour period based on the radioephemeris data. Radiophemeris data is used to extrapolate the location of navigation satellites for up to four hours. This time interval is considered that the location of the navigation satellite can be determined with sufficient accuracy.

6. CONCLUSIONS

The development inMatLab algorithms for radioephemeris processing can be implemented by connecting a GPS receiver; extracting radioephemeris data for single navigation satellite or all available radioephemeris data; with extracted ephemeris data can determine the exact location of navigation satellites for a certain time or for a specified time; calculating the geometric distance between the navigation satellite and fixed point in earth-fixed coordinate system.

The proposed model can be used as a part of virtual reference station.

REFERENCES

[1]. Department of The Army - ***Engineering and Design NAVSTAR GLOBAL POSITIONING SYSTEMS SYRVEYING***, Manual No. 111-1-1003, 2003

[2]. Hofmann-Wellenhof B., Lichtenegger H., Collins J.–***Global Positioning System: Theoryand Practice***

[3]. Navstar Global Positioning System – ***Interface Specification 200 Revision D***

[4]. NMEA, UBX Protocol Specification, u-blox 5 GNSS Receiver, Public Release

[5]. US Department of Defense and US Department of Transportation **"*2001 Federal Radionavigation Systems*",** 2001

STUDY OF A MAPPING FUNCTIONS AND TROPOSPHERE MODELS FOR CALCULATING OF GPS RADIOSIGNALS DELAY

TSVETKOV MIROSLAV

"Nikola Vaptsarov" Naval Academy, Varna, Bulgaria

This paper represents the results of a comparison study of different troposphere models and different mapping functions and combinations between them for calculating the troposphere delay of GPS radio signals. The best accuracy of GPS receiver is used for estimation of the best combination between troposphere model and mapping function. Local meteorological data is used in calculations. The generated data can remove troposphere error and increase the accuracy of GPS measurements.

Keywords: GPS, Troposphere, Models, Mapping, Functions

1. INTRODUCTION

Since their development, GNSS have passed a long way of transformation. They have been constantly subjected to modernization and improvement in order to provide maximum accuracy in positioning the users. Presently the accuracy of GNSS Navstar is 36 meters of horizontal accuracy (2drms) and 77 meters of vertical accuracy (2drms), the accuracy of GNSS GLONASS is similar. The accuracy requirements of various countries and organizations are different, but the common is that, the accuracy must be higher as possible.

Different kinds of augmentation systems have been developed for increasing the GPS measurement accuracy. There are wide area (WAAS, EGNOS, MSAS), regional (SkyFix, StarFix, Eurofix, GRAS) and local (maritime, aeronautical, geodetical) augmentation systems. The best accuracy is achieved when using data from a local reference station situated near the user.

Table 1 summarizes the quantity estimation of error sources, derived from the relevant information, their typical values and elimination of some of them by using data from reference station (differential technique). The typical values are represented in meters and corresponding percentage values.

Table 1 shows that the sum of errors on account of Ionosphere refraction, Troposphere refraction and Ephemeris and Clock errors of Space Vehicle, known as User Range Error (URE) is approximately 82,35 % of the User Equivalent Range Error (UERE).

In other words, if we reduce or eliminate the user range error, we will increase the accuracy of GPS measurements up to approximately 82,35 %. User Equivalent Range Error is defined as formula 1:

$$UERE = \sqrt{\left(URE^2 + UEE\right)}, \tag{1}$$

where UEE is the User Equipment Error, that depends on technical characteristics of user receiver and its antenna. The User Equipment Error includes multipath and receiver noise errors.

Table 1: GPS error budget

Error Source	Symbol		Without differential reference station	
			Value (1-sigma)	**Value [%]**
Ionosphere refraction	URE	Δ_{ION}	7 m	45,75
Ephemeris and clock errors of Space Vehicles	URE	Δ_{SV}	3,6 m	23,53
Troposphere refraction	URE	Δ_{TRO}	2 m	13,07
Multipath	UEE	Δ_{MP}	1,2 m	7,84
Receiver noise	UEE	Δ_{R}	1,5 m	9,81
Total		Δ_{PR}	15,3 m	100

The horizontal Estimated Position Error (EPE) at 95 % confidence level (2drms) can be defined using the following equation 2:

$$EPE_{(2drms)} = 2 \cdot HDOP \cdot UERE\ , \qquad (2)$$

where HDOP is the Horizontal Dilution of Precision, that depends on the actual constellation from navigational satellites (space vehicles) with respect to user's position only.

In summary, reducing or fully eliminating the User Range Error decreases the Estimated Position Error and respectively increases the accuracy of the GPS measurements.

2. CALCULATING TROPOSPHERE REFRACTION ERROR

For calculating the value of error caused by troposphere refraction (Δ_{TRO}) a various combinations of different troposphere models and troposphere mapping functions can be used. The magnitude of Troposphere error can be defined by using the following equation:

$$\Delta_{TRO}\,[m] = ZHD \cdot MF_H + ZWD \cdot MF_W\ , \qquad (3)$$

where ZHD is the Zenith Hydrostatic Delay caused by the "dry" troposphere, ZWD is the Zenith Wet Delay caused by the "wet" troposphere, MF_H and MF_W are the mapping functions respectively, used to transform vertical delay to equivalent delay, that depend on zenith angle z to the navigation satellite.

There are several well-known troposphere models and mapping functions. Different type of meteorological data is used from every one of them.

To provide meteorological data (temperature, relative humidity and surface total pressure) for the troposphere models and the mapping functions, automatic ships meteorological station or databases of the World Meteorological Organization (WMO) can be used. In this study a two troposphere models are compared, they are Hopfield's troposphere model and MOPS troposphere model. The Hopfield's model is pronouncedly local area model basically for geodetic usage, while MOPS model is used for wide areas.

In table 2a different mapping functions are presented, where P – atmosphere pressure, t – temperature, e – pressure of water vapor, H_t – high of troposphere, α – temperature error, φ – latitude of observer, H – altitude of observer, doy – day of year, ε_{min}[°] – minimal zenith angle for correct calculation of data.

Table 2: Mapping functions

Function	coefficients			
	a	B	c	ε_{min}[°]
Marini & Murray	F(P,e)	F(P,t,φ)	not used	2
Chao	constant	constant	not used	10
Black	not used	not used	not used	7
Ifadis	F_{ia}(P,t,e)	F_{ib}(P,t,e)	constant	2
MTT (Herring)	F_{ma}(φ,H,t)	F_{mb}(φ,H,t)	F_{hc}(φ,H,t)	3
NMF (Niell)	F_{na}(φ,H,doy)	F_{nb}(φ,H,doy)	F_{nc}(φ,H,doy)	3
UNBabc	F_{1a}(θ,H)	constant	constant	2

The mapping functions can be divided into two groups as well as troposphere models. The first one of them is geodetic survey oriented and second one is navigational oriented. The mapping functions from the first group are more precise and more complex. There are Ifadis, MTT (Herring) and NMF(Niell) mapping functions. The mapping functions from the second group are simpler and more inaccurate. For more thoroughness of survey a troposphere model of Marini & Murray is included. It consist a mapping function, and it is used basically for laser detection and ranging of space vehicles and radiosonds.

3. COMPARATIVE ANALYSIS

An experiment has been conducted for comparison the efficiency of different combination of troposphere models and mapping functions. Figure 1 illustrates the experiment. The experiment was carried using meteorological data from weather station La Crosse, model WS 3500, one DGPS receiver u-bloxAntaris AEK-4P and one laptop with installed MatLab, u-center and Heavy Weather Pro software.

A MatLab scripts ensured monitoring and recording of all data from the GPS receivers and weather station. The azimuth data for all visible space vehicles (SV's) are extracted from the GPS receiver. The meteorological data (temperature, atmospheric pressure and relative humidity) are extracted from the weather station. The extracted data are input for combinations of troposphere models and mapping functions (see fig. 1). The output data (error caused by troposphere refraction)from each combination is filed to the GPS receiver as pseudo range correction (PRC) in RTCM SC-104 format. In result of consecutively sending of pseudo range corrections from the different combinations to the GPS receiver he switched to DGPS mode. Alternating the source (combination)of pseudo range corrections we can monitor the changes of horizontal accuracy of the GPS receiver.

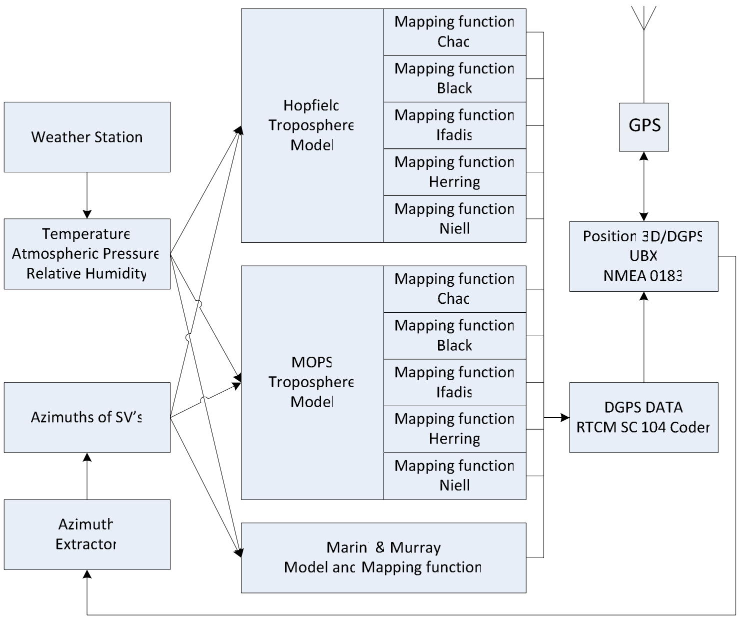

Fig.1. Experimental Diagram

Table 3 illustrates extract from calculated troposphere refraction delay in meters using Hopfield troposphere model and different mapping functions. For comparison a Marini & Murray(M&M) model and function results are included.

Table3: Troposphere refraction (in meters) using Hopfield troposphere model in different combinations

Elevation [°]	Mapping function					
	M&M	Chao	Black	Ifadis	Herring	Niell
10	12,40	13,22	17,20	13,29	13,34	13,34
20	6,64	6,93	7,83	6,93	6,95	6,95
30	4,60	4,77	5,13	4,77	4,78	4,78
40	3,60	3,72	3,90	3,72	3,72	3,72
50	3,03	3,12	3,22	3,12	3,12	3,12
60	2,69	2,76	2,82	2,76	2,76	2,76
70	2,48	2,55	2,58	2,54	2,55	2,55
80	2,37	2,43	2,44	2,43	2,43	2,43
90	2,33	2,39	2,39	2,39	2,39	2,39

In the same way as table 3, the table 4 illustrates extract from calculated troposphere refraction delay using MOPS troposphere model and different mapping functions. A MatLab scripts are used for calculation of the troposphere errors; transform it to pseudo range corrections in RTCM SC-104 format and sending to GPS receiver every second. On every five seconds the source of the corrections (combination) was changed.

Table 4: Troposphere refraction (in meters) using MOPS troposphere model in different combinations

Elevation [°]	Mapping function					
	M&M	Chao	Black	Ifadis	Herring	Niell
10	12,40	13,05	20,23	13,09	13,16	13,17
20	6,64	6,84	8,48	6,84	6,85	6,85
30	4,60	4,71	5,37	4,70	4,71	4,71
40	3,60	3,67	4,00	3,66	3,67	3,67
50	3,03	3,08	3,26	3,08	3,08	3,08
60	2,69	2,73	2,83	2,72	2,73	2,73
70	2,48	2,51	2,57	2,51	2,51	2,51
80	2,37	2,40	2,42	2,40	2,40	2,40
90	2,33	2,36	2,36	2,36	2,36	2,36

4. RESULTS

An experiment has been conducted in Nikola Vaptsarov Naval Academy campus on 11-th February 2013.

During the experiment, 1440 position reports (24 hours, every second) from GPS receiver have been recorded. The data is collected using ASCII NMEA 0183 format and UBX binary data format, especially NAV-POSLLH message (see Figure 2).This massage carries information about horizontal accuracy estimate (hAcc).

Message	NAV-POSLLH				
Description	**Geodetic Position Solution**				
Type	Periodic/Polled				
Comment	This message outputs the Geodetic position in the currently selected Ellipsoid. The default is the WGS84 Ellipsoid, but can be changed with the message CFG-DAT.				
	Header	ID	Length (Bytes)	Payload	Checksum
Message Structure	0xB5 0x62	0x01 0x02	28	see below	CK_A CK_B

Payload Contents:

Byte Offset	Number Format	Scaling	Name	Unit	Description
0	U4	-	iTOW	ms	GPS Millisecond Time of Week
4	I4	1e-7	lon	deg	Longitude
8	I4	1e-7	lat	deg	Latitude
12	I4	-	height	mm	Height above Ellipsoid
16	I4	-	hMSL	mm	Height above mean sea level
20	U4	-	hAcc	mm	Horizontal Accuracy Estimate
24	U4	-	vAcc	mm	Vertical Accuracy Estimate

Fig.2. UBX (u-blox) binary data protocol, NAV-POSLLH message

Table 5 and table 6 illustrate extract from calculated troposphere refraction delay in meters at 12:00:00UTC for day of year 42 (Feb 11, 2013) for all visible space vehicles from Nikola Vaptsarov Naval Academy campus at this moment. The tables are consist of pseudo random number (PRN) – number of space vehicles, azimuth (Az) and elevation (El) to space vehicles at this moment, and troposphere refraction delay in meters calculated in all different combinations and including Marini & Murray(M&M) model and function results.

PRN	Az	El	M&M	Troposphere model - Hopfield				
				Chao	Black	Ifadis	Herring	Niell
1	155,6	38,6	3,7026	3,8240	4,0217	3,8222	3,8277	3,8277
3	190,6	49,1	3,0677	3,1603	3,2655	3,1583	3,1626	3,1626
11	296,0	19,4	6,8258	7,1358	8,0993	7,1395	7,1537	7,1537
14	113,9	52,2	2,9370	3,0242	3,1124	3,0221	3,0262	3,0262
18	56,2	11,7	10,8084	11,4641	14,3247	11,5051	11,5378	11,5410
19	251,0	69,7	2,4818	2,5512	2,5825	2,5488	2,5522	2,5522
22	53,1	50,8	2,9956	3,0852	3,1810	3,0831	3,0873	3,0873
32	40,4	76,2	2,3983	2,4647	2,4839	2,4622	2,4654	2,4654

Table6: Troposphere refraction (in meters)for visible space vehicles

PRN	Az	El	M&M	Troposphere model - MOPS				
				Chao	Black	Ifadis	Herring	Niell
1	155,6	38,6	3,7026	3,7722	4,1326	3,7696	3,7757	3,7757
3	190,6	49,1	3,0677	3,1174	3,3091	3,1150	3,1196	3,1196
11	296,0	19,4	6,8258	7,0397	8,7938	7,0389	7,0569	7,0570
14	113,9	52,2	2,9370	2,9831	3,1438	2,9807	2,9850	2,9850
18	56,2	11,7	10,8084	11,3124	16,4906	11,3348	11,3834	11,3863
19	251,0	69,7	2,4818	2,5165	2,5734	2,5140	2,5175	2,5175
22	53,1	50,8	2,9956	3,0433	3,2178	3,0409	3,0454	3,0454
32	40,4	76,2	2,3983	2,4312	2,4659	2,4285	2,4319	2,4319

During the experiment the best horizontal position accuracy has been achieved by using the Hopfield's troposphere model and Black's mapping function.

The average circular error probable (CEP) of GPS position was alternating between 1.362 meters and 1.725 meters, in other words the average horizontal accuracy at 95% confidence level (2 drms) was alternating between 3.28 meters and 4.14 meters.

5. CONCLUSIONS

As a result of comparative analysis of different combinations of well-known troposphere models and mapping functions the best one with respect to horizontal position accuracy was discovered.

The discovered combination of troposphere model and mapping function and supported algorithms can be used in real time for generation of pseudo range corrections for GPS measurementsusing local meteorological data.

This method can be used for reducing or eliminating the troposphere refraction errors and for example can be part of virtual reference station.

REFERENCES

[1]. Department of The Army - ***Engineering and Design NAVSTAR GLOBAL POSITIONING SYSTEMS SYRVEYING***, Manual No. 111-1-1003, 2003

[2]. Hofmann-Wellenhof B., Lichtenegger H., Collins J.– ***Global Positioning System: Theoryand Practice***

[3]. Jianguo Jack Wang, Jinling Wang, ***Tropospheric Delay Estimation for Pseudolite Positioning***, Journal of Global Positioning Systems vol.4, No. 1-2-106-112, 2005

[4]. ***NMEA, UBX Protocol Specification***, u-blox 5 GNSS Receiver, Public Release

[5]. RTCM RECOMMENDED STANDARDS FOR DIFFERENTIAL GNSS SERVICE VER.2.2

[6]. US Department of Defense and US Department of Transportation “2001 Federal Radio navigation Systems”

MEASURES TO ENHANCE SAFETY OF CONTAINERIZED CARGO TRANSPORT BY REVIZING STANDARDS FOR CARGO INFORMATION AND EDI BAPLIE AND MOVINS MESSAGES STRUCTURE

VELINOV SVILEN

"Nikola Vaptsarov" Naval Academy, Varna, Bulgaria

The intensified containerization during last decades and the increased capacity of container ships in combination with unverified container weights and EDI techniques which do not fully comply with SOLAS Ch VI requirements have led to a number of incidents involving loss of containerized cargo. This paper analyses both present SOLAS requirements for proper cargo information, including the IMO's recently proposed amendments, and the modern techniques and standards for EDI. An introduction of obligatory verification of container weights at container terminal gates is proposed which together with revised BAPLIE and MOVINS EDI standards as suggested by author would form an efficient safety barrier contributing to the safety of maritime container transport.

Keywords: Container transport safety, Container weights verification, Cargo information, BAPLIE

1. EVOLUTION OF WORLD CONTAINER FLEET AND EDI STANDARD MESSAGES IN CONTAINER SHIPPING

With the internationalization and globalization of economies, shipping has obtained a central role in world trade. Most of the general cargo nowadays is transported in containers. As per Lloyd's List Intelligence (2012) the estimated total activity of world's container fleet for 2011 had been 18 756 billion dwt-miles compared to only 2 472 billion dwt-miles for the general cargo fleet for the same period. The increase in volume of containerized cargo was an obvious tendency for the last decades. Economies of scale have been continuously pushing through the years for the construction of larger containerships. The size limit of the Panama Canal, which is still known as the *panamax standard*, was reached in 1985. Later on in 1988 APL introduced the first *post panamax* containership which together with the global economy growth gave a quick increase of container vessel maximum capacity to about 8000 TEU. With the maximum size of the new Panama Canal locks, expected to open in 2014, came a new class of ships – the *new panamax (NPX)*. For containerships this capacity limit will be about 13000 TEU. The era of the *post new panamax* containerships started in 2006 when the maritime operator Maersk introduced the Maersk E-class ships (Emma Maersk). In February 2013 Maersk launched the world's largest containership ever built, the first of the series Triple-E class Maersk Mc-Kinney Moller, which is currently the world's largest vessel. The Triple-E will consume approximately 35 percent less fuel per container than the 13100 TEU vessels being delivered to other container shipping lines in the next few years. With such economy of scale it would be quite natural to expect vessels of even larger size on the Asia-Europe route in the next decade. These will be the so called *"Malacca Max"* class containerships which are currently on the drawing boards and would have capacities of about 27000-30000 TEU.

The expansion of world's container fleet and capacities of containerships did not happen without the facilitation to shipping industry brought by advanced computer technologies and the development of EDI (Electronic Data Interchange) standards, which have been developed during last decades. Nowadays it seems impossible for the container shipping industry to function without modern technical aids, such as computer cargo planning software for terminals and for ships and the EDI standard messages. The implementation of global standards for EDI messages did not come easy. It was the SMDG (User Group for Shipping Lines and Container Terminal) as an official Pan European User Group, recognized by the UN/EDIFACT Board, which in 1991 presented the first BAPLIE structure, based on the 91.1 Edifact Directory. It took few years more for BAPLIE 1.1 to be finally accepted as stable for use. Later on BAPLIE was updated by versions 1.5, 2.0 and 2.1 which all are still in use. In 2007 a newer version 3.0 was proposed. This version has still not been officially declared stable despite the considerable number of additional options it offers. Today, cargo information interchange when dealing with CTUs seems impossible without the use of various EDI standard messages. SMDG estimates that only BAPLIE messages are used worldwide minimum 50000 times per day.

2. PRESENT SOLAS REGULATIONS CONCERNING CARGO INFORMATION, AND CONTAINERIZED CARGO STOWAGE AND SECURING

SOLAS Regulation VI/2 requires the shipper of containerized goods to provide the ship's master or his representative with appropriate information on the cargo, prior to ships loading. Such information shall be confirmed in writing and by appropriate shipping documents. A reference to this regulation states that EDP and EDI transmission techniques can be used as an aid to paper documentation. This option is widely used today and hard copies of bay plans are rarely delivered onboard.

To fulfil the requirements, as an aid to paper documentation, BAPLIE standard must be fully capable of transmitting all the necessary cargo information as required by SOLAS. The applicable text of Regulation VI/2 puts the shipper under the obligation to declare the general description of the cargo, the gross mass of the cargo units, and any relevant special properties of the cargo. Furthermore, the regulation requires that the shipper shall ensure that the gross mass of the loaded (or "stuffed") container is in accordance with the gross mass declared on the shipping documents. For the purpose of this regulation the following requirements for cargo information given in sub-chapter 1.9 of the CSS Code are made mandatory:

- Prior to shipment the shipper should provide all necessary information about the cargo to enable the shipowner or ship operator to ensure that:
  - the different commodities to be carried are compatible with each other or suitably separated;
  - the cargo is suitable for the ship;
  - the ship is suitable for the cargo; and
  - the cargo can be safely stowed and secured on board the ship and transported under all expected conditions during the intended voyage.
- The master should be provided with adequate information, regarding the cargo to be carried so that its stowage may be properly planned for handling and transport.

SOLAS Regulation VI/5, dealing with stowage and securing, requires that freight containers shall not be loaded to more than the maximum gross weight indicated on the Safety Approval Plate under the CSC 72, as amended.

3. RECENT INCIDENTS WITH CONTAINERIZED CARGO INVOLVING MISDECLARED CONTAINER WEIGHTS AND INCORRECT CARGO INFORMATION

Regulatory instruments, such as above SOLAS requirements, regarding proper cargo information, stowage and securing of CTUs, together with the CSC 72's system of inspection and certification of containers, might seem sufficient to provide safety of container transport at sea.

Unfortunately, incidents with losses of containerized cargo at sea continued through the last decade. IMO officially listed in DSC 17/INF.5, 2012 ("Development of measures to prevent loss of containers") some recent incidents with containers. It was clearly stated in the document that it did not purport to provide a comprehensive summary of all incidents involving misdeclared container weights in the recent years, but rather the purpose of the document was to provide illustrative examples of the significant safety issues that misdeclared container weights may give rise to on shore and on ships. It was clearly noted in the paper that the incidents listed may have involved contributing causes separate from misdeclared weights. Nevertheless the main causes of incidents, even if not always acting independently, were the misdeclared container weights. Some of those cases are listed below:

- June 2011: Containership Deneb in Algeciras: The ship suffered a significant stability incident. A review after the incident found that out of the 168 containers on the load list, 16 – or roughly 1 out 10 – containers had actual weights far above the declared weights. The actual weights exceeded the declared weights in a range from between 1.9 times as much as the declared weights to as much as 6.7 times the declared weights. The total actual weight of these 16 containers was more than 278 tonnes above their total declared weight of about 93 tonnes or four times higher than their declared weight.
- February 2011: On February 25, 2011 a 28-tonne container fell from height of 12 meters down on the pier and narrowly missed two workers at the Australian Darwin Port. It was the third accident in a month at Darwin Port. The container was severely overloaded. Listed as only four tonnes, it actually weighed 28 tonnes and exceeded the crane's load limit.
- January 2007: About 660 containers stowed on deck, which had remained dry after grounding of MSC Napoli, were weighed. The weights of 137 (20%) of these containers were more than 3 tonnes above their declared weights. The largest difference was 20 tonnes, and the total weight of the 137 containers was 312 tonnes heavier than on the cargo manifest.
- February 2007: A container stack on board MV Limari collapsed due to stack overweight in Damietta port. Excessively heavy units had been loaded in the upper tiers and the maximum stack weight had been exceeded considerably in some rows. Exceeding permissible weight distribution and/or exceeding the maximum stacking weight in stacks resulted in overstressed stowage/securing elements and overstressed containers. The actual container weights were established by the devices on the gantry crane when lifting and shifting the collapsed containers. The actual container weights exceeded the declared weights by 362% (Row 08), 393% (Row 06), 407% (Row 04) and 209% (Row 02) in Bay 52 where the collapse occurred.

- January 2006: Misdeclared container weights contributed to an incident onboard P&O Nedlloyd Genoa. “The declared weight of a container provided by the shipper and used for all stow planning and onboard stability purposes can, if inaccurate, cause major discrepancies between actual and declared weights. Furthermore, incorrect weight can result in stack overload and the application of excessive compression and racking forces on containers and their lashings. Although there are no financial gains to be made by the shipper who declares less than actual weight, the industry acknowledges that overweight containers are a problem. However, as yet this has not justified a requirement for compulsory weighing of containers prior to loading" (Source: "Report on the investigation of the loss of containers overboard from P&O Nedlloyd Genoa", U.K. Marine Accident Investigation Branch, Report 20/2006, August 2006, pages 19, 30 and 31)

4. NEW SOLAS AMENDMENT PROPOSED BY IMO

These incidents were considered by the IMO’s DSC Sub-committee, which together with their partners, BIMCO, the International Association of Ports and Harbors (IAPH), the International Chamber of Shipping (ICS), the International Transport Workers Federation (ITF) and the World Shipping Council (WSC), discussed whether and how to amend SOLAS to require verification of containers’ actual weight before loading onto a SOLAS regulated ship.

As noted above, Regulation VI/2 addresses the issue of container weights by requiring containerized cargo shippers to provide accurate container weight declarations. Shippers, however, are generally located outside the effective regulatory reach of the SOLAS ship-port regulatory interface. The shipper may be domiciled in a jurisdiction beyond the port state where the ship is being loaded. There is no SOLAS signatory that institutes enforcement actions against shippers under regulation VI/2 for providing substantially incorrect container weights.

Most stuffed cargo containers delivered to port facilities for export have not been weighed to verify their weight prior to delivery to port facilities. Although many, if not most, port facilities have scales or other equipment capable of weighing loaded export containers upon receipt or during yard operations, a very substantial percentage of loaded containers are not weighed. Neither Regulation VI/2, Regulation VI/5, nor any other provision of SOLAS requires weighing a loaded container prior to vessel stowage. It is obvious that unless such containers are weighed presently the vessel and the port facility rely only on shipper’s weight declaration.

The vast majority of container vessels do not have cranes or other equipment that can weigh containers. Thus, by necessity, container vessels must rely on any container weight verification to be performed onshore. Most shippers too do not have weigh scales at their container stuffing locations, and further, even if scales are available within the country where the shipper is domiciled, they may not be conveniently located between the container stuffing location and the receiving port facility. It would be impractical for the tens of thousands of different shippers of containerized goods around the world to install container weighing devices on their premises.

As port facilities have container weighing technology and as they are the “choke points” through which all container traffic must pass, it is natural that IMO addressed the issue for future SOLAS amendment concerning container weight verification mostly to container terminals, which together with the shipper and the ship’s master have an important role to play.

DSC proposed following amended text of SOLAS Regulation VI/2: “A freight container containing cargo shall not be loaded aboard a ship unless the master or his representative and the terminal representative have the verified gross weight of the container obtained by a weighing of the container. Such verified weights shall be available sufficiently in advance of vessel loading to be used in the vessel stowage plan.” “Terminal representative” will have the same meaning as in SOLAS Regulation VI/7, i.e. this will be a person appointed by the terminal who will be held responsible for the loading/unloading operations in regard to the particular ship.

5. FURTHER SAFETY ISSUES RELATED TO THE INADEQUATE CARGO INFORMATION CONCERNING CONTAINERIZED CARGO

Unfortunately, the newly proposed SOLAS amendment, as described in section 4, still does not require a container to be weighed by the terminal before loading aboard a vessel. Such practice already exists in the U.S., where Occupational Safety and Health Administration require export containers to be weighed before loading. Other nations have no similar requirements. There is a strong opposition to the idea of the compulsory weight verification mostly led by The European Shippers’ Council. It claims that shippers have not been deliberately misdeclaring the weight of containers “so they can move more cargo in fewer boxes and so save money”. Shippers were also claiming that the shipping lines were failing to use the latest information about the shipments they carried. And until various parties concerned are negotiating on how and when SOLAS to be amended containerized cargo is still being loaded with unverified weights and crews’ and terminal personnel’s safety is put into danger.

It is obvious that if terminals are not directly involved in solving the issue with the misdeclared weights the practice of loading cargo with only estimated weights will not be ceased. What’s more, with the use of modern container terminal equipment nowadays it would not be time consuming or expensive to verify the weight of all export containers, even the empties. Such practice will as well contribute to terminals security as in integral part of the overall safety.

As mentioned in section 2 above, present text of Regulation VI/5 requires that a freight container shall not be loaded to more than the maximum gross weight (MGW) as per Safety Approval Plate. According to IMO/ILO/UNECE Guidelines for Packing of Cargo Transport Units (CTUs) it is the responsibility of the person in charge for packing a container to verify that the MGW of container is not exceeded, i.e. that the unit is not overloaded. Much alike weight verification, there is no further control to confirm that a unit is not overloaded. Actually, if the estimated amount of cargo at the container stuffing place is wrong and once a container is overloaded when stuffed later on it can easily be loaded aboard and no authority will further double check for the CSC’72 compliance. Neither the terminal, nor the ship’s crew is obliged to monitor the compliance with MGW, stated on the Safety Approval Plate. The problem does not end with that as both ship’s master and the “terminal representative” do not receive from shipper information about the MGW of a container. The reason is that standard EDI formats currently used for exchanging information about containerized cargo for loading between shipping lines, terminals and vessels (BAPLIE and MOVINS) do not include segments containing the MGW of each CTU. This way it is impossible for a ship master to evaluate cargo fitness as required by sub-chapter 1.9 of the CSS Code mentioned in section 2. There is no way for a master to verify that “cargo can be safely stowed and secured on board the ship” as he doesn’t receive important information via EDI about CTU’s MGW and CTU’s verified weight.

Additionally, if such information is being received by terminals as “cargo information” via MOVINS standard by verifying a container weight when a container enters a terminal it would be possible to compare the unit's verified weight with its MGW and compliance with the CSC'72 could be easily confirmed by the EDI processing software. On loading stowage plan in BAPLIE format the ship's side will also have the option to check that each container offered for loading is not overloaded.

Such enhancement for safety of container stowage planning would be impossible if current SMDG's standards BAPLIE and MOVINS are not revised. The draft version of the latest BAPLIE 3.0 offers additional options compared to the older versions. Such new feature, contributing to container stowage safety, is the new qualifier "MEA+ASW". It is supposed to mark the maximum allowable stacking weight (MASW) of a unit in case it is less than 192000 kg. The qualifier is introduced to be in line with the 2010 amendments to the CSC'72 (IMO Res MSC.310(88)) which require containers with stacking or racking values of less than 192000 kg and 150 kN, respectively, to be considered as having limited stacking and racking capacity and to be marked accordingly. Unfortunately, the new BAPLIE "MEA+ASW" qualifier is not considered as mandatory. Such approach will not solve the safety issue of verifying that the MASW of each container on board is not exceeded. Stability and lashing programs which are presently used on board container vessels are not designed to calculate the mass of cargo stacked on each container as per actual stowage plan. Some of them can accept BAPLIE 3.0 standard but as the "MEA+ASW" qualifier is not mandatory, in case it is not used, the MASW of a unit is assumed to be 192000 kg. This way software will not give any warning in case of an exceeded MASW.

For cargo stowage planning safety the actual stacking weight calculation and a comparison with the MASW for each unit onboard (or at least for lower tiers inside holds) should be made mandatory. The example below demonstrates a dangerous situation which may evolve if such calculation is not performed. Figure 1 is a printout from the stability program TSB Supercargo of a 13100 TEU vessel. Cargo holds can accommodate up to 11 tiers with maximum mass of 335.5 tonnes for a 40' container stack (each container weighing up to 30.48 tonnes) and 255 tonnes for 20' container stack (each 20' container weighing up to 24.00 tonnes and one 40' container on row 22 weighing 30.48 tonnes). The example shows that the container MASW is exceeded (even if containers are designed as per increased strength standards of ISO 1496-1/Amd.3:2005(E) for MASW 213360 kg) for containers at lower 3 tiers (tiers 02, 04 and 06) at the 40' stack (row 01) and is also exceeded for the tier 02 at the 20'/40' combined stack (row 03). In case of containers designed as per earlier ISO 1496-1 standard (for MASW 192000 kg) containers structure as per same stowage example will be overstressed on tiers 02, 04, 06 and 08 for row 01 and also on tiers 02 and 04 for row 03. As local stacking weight for ship's double bottom in this case is not exceeded there is no warning given by the software about a stowage problem concerning container weights.

The problem with container strength for the under deck stowage may additionally grow worse in case container vessels reach the *Malacca Max* size as such vessels are expected to have 13 container tiers inside hold (Wijnolst, Scholtens, Waals, 1999). Presently, a verification that a container MASW is not exceeded for all CTUs on board is not offered by software makers as this is not in the scope of IMO's and IACS's documents concerning preparation of Stability Instruments and Loading Instruments (The Recommendation on loading instruments, adopted by resolution 5 of the 1997 SOLAS Conference; IACS Requirement 1971 / Rev.7 2010; IACS Recommendations No 48 1997; MSC Circular 891; MSC.1/Circ.1229, 11 January 2007).

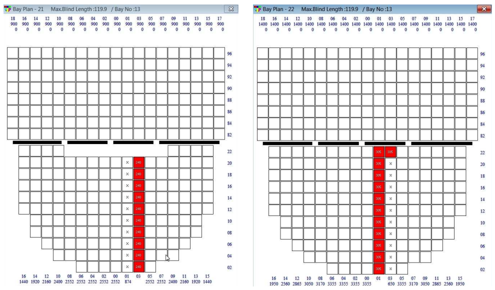

Fig. 1. Example of containers stacked inside 13 100 TEU container ship cargo hold

If SMDG successfully develops and implements future revised versions of BAPLIE and MOVINS, requiring mandatory segments for MGW and MASW, makers of ship's loading software would need to update the software they offer with two additional automated cargo stowage checks – a check that each unit offered for loading has mass less than the MGW; and that no container on board is stacked with mass exceeding the maximum permissible stacking weight as per Safety Approval Plate. Such software features expansion can be provided in form of software new versions and would not require significant research and investments.

The recent marine accident investigations involving loss of containers revealed three main groups of factors that have caused loss of containerized cargo. These are:

- human error (human factor);
- technical reason;
- extreme weather.

In most of the cases not just one but several factors acted simultaneously and they belonged very often to different groups as defined above. In case of cargo loss it have been a common practice during last decades to look desperately for a "human error". A human error explanation is an easy solution and somehow fits all major parties involved in an investigation. Ship's crew and/or terminal planners have been blamed for the improper stowage and overstressing of containers construction despite the fact that they do not receive information about containers MASW and the MGW.

This paper proposes a different approach to the issue. The shortage in cargo information as mentioned above cannot be labelled as a "human error" as it is a pure system error – an error in the cargo information exchange system. There is no actual verification of container weights. There is no proper cargo information delivered on board container vessels about containers offered for loading that includes MGW and MASW. As a result today container stowage plans are often checked and approved with estimated weights and such calculations may give just estimated results. Of course such approach cannot be accepted anymore as human lives are put in danger.

6. CONCLUSION – PROPOSED MEASURES TO ENHANCE CONTAINER TRANSPORT SAFETY

A variety of risk assessment and risk management techniques may be used for risk mitigation purposes in containerized cargo maritime transportation. Irrespective of the particular method chosen its main target would be to build up a safety barrier to avoid the "domino effect" first presented by Heinrich back in 1950.

An obligatory verification of container weights at container terminal gates will act as an efficient safety barrier and would contribute to container transport safety in following ways:

- **safer container handling inside container terminals** including and not limited to: lifting, shifting, transportation inside terminal, loading to and unloading from container ships;
- **safer cargo planning** as a result of an increased accuracy of seaworthiness calculations using container actual weights; and early verification of weights (in comparison to a verification prior to loading on board) which would give enough time for the terminal planner in charge for the vessel to prepare a prestow plan with actual weights instead of estimated container weights;
- **confirmation that container MGW as per CSC'72 is not exceeded** by enabling the use of container cargo information processing software to compare the verified container weight with the MGW for which a container is certified;
- **increased security for terminals and ships** by providing an early alert in case of a misdeclared container.

Development of new standards for BAPLIE and MOVINS messages that will include mandatory qualifiers for containers' MGW and MASW will additionally contribute to the overall container transport safety by:

- **ensuring full compliance with SOLAS VI/2 requirements** regarding cargo information;
- **enabling instant verification that containers' MGW is not exceeded** and the units are not handled if overloaded;
- **enabling verification that the MASW is not exceeded** for each container according to a ship's container stowage plan.

REFERENCES

[1]. Heinrich H. – ***Industrial Accident Prevention,*** McGraw-Hill, 1950

[2]. IACS – ***Recommendations on Loading Instruments No 48,*** IACS, 1997

[3]. IACS – ***Requirement for Loading Conditions, Loading Manuals and Loading Instruments 1971/Rev.7 2010,*** IACS, 2010

[4]. IMO – ***DSC 17/INF.5 "Development of measures to prevent loss of containers",*** IMO, 2012

[5]. IMO –***International Convention for Safe Containers CSC'72, Edition IB282E,*** IMO, 2012

[6]. IMO – ***MSC Circular 891 "Guidelines for the On-board use and Application of Computers",*** IMO

[7]. IMO – ***MSC.1/Circ.1229 "Guidelines for the Approval of Stability Instruments",*** IMO, 2007

[8]. IMO – ***The recommendation on loading instruments, adopted by resolution 5 of the 1997 SOLAS Conference,*** IMO, 1997

[9]. IMO – ***Resolution MSC.310(88) Adoption of Amendment to the International Convention for Safe Containers (CSC), 1972*** IMO, 2010

[10]. IMO – ***SOLAS Consolidated Edition,*** IMO, 2009

[11]. IMO/ILO/UNECE – ***Guidelines for Packing of Cargo Transport Units (CTUs),*** IMO/ILO/UNECE, 1997

[12]. ISO – ***ISO 1496-1(E) Series 1 freight containers – Specifications and testing, fifth edition,*** ISO, 1990

[13]. ISO – ***ISO 1496-1(E) Series 1 freight containers – Specifications and testing, fifth edition, 1990 Amendment 3,*** ISO, 2005

[14]. SMDG – ***User Manual UN/EDIFACT Bayplan Message Ver 2.2.1,*** SMDG, 2007

[15]. U. K. Marine Accident Investigation Branch – ***Report 20/2006. Report on the investigation of the loss of containers overboard from P&O Nedlloyd Genoa,*** 2006

[16]. U. K. Marine Accident Investigation Branch – ***Report 9/2008. Report on the investigation of the structural failure of MSC Napoli,*** 2008

[17]. UNCTAD – ***Review of Maritime Transport 2012,*** UNCTAD, 2012

[18]. Wijnolst N., Scholtens M., Waals F. – ***Malacca-Max. The Ultimate Container Carrier***, Delft University Press, 1999.

[19]. **http://theloadstar.co.uk/dutch-u-turn-throws-mandatory-container-weighing-into-doubt/**

[20]. **http://www.smdg.org/upload/BAPLIE3htm.zip**

For Authors

Are edited scientific papers in topics, written in English. Papers are selected after a peer review. Each participant is allowed to send maximum 2 papers as first author. Authors should make sure that the manuscripts submitted are ready for refereeing. The papers that are to be published must bring scientific contributions to the journal. The papers also have to contain the results of some of your work. It is strongly recommended an even number of pages, no longer than 6-10 pages. The papers that do not respect the publishing conditions and which are not integrated in the thematic of this journal will be rejected from the start by the Editorial Board. Authors submitting an article affirm that the same manuscript is not concurrently submitted to another publication. The authors are entirely responsible for the content of their papers.

PUBLISHED SINCE 2008
ISSN:1844-6116
ON LINE SINCE: 2008
PUBLISHED BY: Editura Nautica/ Constanta Maritime University